

Dissertation
submitted to the
Combined Faculties for the Natural Sciences and for Mathematics
of the Ruperto-Carola University of Heidelberg, Germany
for the degree of
Doctor of Natural Sciences

presented by
Cletus Adiyaga Wezena, M.Sc. Medical Microbiology
born in Navrongo, Ghana

Oral examination: 11.05.2018

**The cytosolic glyoxalase systems of the host-parasite unit
are dispensable during asexual blood-stage development of
the malaria parasite *Plasmodium falciparum***

Referees: Prof. Dr. Michael Lanzer

Prof. Dr. Marcel Deponste

Dedication

To my mother, Mary-Paula Peyegu Adiyaga, and late sister, Mrs Rose Abadandi, for all the sacrifices they made towards my education.

Declaration

I hereby declare that this thesis has been composed solely by myself and is an original report of my research work which I performed under the supervision of Prof. Dr. Marcel Deponte. The experimental results are almost entirely by my own efforts. Collaborative contributions, supporting literatures and resources, and any form of help received from colleagues have been indicated clearly in text, acknowledged and duly referenced. I declare that this thesis contains no material which has been accepted for the award of any other degree or diploma in any university or other tertiary institution.

Parts of this work have been published in:

Cletus A. Wezena, Miriam Urscher, Robert Vince, Swati S. More & Marcel Deponte. (2016). Hemolytic and antimalarial effects of tight-binding glyoxalase 1 inhibitors on the host-parasite unit of erythrocytes infected with *Plasmodium falciparum*. *Redox Biology*, **8**:348–353.

Cletus A. Wezena, Johannes Krafczyk, Verena Staudacher & Marcel Deponte. (2017). Growth inhibitory effects of standard pro- and antioxidants on the human malaria parasite *Plasmodium falciparum*. *Experimental Parasitology*, **180**:64-70.

Cletus A. Wezena, Romy Alisch, Alexandra Golzmann, Linda Liedgens, Verena Staudacher, Gabriele Pradel and Marcel Deponte. (2018). The cytosolic glyoxalases of *Plasmodium falciparum* are dispensable during asexual blood-stage development. *Microbial Cell*, **5**(1):32-41.

.....

Date

.....

Cletus Adiyaga Wezena

Acknowledgments

First and foremost, all praises and thanks to the Almighty God for granting me His blessings, the good health and energy to successfully complete my study.

I also wish to sincerely thank Prof. Dr. Michael Lanzer for offering me the opportunity to undertake my PhD studies in the Department of Parasitology of the Center for Infectious Diseases. He did not only introduce me to the Department and my supervisor but is also my first thesis advisor. He patiently and promptly wrote several support letters to the DAAD on my behalf, a very generous act that helped me secure the much needed financial support for my study. I am very grateful for his invaluable support.

To my supervisor, Prof. Dr. Marcel Deponte, I wish to sincerely thank him for the opportunity to join his group. He was always interested, enthusiastic and patient when I needed his direction and advice. He had time to personally demonstrate some experiments to me and always showed interest in my progress. I am also very thankful to him for the many letters he wrote to Ghana and the DAAD to support my study and for his help with the publications that we produced during the time of my study. I am also very grateful to him for taking time to correct my reports and this manuscript. It was a wonderful time and I have learnt so much under his guidance that I am very proud and happy about.

The working environment was always conducive and fun. I thank my colleagues in the group: Verena, Linda, Sandra, Gino, Johannes and Kristina. I am particularly thankful to Linda, for her help with the purification of my antibodies, performing some of my western blot analyses and taking time to read my manuscript and translate parts of it to the German language, and to Verena for introducing me to many of the techniques I used for my project. I also thank Sonia, Jessica, Dennis, Catherine, Katharina, Mendi, Mirko and the members of the Department of Parasitology for their advice and suggestions for some of my experiments.

It has been quite a long personal journey to this point. I wish to thank Mr. and Mrs. Sam Janse and Madam Louise Porteus for their kind words and support at various stations of this journey. I am also grateful to Mrs Dorothee-Julia Schaefer-Winkler for her support during my study.

I wish also to sincerely thank the DAAD and the Ministry of Education of Ghana for jointly funding my study by providing me a scholarship.

Finally, I wish to thank my family for their support, encouragement and prayers throughout my journey in search for academic laurels, especially during the course of this PhD study. I particularly appreciate the patience and understanding of my wife during the time of my study. May the good Lord, continue to bless us all.

Abstract

Human malaria is caused by protozoan parasites of the genus *Plasmodium* and is a major contributor to global morbidity and mortality. *Plasmodium falciparum* is the most virulent of five *Plasmodium* species that infect human. As in the other species, *P. falciparum* develops and proliferates in the nutrient-rich anucleated erythrocyte, consuming glucose for energy and metabolizing haemoglobin as a source of amino acids. In the erythrocyte, the parasite is also able to avoid some of the host's immune responses during infection. To support the high growth rate of the parasite during infection, glucose consumption in the infected erythrocytes increases by up to 75-fold in comparison with uninfected erythrocytes. As a consequence, a high amount of the 2-oxoaldehyde methylglyoxal, a toxic by-product of glycolysis, is spontaneously formed in the parasite. Methylglyoxal reacts with and damages nucleic acids and proteins leading to the formation of the so-called advanced glycation end-products (AGE) in the cell. Glyoxalases 1 and 2 (Glo1 and Glo2) of the ubiquitous glyoxalase system catalyze the glutathione-dependent detoxification of methylglyoxal and other 2-oxoaldehydes to non-toxic 2-hydroxycarboxylic acids.

In the *P. falciparum* infected erythrocyte, two functional glyoxalase systems operate; one in the cytosol of the erythrocyte (hGlo1 and hGlo2) and the other in the parasite cytosol (*Pf*Glo1 and *Pfc*Glo2). In addition to the cytosolic enzymes, *P. falciparum* also encodes a functional apicoplast-targeted Glo2 enzyme (*Pf*ΔGlo2), and an inactive Glo1-like protein (*Pf*GILP) that also carries an apicoplast-targeting sequence. On account of the detoxification role the glyoxalase system plays during *Plasmodium* infection, there has been a long-standing hypothesis that inhibition or knockout of the *Plasmodium* glyoxalase-encoding genes would lead to an accumulation of methylglyoxal (2-oxoaldehydes) in the host-parasite unit and result in parasite death. And so, the glyoxalase system(s) of the host-parasite unit could be targeted for antimalarial drug development.

This thesis investigated the relevance of the glyoxalase system to the blood-stage parasite survival by generating clonal *PFGLO1* and *PFcGLO2* knockout lines of *P. falciparum* 3D7 strain using the CRISPR-Cas9 system. SYBR green-based growth assays of the knockout clones showed that the 3D7Δ*glo1* knockout clones had an increased susceptibility to the external 2-oxoaldehyde glyoxal compared with the 3D7Δ*cglo2* knockout clone and the 3D7 wild-type strain. Western blot analyses also supported the accumulation of selected modified proteins in 3D7Δ*glo1* and 3D7Δ*cglo2* knockout strains in comparison with the 3D7 wild-type strain. The 3D7Δ*glo1* and 3D7Δ*cglo2* knockout lines were, however, viable and showed no significant morphological or growth phenotype under standard growth conditions. Furthermore, the lack of *Pfc*Glo2, but not *Pf*Glo1, resulted in increased gametocyte induction and gametocytogenesis in the knockout lines. *Pf*Glo1 and *Pfc*Glo2 are therefore dispensable during asexual blood-stage development and the loss of *Pfc*Glo2 may actually contribute to the transmission of the malaria parasite. The results show that *Pf*Glo1 and *Pfc*Glo2 are non-essential and most likely not suitable for targeted antimalarial drug development.

Several attempts to generate knockout clonal lines for the apicoplast targeted glyoxalase enzymes were unsuccessful. Transfectants resistant to both positive and negative selection were obtained in three knockout trials but were all confirmed to be false-positive transgenic parasites. The most

probable explanation for this outcome is an off-target or unwanted integration of the positive selectable marker into the parasite genome. Methodological limitations, rather than the essentiality of the two enzymes, are therefore most likely the cause of the negative knockout results.

The thesis also investigated the relevance of the hGlo1 enzyme to the survival of the parasite in the host-parasite unit using three tight-binding Glo1 inhibitors. Inhibitor treatments of uninfected erythrocytes showed an extremely slow inactivation of the host cell glyoxalase. Esterification did not confer improved pharmacokinetics nor increased the potency of the inhibitors. Inhibition of the erythrocyte Glo1 enzyme did not affect parasite development in the host cell, pointing to a potential dispensability of the host cell enzyme for parasite survival in the host-parasite unit.

Finally, as a way of addressing the relevance of the so-called oxidative stress on parasite development, the thesis investigated the effects of the prooxidant H₂O₂ and the so-called antioxidants NAc, ascorbate, and DTT on the survival of *P. falciparum* 3D7 strain. IC₅₀ values for the redox agents were determined for ring-stage synchronized parasites using a SYBR green-based growth assay. An IC₅₀ value of 78 mM for H₂O₂ revealed the compound as a very poor prooxidant in parasite culture. The host-parasite unit appears to be very robust against challenges with H₂O₂ and parasite killing required extremely high concentrations with implications for host defence mechanisms. The reductants NAc, ascorbate and DTT also had antiproliferative instead of growth-promoting effects with IC₅₀ values around 16, 4 and 0.3 mM, respectively. Taken together, the host-parasite unit appears more tolerant to high levels of H₂O₂, ascorbate and NAc, but is more susceptible to DTT. The inhibitory effect of the so-called antioxidants has implications for clinical trials and studies on oxidative stress.

Zusammenfassung

Menschliche Malaria wird von Protozoenparasiten der Gattung *Plasmodium* verursacht und gehört zu den Hauptursachen der globalen Morbidität und Sterblichkeit. *Plasmodium falciparum* ist der virulenteste der fünf humanpathogenen Malaria-Arten. Wie auch die anderen Arten, entwickelt und vermehrt *P. falciparum* sich in nährstoffreichen zellkernlosen Erythrozyten, nutzt Glucose als Energiequelle und metabolisiert Hämoglobin als Aminosäurequelle. Innerhalb der roten Blutkörperchen ist der Parasit teilweise auch in der Lage, sich der Immunantwort des Wirts während der Infektion zu entziehen. Als Folge der hohen Wachstumsrate des Parasiten während der Infektion erhöht sich der Glucoseverbrauch des infizierten Erythrozyten um das bis zu 75-fache im Vergleich zu nicht infizierten Erythrozyten. Als eine Konsequenz entsteht spontan eine große Menge des 2-Oxoaldehyds Methylglyoxal als toxisches Nebenprodukt der Glykolyse im Parasiten. Glyoxalase 1 und 2 (Glo1 und Glo2) des ubiquitären Glyoxalase Systems katalysieren die glutathionabhängige Entgiftung von Methylglyoxal und anderen 2-Oxoaldehyden zu ungiftigen 2-Hydroxycarbonsäuren. In mit *P. falciparum* infizierten Erythrozyten sind zwei funktionale Glyoxalase-Systeme tätig; eins im Zytosol des Erythrozyten (hGlo1 und hGlo2) und das andere im Zytosol des Parasiten (*PfGlo1* und *PfcGlo2*). Zusätzlich zu den zytosolischen Enzymen, codiert *P. falciparum* für das funktionelle Glo2-Enzym (*PfGlo2*) mit Apicoplast-Zielsequenz und ein inaktives Glo1-ähnliches Protein (*PfGILP*), welches auch eine Apicoplast-Zielsequenz aufweist. Aufgrund der Entgiftungsrolle des Glyoxalase-Systems während einer Plasmodien-Infektion, gibt es seit langer Zeit die Hypothese, dass eine Inhibition oder das Ausschalten der Glyoxalasen in *Plasmodium* zu einer Anreicherung von 2-Oxoaldehyden in der Wirt-Parasiten-Einheit führen könnte, welche zum Tod des Parasiten führen könnte. Deshalb könnte das Glyoxalase-System der Wirt-Parasiten-Einheit ein mögliches Angriffsziel für die Entwicklung von Antimalariawirkstoffen sein. In dieser Arbeit wurde die Relevanz des Glyoxalase-Systems für das Überleben des Parasiten in Blutzellstadien untersucht, indem klonale *P. falciparum* 3D7 Knockout Stämme für *PFGL1* und *PFcGLO2* mithilfe der CRISPR-Cas9 Technologie erzeugt wurden. Auf SYBR-green basierte Wachstumsstudien der Knockout Klone zeigten, dass die 3D7Δ*glo1* Knockout Klone eine erhöhte Empfindlichkeit gegenüber externem Glyoxal im Vergleich zu den 3D7Δ*glo2* Knockout Klonen und Wildtypparasiten zeigten. Western Blot Untersuchungen zeigten ebenfalls eine Anreicherung von ausgewählten modifizierten Proteinen in den 3D7Δ*glo1* and 3D7Δ*glo2* Knockout Stämmen im Vergleich zum 3D7 Wildtypstamm. Allerdings waren alle klonalen Linien des 3D7Δ*glo1* und 3D7Δ*glo2* Knockouts überlebensfähig und zeigten keinen signifikanten morphologischen oder Wachstums-Phänotyp unter Standardwachstumsbedingungen. Außerdem resultierte das Fehlen von *PfcGlo2*, aber nicht das Fehlen von *PfGlo1*, überraschenderweise in einer erhöhten Gametozytenbildung in den Knockout-Stämmen. *PfGlo1* und *PfcGlo2* sind daher entbehrlich während der asexuellen Blutstadienentwicklung und der Verlust von *PfcGlo2* könnte tatsächlich zur Übertragung des Malariaparasiten beitragen. Die Daten zeigen, dass *PfGlo1* und *PfcGlo2* nicht essentiell und daher höchstwahrscheinlich nicht für die zielgerichtete Entwicklung eines Malariamedikaments geeignet sind. Mehrere Versuche klonale Knockout-Stämme für die Glyoxalasen des Apicoplasten zu generieren waren erfolglos. Transfektanten, welche sowohl gegen positive als auch negative Selektion resistent waren, wurden in drei Knockout-Versuchen erzielt, wurden aber alle als falsch

positive transgene Parasiten identifiziert. Die wahrscheinlichste Erklärung für dieses Ergebnis sind unerwünschte Integrationen des positiven Selektionsmarkers in das Genom des Parasiten. Methodische Einschränkungen sind daher plausibler als Erklärung der negativen Knockout Ergebnisse als dass die zwei Enzyme essentiell sind. In diesem Projekt wurde außerdem die Relevanz des hGlo1 Enzyms auf das Überleben des Parasiten in der Wirt-Parasiten-Einheit untersucht, indem zwei Inhibitoren der Glyoxalase Glo1 und deren Carboxyl *tert*-butyl Ester Derivate eingesetzt wurden. Die Behandlung nicht-infizierter Erythrozyten mit Inhibitor zeigte eine extrem langsame Inaktivierung der Wirtszellglyoxalase. Eine Veresterung führte weder zu verbesserter Pharmakokinetik noch erhöhte sich die Wirksamkeit des Inhibitors. Die Inhibition des Glo1-Enzyms des Erythrozyten hatte keinen Effekt auf die Entwicklung des Parasiten was auf eine mögliche Entbehrlichkeit des Wirtsenzyms für das Überleben des Parasiten in der Wirt-Parasiten-Einheit deutet. Schließlich wurde in dieser Arbeit der Effekt des Prooxidants H₂O₂ und der sogenannten Antioxidantien NAc, Ascorbat und DTT auf das Überleben des 3D7-Stamms von *P. falciparum* untersucht, um Einblicke in die Relevanz von sogenanntem oxidativem Stress auf die Entwicklung des Parasiten zu gewinnen. Für die Redoxmittel wurden IC₅₀-Werte mit synchronisierten Parasiten im Ringstadium mittels SYBR-green basierten Wachstumskurven bestimmt. Ein IC₅₀-Wert von 78 mM für H₂O₂ zeigte, dass H₂O₂ ein sehr schwaches Prooxidants in der Parasitenkultur ist. Die Einheit aus Wirt und Parasit scheint sehr widerstandsfähig gegen die Behandlung mit H₂O₂ zu sein, und um den Parasiten zu töten waren extrem hohe Konzentrationen nötig, die auch Auswirkungen auf den Verteidigungsmechanismus des Wirts haben. Die Reduktionsmittel NAc, Ascorbat und DTT hatten auch einen antiproliferativen anstatt wachstumsfördernden Effekt mit entsprechenden IC₅₀-Werten von 12, 3 und 0,4 mM. Zusammengefasst scheint die Einheit aus Wirt und Parasit toleranter gegen hohe Konzentrationen von H₂O₂, Ascorbat und NAc zu sein, aber anfälliger für DTT. Der hemmende Effekt der sogenannten Antioxidantien hat Auswirkungen für klinische Versuche und Studien zum oxidativen Stress.

Table of Contents

<i>Acknowledgments</i>	v
<i>Abstract</i>	vi
<i>Zusammenfassung</i>	viii
<i>Table of Contents</i>	x
<i>Abbreviations</i>	xiii
<i>Index of Figures</i>	xvi
<i>Index of Tables</i>	xvii
1. INTRODUCTION	1
1.1. Introduction to malaria and <i>Plasmodium</i> species.....	1
1.1.1. Malaria – a brief history	1
1.1.2. Insect vector.....	2
1.1.3. <i>Plasmodium</i> species - the complex life cycle	3
1.1.4. Morphology and metabolism of <i>P. falciparum</i>	9
1.2. Control of malaria.....	11
1.2.1. Prevention of transmission.....	11
1.2.2. Diagnosis of malaria	13
1.2.3. Drug treatment of malaria	13
1.2.4. Emergence and implications of drug resistance	15
1.3. Molecular biology and genetic manipulation of <i>P. falciparum</i>	16
1.3.1. Historical and general aspects	16
1.3.2. The CRISPR-Cas9 genome-editing strategy	19
1.4. The glyoxalase system.....	21
1.4.1. History and general aspects	21
1.4.1.1. History.....	21
1.4.1.2. Glo1	23
1.4.1.3 Glo2.....	24
1.4.1.4. 2-Oxoaldehydes	25
1.4.1.5. Other pathways of methylglyoxal metabolism	26
1.4.2. Glyoxalase system of the human erythrocyte	27
1.4.3. Glyoxalase system and methylglyoxal metabolism in <i>P. falciparum</i>	28
1.4.4. Glyoxalase systems of the host-parasite unit as a potential drug target	30
1.5. Inhibitory effects of standard pro- and antioxidants on <i>P. falciparum</i>	33

1.6. Hypothesis and aims of the study	34
2. MATERIALS.....	35
2.1. Technical equipment	35
2.2. Chemicals, Consumables and kits	36
2.3. Plasmids, Primer and Strains.....	37
3. METHODS	40
3.1. Design of strategy for <i>P. falciparum</i> glyoxalase gene disruption	40
3.2. Design and purification of peptide antibodies	40
3.3. Plasmid constructs	41
3.3.1. Cloning strategy of knockout plasmids.....	41
3.3.2. PCR amplification of homologous regions.....	41
3.3.3. TOPO cloning of homologous regions	42
3.3.4. Plasmid minipreparation from <i>E. coli</i> cells.....	42
3.3.5. Cloning of homologous regions into the pL6 plasmid.....	43
3.3.6. Cloning of guide sequence into the pL6 plasmid.....	44
3.3.7. Maxipreparation of pL7 plasmid for transfection.....	45
3.4. <i>P. falciparum</i> cell culture	46
3.4.1. <i>P. falciparum</i> parasite culture	46
3.4.2. Thawing and cultivation of parasite strains	47
3.4.3. Splitting the culture.....	48
3.4.4. Determination of parasitemia and culture viability	48
3.4.5. Synchronization of parasite growth	48
3.4.6. Cryopreservation of <i>P. falciparum</i> parasites	49
3.5. Transfection and selection of transgenic parasites	49
3.5.1. Transfection of the pUF1-Cas9 plasmid	50
3.5.2. Transfection of the pL7 plasmid.....	51
3.5.3. Limiting dilution and generation of single knockout clones	51
3.6. Genome and western blot analyses of clonal knockout lines	52
3.6.1. Saponin lysis of infected erythrocytes and purification of parasites	52
3.6.2. Isolation and purification of genomic DNA of knockout strains.....	53
3.6.3. Genotyping of wild-type parasites and clonal knockout lines.....	54
3.6.4. SDS-PAGE and western blot analyses of wild-type parasites and knockout lines	55
3.7. Growth and morphological analyses of knockout strains.....	57
3.7.1. Growth analysis	57
3.7.2. Gametocyte formation assay.....	57
3.7.3. Determination of IC ₅₀ values for external 2-oxoaldehydes for knockout strains .	58
3.8. Relevance of host cell Glol activity for <i>P. falciparum</i> growth.....	59

3.9. Glyoxalase activity assays of erythrocytes and knockout strains.....	60
3.9.1. Preparation of erythrocyte lysate for enzyme assays.....	60
3.9.2. Preparation of parasite lysate for enzyme assays.....	60
3.9.3. Measurement of erythrocyte hemoglobin concentration	61
3.9.4. Bradford assay	61
3.9.5. Glyoxalase 1 activity assay.....	62
3.9.6. Glyoxalase 2 activity assay.....	63
3.10. IC ₅₀ value determination for standard pro- and antioxidants for <i>P. falciparum</i> 3D7 parasites.....	63
3.11. Growth analysis of ascorbate treated <i>P. falciparum</i> 3D7 parasites.....	64
4. RESULTS.....	65
4.1. Effect of the host cell Glo1 activity on <i>P. falciparum</i> blood-stage cultures	65
4.2. pL7-knockout constructs to disrupt the glyoxalase genes in <i>P. falciparum</i>	66
4.3. Generation of single knockout clones by limiting dilution	69
4.4. PCR and western blot analyses of 3D7 Δ <i>glo1</i> and 3D7 Δ <i>cglo2</i> clones	69
4.5. Attempts to disrupt the <i>PfGlo2</i> - and <i>PfGILP</i> -encoding genes were not successful....	70
4.6. Growth curve and morphological analyses of knockout strains.....	71
4.7. Glo1 and Glo2 activities of glyoxalase knockout strains	72
4.8. Susceptibility of glyoxalase knockout strains to 2-oxoaldehydes	73
4.9. AGE accumulation in glyoxalase knockout strains.....	74
4.10. Gametocytogenesis of glyoxalase knockout strains	76
4.11. Antiproliferative effects of H ₂ O ₂ , ascorbate, NAc and DTT	76
5. DISCUSSION	78
5.1. A revolutionary CRISPR-Cas9 system for <i>P. falciparum</i> genome editing.....	79
5.2. Human Glo1 appears to be dispensable for asexual blood-stage development.....	80
5.3. Cytosolic glyoxalases of <i>P. falciparum</i> are dispensable for blood-stage development	81
5.4. Loss of <i>PfcGlo2</i> in the asexual blood stages increased gametocytogenesis.....	83
5.5. Disruption of <i>PfGLO2</i> and <i>PfGILP</i> genes is challenging.....	84
5.6. Standard redox agents inhibit the growth of <i>P. falciparum</i> in cell culture.....	84
5.7. Conclusion.....	87
References.....	88

Abbreviations

ACTs	Artemisinin-based combination therapies
AGE	Advanced Glycation Endproducts
<i>A. gambiae</i>	<i>Anopheles gambiae</i>
BC	Before Christ
bp	Base pair(s)
Cas	CRISPR-associated protein
CD	Cytosine deaminase
CRISPR	Clustered regularly interspaced short palindromic repeats
DDT	Dichlorodiphenyltrichloroethane
DHAP	Dihydroxyacetone-phosphate
DHFR	Dihydrofolate reductase
DHPS	Dihydropteroate synthase
DNA	Deoxyribonucleic acid
DSB	Double strand break
DTT	Dithiothreitol
<i>E. coli</i>	<i>Escherichia coli</i>
5-FC	5-Fluorocytosine
g	Earth's gravitational force
gDNA	Genomic deoxyribonucleic acid
gRNA	Guide ribonucleic acid
GILP	Glo1-like protein
Glo1	Glyoxalase I
Glo2	Glyoxalase II
Glo3	Glyoxalase III
GSH	Reduced glutathione
<i>HAGH</i>	Hydroxyacylglutathione hydrolase gene
Hb	Haemoglobin
<i>hdhfr</i>	Human dihydrofolate reductase gene
hGlo1	Human glyoxalase I
hGlo2	Human glyoxalase II
hr	Hour(s)
HR	Homologous region
H ₂ O ₂	Hydrogen peroxide
IC ₅₀	Half maximal inhibitory concentration
IRS	Indoor residual spraying
ITNs	Insecticide-treated mosquito nets
kDA	Kilodalton
kb	Kilobase pair(s)
K_i^{app}	Apparent inhibition constant
K_M	Michaelis-Menten constant
kV	Kilovolts

M	Molar
Mb	Mega bases
MG	Methylglyoxal
μ F	Microfarad
μ L	Microliter
μ M	Micromolar
μ U	Microunit(s)
mm	Millimeter
mM	Millimolar
mL	Milliliter
min	Minute(s)
NAc	<i>N</i> -Acetylcysteine
ng	Nanogram
nm	Nanometer
PAM	Protospacer adjacent motif
PBS	Phosphate buffered saline
<i>Pb/P. berghei</i>	<i>Plasmodium berghei</i>
PCR	Polymerase chain reaction
<i>Pf/P. falciparum</i>	<i>Plasmodium falciparum</i>
<i>Pf</i> Glo1	<i>P. falciparum</i> glyoxalase I
<i>Pf</i> GILP	<i>P. falciparum</i> GloI-like protein
<i>Pfc</i> Glo2	<i>P. falciparum</i> cytosolic glyoxalase II
<i>Pft</i> Glo2	<i>P. falciparum</i> apicoplast-targeted glyoxalase II
3D7 Δ <i>glo1</i>	<i>P. falciparum</i> glyoxalase I knockout line
3D7 Δ <i>cglo2</i>	<i>P. falciparum</i> cytosolic glyoxalase II knockout line
3D7 Δ <i>tglo2</i>	<i>P. falciparum</i> apicoplast-targeted glyoxalase II knockout line
3D7 Δ <i>gilp</i>	<i>P. falciparum</i> GloI-like protein knockout line
RBC	Red blood cell(s)
RDTs	Rapid diagnostic kits
rpm	Revolutions per minute
RNA	Ribonucleic acid
RPMI	Roswell Park Memorial Institute
s	Second(s)
SDS	Sodium dodecyl sulphate
SLG	<i>S</i> -D-lactoylglutathione
sgRNA	Single-guide RNA
SNP	Single nucleotide polymorphism
TALENs	Transcription activator-like type II effector nucleases
tBOOH	<i>Tert</i> -butyl-hydroperoxide
TEMED	<i>N, N, N', N'</i> -Tetramethylethylenediamine
TCA	Tricarboxylic acid
tracrRNA	<i>Trans</i> -encoded CRISPR RNA
U	Unit(s)

UTR	Untranslated region
v/v	Volume/volume
WR	WR99210
w/v	Weight/volume
<i>ydhodh</i>	Yeast dihydroorotate dehydrogenase gene
<i>yfcu</i>	Yeast fusion cytosine deaminase and uridyl phosphoribosyl transferase
ZFNs	Zinc-finger nucleases

Index of Figures

Figure 1.1.	Global status of malaria in 2016.....	2
Figure 1.2.	The life cycle of <i>P. falciparum</i>	5
Figure 1.3.	Developmental stages of <i>P. falciparum</i> in the erythrocyte.....	6
Figure 1.4.	Schematic representation of the morphological stages of <i>P. falciparum</i> gametocytes.....	8
Figure 1.5.	Scheme of type II CRISPR-mediated DNA double-strand breaks.....	20
Figure 1.6.	Two plasmids for targeted <i>P. falciparum</i> genome editing using sgRNA:Cas9.....	21
Figure 1.7.	The glyoxalase detoxification system.....	22
Figure 1.8.	Formation, reactivity and detoxification of methylglyoxal in parasitized erythrocytes.....	31
Figure 3.1.	Structures of Glo1 inhibitors and esterified analogues used in inhibition studies.....	60
Figure 4.1.	Effect of the host cell Glo1 activity on <i>P. falciparum</i> blood-stage cultures.....	65
Figure 4.2.	Generation and validation of <i>P. falciparum</i> <i>GLO1</i> and <i>cGLO2</i> knockout clonal lines.....	67
Figure 4.3.	Strategy for the generation of <i>P. falciparum</i> <i>PFtGLO2</i> and <i>PFGILP</i> knockout clones.....	68
Figure 4.4.	Growth curve analysis and general morphology of <i>P. falciparum</i> knockout strains 3D7 Δ <i>glo1</i> and 3D7 Δ <i>cglo2</i>	71
Figure 4.5.	Glo1 and Glo2 activity measurements of <i>P. falciparum</i> 3D7 Δ <i>glo1</i> and 3D7 Δ <i>cglo2</i> knockout strains after erythrocyte removal by saponin lysis.....	73
Figure 4.6.	Summary of growth inhibitory effects of exogenous 2-oxoaldehydes on 3D7 Δ <i>glo1</i> and 3D7 Δ <i>cglo2</i> knockout strains.....	74
Figure 4.7.	Detailed results of growth inhibitory effects of exogenous 2-oxoaldehydes on synchronous ring-stage cell cultures of <i>P. falciparum</i> 3D7 Δ <i>glo1</i> and 3D7 Δ <i>cglo2</i> knockout strains.....	74
Figure 4.8.	Western blot detection of AGE in parasite extracts from <i>P. falciparum</i> 3D7 Δ <i>glo1</i> and 3D7 Δ <i>cglo2</i> knockout strains after erythrocyte removal by saponin lysis.....	75
Figure 4.9.	Analysis of gametocyte development of the <i>P. falciparum</i> 3D7 Δ <i>glo1</i> and 3D7 Δ <i>cglo2</i> knockout strains.....	76
Figure 4.10.	Growth inhibitory effects of hydrogen peroxide and three reducing agents, NAc, ascorbate and DTT, on <i>P. falciparum</i> 3D7 wild-type strain cultures.....	77

Index of Tables

Table 1.1. Summary of properties of the glyoxalases in the host-parasite unit.....	27
Table 2.1. Table of plasmids used.....	37
Table 2.2. Oligonucleotides used.....	37
Table 2.3. Table of bacterial and <i>P. falciparum</i> strains used.....	39
Table 3.1. 5' and 3' HRs and primers used for PCR amplifications.....	40
Table 3.2. Summary of <i>P. falciparum</i> 3D7 wild-type and knockout genotype PCR.....	55
Table 4.1. Summary of the IC ₅₀ values determined in this study compared with previously determined values from the Dd2 strain.....	78

1. INTRODUCTION

1.1. Introduction to malaria and *Plasmodium* species

1.1.1. Malaria – a brief history

Malaria is a major parasitic protozoan disease of humans that is transmitted by the bite of an infected female *Anopheles* mosquito (Cox, 2010; Neghina *et al.*, 2010; Webb, 2010; Kamareddine, 2012). The characteristic symptoms of the disease are rhythmic or fluctuating fevers, splenomegaly, malaise and anaemia, which when untreated can lead to a varied box of life-threatening complications such as coma (Webb, 2010; Clark *et al.*, 2004; Bartoloni & Zammarchi, 2012). The incubation period of the disease, depending on the parasite transmitted and status of the host, ranges from seven to fifteen days after a bite by the infected vector (Bartoloni & Zammarchi, 2012; WHO, 2017a; Kim *et al.*, 2013).

Earliest description of human infections similar to malaria can be traced back to Chinese documents around 2700 BC, and to records of Mesopotamia and ancient Egypt around 1500 BC. Hippocrates (400 BC), the famous early Greek physician, and his compatriots observed and associated poor health, fevers and enlarged spleens (which are malaria-like symptoms) to individuals living in marshy places (Cox, 2010; Neghina *et al.*, 2010). Thus, for over 2500 years after this initial association, miasmas emanating from swampy areas were connected with and thought to be the cause of poor health among people living in these areas. The name malaria was later adopted to describe the condition of poor health common among people living in marshy areas and is widely believed to have originated from the Italian phrase *mal'aria*, which means *spoiled air* (Cox, 2010; Neghina *et al.*, 2010; Webb, 2010). With the advancement of science, the miasma theory lost favour and in 1880, C. L. Alphonse Laveran discovered that the actual causative agent of malaria was a parasitic protozoan (Cox, 2010). The role of the *Anopheles* mosquito as the transmitting vector of *Plasmodium* parasites was subsequently discovered by Ronald Ross seventeen (17) years later (Cox, 2010; Neghina *et al.*, 2010). Despite the long history and many years of dedicated scientific research to control *Plasmodium* infection, malaria still remains one of the most dilapidating diseases in the history of mankind. In the past, malaria had played its part in the rise and decline of nations and helped model civilizations (Neghina *et al.*, 2010; Webb, 2010). At the present, although some important advances have been made, malaria still remains a huge socio-economic and health issue in many countries especially those in sub-Saharan Africa (Neghina *et al.*, 2010; Webb, 2010; WHO, 2016b). An estimated 297 million new malaria cases were recorded in 2015 with 731 000 fatal consequences (Vos *et al.*, 2016; Wang *et al.*, 2016). Of all deaths caused by malaria globally, 90% occur in sub-Saharan Africa alone. The reason for this is partly due to the warm and conducive climate for vector development in this region, and also as a result of the continuous sustenance of the disease by poverty (Webb, 2010; WHO, 2016b; Vos *et al.*, 2016; WHO, 2016a; Cruz *et al.*, 2013). High rates of malaria infections are also recorded in the South-East Asian, the Eastern Mediterranean and the South American regions of the world (WHO, 2017a; Cruz *et al.*, 2013). A majority of malaria deaths are among pregnant women and children under the age of five (5) years (Webb, 2010; WHO, 2016b; Vos *et al.*, 2016; WHO, 2016a). In 2015 alone, 2.9 billion US\$ was allocated to the fight against

malaria but the disease remains endemic in 91 countries putting nearly half of the world's population at risk (WHO, 2017a, 2016a). An upsurge in malaria research and the sequencing of the complete *Plasmodium falciparum* genome has helped in better understanding the transmission of the disease and the biology of the parasite. By combined efforts of donors, researchers and governments, the European region has been declared free of locally acquired malaria infections for many years now (WHO, 2016b). Several other countries are winning their fight against malaria and are now declared non-endemic to the disease (Figure 1.1) (WHO, 2016b). Nevertheless, the eradication and total control of the disease through new drugs and potential vaccines have so far been daunting to achieve in many parts of the world. Considering the challenging effects of drug resistance, climate change, global warming and a rise in international travel, chances are high for malaria transmission to increase or re-emerge even in areas now known to be free of the disease (Lee *et al.*, 2013; Mirski *et al.*, 2011; Bai *et al.*, 2013; Hurd *et al.*, 2005).

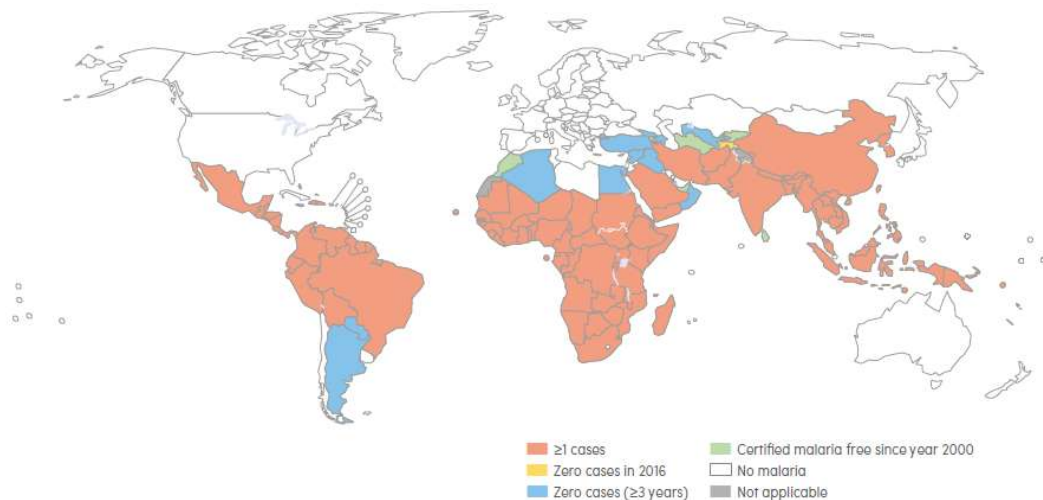


Figure 1.1. Global status of malaria in 2016. Taken from (WHO, 2017b).

1.1.2. Insect vector

To date, over 460 mosquito species of the genus *Anopheles* have been identified, 100 of which can act as potential vectors and definitive hosts for the malaria parasite (Webb, 2010; Kamareddine, 2012; Arrow *et al.*, 2004; Pimenta *et al.*, 2015; Sinka *et al.*, 2012). Of these potential vectors, 30-40 species are of major public health importance because of the efficiency of which they transmit the disease worldwide (Kamareddine, 2012; Arrow *et al.*, 2004; Sinka *et al.*, 2012). In sub-Saharan Africa where most of the world's transmission of the disease occurs, *A. gambiae*, *A. arabiensis* and *A. funestus* co-dominate as vectors (Arrow *et al.*, 2004; Sinka *et al.*, 2012). Only female *Anopheles* mosquitoes are known to transmit *Plasmodium* species to their intermediate host (Webb, 2010; Kamareddine, 2012; Arrow *et al.*, 2004). The life cycle of the mosquito comprises four developmental stages; egg, larva, pupa and adult (imago) (Arrow *et al.*, 2004). The adult female mosquito would normally bite an intermediate host for a blood meal. The mosquito needs blood to nurture its developing eggs to maturity. In the process of feeding, the mosquito may also suck up parasite

gametocytes from an infected host along with the blood, or introduce parasite sporozoites from its salivary glands into the host skin (WHO, 2017a; Arrow *et al.*, 2004; Pimenta *et al.*, 2015). Apart from a human intermediate host, *Anopheles* mosquitoes also feed on other warm-blooded animal such as other mammals. If the mosquito species prefers a human host, the species is termed anthropophagic or anthropophilic. If the species prefers to feed on other animals, it is termed zoophagic or zoophilic (Arrow *et al.*, 2004). The *A. gambiae* mosquito is particularly responsible for most cases of malaria in the African region because of its strong preference for human blood and its relatively longer lifespan compared to other species (WHO, 2017a; Arrow *et al.*, 2004; Cohuet *et al.*, 2010).

1.1.3. *Plasmodium* species – the complex life cycle

Malaria parasites are Apicomplexan protozoan belonging to the genus *Plasmodium* (Rich & Ayala, 2006). Presently, there are over 200 known *Plasmodium* species that infect and cause malaria in various vertebrates including humans, other mammals, birds and reptiles (Rich & Ayala, 2006; Perkins & Austin, 2009; Ramasamy, 2014; Lee & Vythilingam, 2013). *Plasmodium* species that infect other animals may be transmitted by different insect species apart from mosquitoes (or *Anopheles* species) (Sinden, 2002). In humans, malaria is caused by five morphologically and immunologically different *Plasmodium* species: *P. falciparum*, *P. vivax*, *P. malariae*, and *P. ovale* and the relatively new zoonotic addition, *P. knowlesi* (Cox, 2010; WHO, 2017a; Tuteja, 2007). The classical symptoms of the disease mentioned above are common to all five *Plasmodium* species even though their severity, manifestations and possible relapse pattern vary from species to species (Tuteja, 2007).

P. falciparum is the most virulent human malaria parasite, accounting for more than 85% of global malaria cases and deaths (Lee & Vythilingam, 2013; Tuteja, 2007; Rich & Ayala, 2006). It is also the most prevalent *Plasmodium* species in the African region (WHO, 2017a; Bousema & Drakeley, 2011). Infections by this species are characterized by severe anemia caused by high parasitemia during infection and the fever presented is usually asynchronous. *P. falciparum* infections often lead to fatal organ complications and cerebral malaria in children (Tuteja, 2007).

P. vivax causes a milder disease and is rarely fatal, similar to disease caused by *P. malariae* and *P. ovale*. This species is the most geographically widespread and infections cause the so-called mild tertian malaria which is characterized by mild anemia and fevers that reoccur every 48 hours (Antinori *et al.*, 2012). *P. vivax* typically forms hypnozoites, intrahepatic-stage parasites that are responsible for the relapse of the disease after many months of dormancy (Tuteja, 2007; Antinori *et al.*, 2012; Bousema & Drakeley, 2011). *P. vivax* is prevalent throughout the tropics especially in South-East Asia and South America (WHO, 2017a; Rich & Ayala, 2006; Lee & Vythilingam, 2013; Bousema & Drakeley, 2011; Antinori *et al.*, 2012). *P. ovale* is the least common malaria parasite and is present mostly in West Africa. Two morphologically indistinguishable genetic haplotypes (or species) of this species, *P. ovale curtisi* and *P. ovale wallikeri*, occur in sympatry (Tuteja, 2007; Antinori *et al.*, 2012). Infections by this species cause mild and easily managed disease. Similar to *P. vivax* infection, *P. ovale* can also cause relapses in malaria infections from dormant hypnozoites (Antinori *et al.*, 2012; Tuteja, 2007).

P. malariae is responsible for only a low frequency of human infections although it also has a worldwide distribution (Tuteja, 2007). The species is responsible for the so-called quartan malaria, the hallmark of which is 72 hours recurring fevers with a low grade parasitemia and mild anemia (Antinori *et al.*, 2012; Rosenberg, 2008). Even though no hypnozoites have been identified for this parasite, blood-stage parasites are capable of surviving at low parasitemia for long periods with the potential of causing disease recrudescence (Antinori *et al.*, 2012; Lee & Vythilingam, 2013; Garcia, 2010).

P. knowlesi is naturally a simian malaria parasite infecting macaque monkeys but has now been confirmed to have the potential of crossing over the species barrier to infect humans (Lee & Vythilingam, 2013; Galinski & Barnwell, 2009; Cox-Singh *et al.*, 2008; White, 2008). Records show that, due to the morphological similarities this species shares with *P. malariae*, many *P. knowlesi* infections have in the past been misdiagnosed as *P. malariae* infections. However, as a result of improved and more sensitive diagnostic methods, the species is now gaining grounds especially in South-East Asia as an important cause of malaria in humans (Lee & Vythilingam, 2013; Galinski & Barnwell, 2009; Cox-Singh *et al.*, 2008). Human infections of *P. knowlesi* are characterized by severe anemia. Disease manifestations caused by high level parasitemia have also been reported similar to the infection pattern of *P. falciparum* (White, 2008; Antinori *et al.*, 2012). Renal failure, jaundice and fevers that recur every 24 hr (quotidian cycle) are common symptoms of *P. knowlesi* infection (White, 2008).

The life cycle of the malaria parasite is complex and involves several tissues and developmental forms in two different hosts, vertebrate and invertebrate (Fig.1.2). Asexual development takes places in the vertebrate (intermediate) host (Fig 1.3) while sexual development occurs in the invertebrate (definitive) host (Spinello, 2012). All the five human malaria parasites undergo a similar life cycle, sharing a human vertebrate host and female *Anopheles* as the intermediate host. In the exemplified life cycle of *P. falciparum*, the endogenous asexual phase, also called schizogony, commences when infective sporozoites (1n=haploid) from the salivary gland of the *Anopheles* mosquito are injected into the skin of the human host during a blood meal. The sporozoites will later find their way from the skin dermis through the capillaries into the host blood circulation (Antinori *et al.*, 2012). Sporozoites are usually delivered along with mosquito saliva containing anticoagulant and anti-inflammatory enzymes. These components of saliva ensure an easy flowing blood meal and minimize the pain-reaction caused by the bite (Lee & Vythilingam, 2013; Tuteja, 2007; Garcia, 2010; Garcia *et al.*, 2006). Around 20-200 sporozoites are transmitted in an infected bite, most of which are rapidly cleared from the blood circulation by the host's immune system leaving only a few to find and infect the liver hepatocytes (Rosenberg, 2008; Garcia *et al.*, 2006). The sporozoites are able to glide at considerable speed through the skin and into the blood vessels enabled by specialized parasite proteins (Boucher *et al.*, 2018). Exhibiting the same gliding motility, the sporozoites are then able to traverse liver sinusoidal cell layer including the kuffer cells, some hepatocytes and finally invade the hepatocytes to establish an infection (Boucher *et al.*, 2018). Parasite proteins such as thrombospondin-related anonymous protein (TRAP) are necessary for parasite active mobility and invasion, using power generated by an actomysin motor (Boucher *et al.*, 2018). At the liver-stage, each sporozoite penetrates one hepatocyte, differentiates into a liver trophozoite (1n) and undergoes a phase of asexual reproduction (mitosis) called pre-erythrocytic schizogony resulting in the production of tissue schizonts (1n) containing up to 30000 (compared to about 10000 in *P. vivax* or *P.*

ovale) uninucleated motile merozoites (1n) (Lee & Vythilingam, 2013; Antinori *et al.*, 2012; Rosenberg, 2008; Collins & Jeffery, 2007).

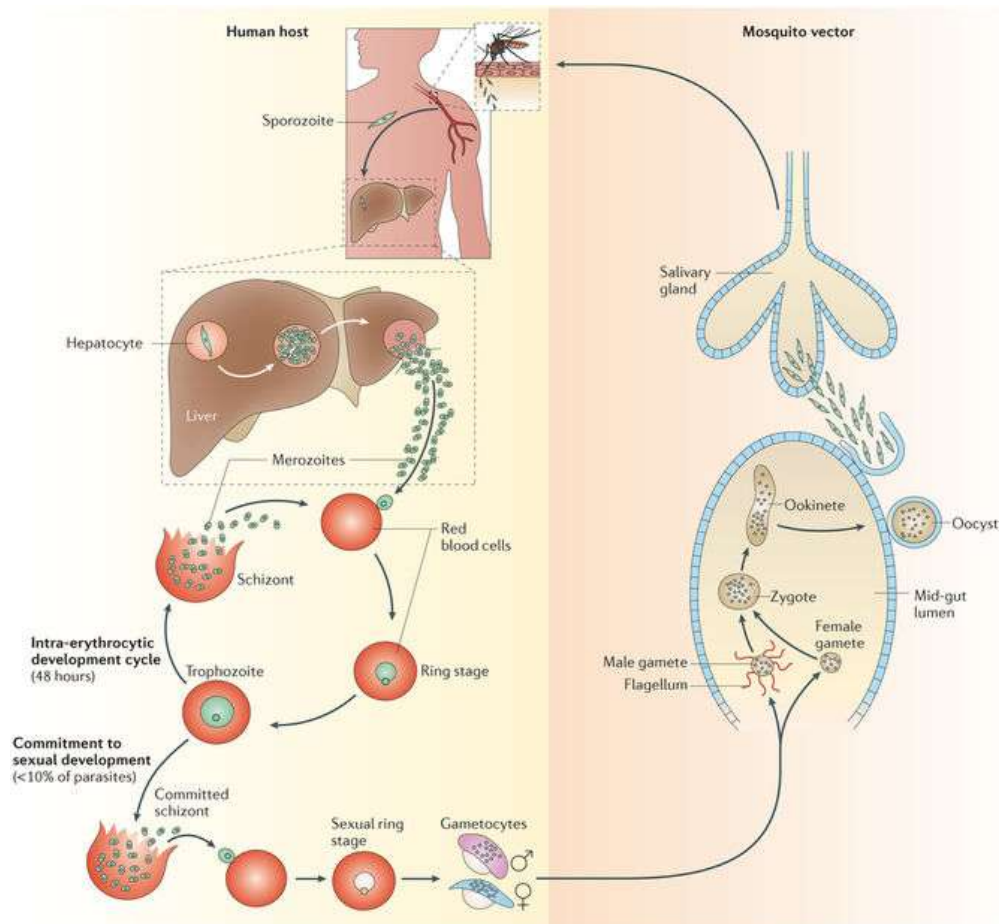


Figure 1.2. The life cycle of *P. falciparum*. Infectious sporozoites are injected into the human skin through the bite of an infected female *Anopheles* mosquito. Sporozoites travel through the blood stream to the liver and develop in the liver hepatocytes to produce tens of thousands of merozoites (extra-erythrocytic schizogony) by asexual reproduction. Merozoites are released into the blood and invade red blood cells, undergoing repeated rounds of asexual multiplication (intra-erythrocytic schizogony). Parasite development in the erythrocyte progresses through ring, trophozoite- and schizont-stages in one cycle. After a number of cycles, a small proportion (<10%) of merozoites leave the regular asexual cycle and instead begin to develop into the male and female sexual gametocytes. After 10–12 days of gametocytosis, gametocytes are taken up by the mosquito during a blood meal to begin the sexual phase of the life cycle in the mid-gut. Gametocytes differentiate into male and female gametes and undergo fertilization to form a zygote, which develops through the motile ookinete-stage to form the oocyst. Upon rupture of the oocyst, haploid sporozoites are released which migrate to the salivary glands and can then be transmitted to humans. Taken and modified from (Josling & Llinás, 2015).

At maturity, the liver schizont together with the infected hepatocyte burst to release packages of merozoites known as merozoites (through the liver) into the host blood stream (Tuteja, 2007; Gerald *et al.*, 2011). On average, the pre-erythrocytic phase takes between 5-6 days in *P. falciparum* (8-9 days for *P. ovale*, *P. vivax* and *P. knowlesi*, and 13-16 days for *P. malariae*) (Lee & Vythilingam, 2013; Antinori *et al.*, 2012; Gerald *et al.*, 2011). In the rodent *Plasmodium* species *P. berghei*, merozoites, which are membrane-bound vesicles derived

from hepatocyte material including membranes, are thought to protect the merozoites from the liver immune kupffer cells while they migrate to the host blood stream (Tuteja, 2007; Gerald *et al.*, 2011; Sturm *et al.*, 2006). The merozoites therefore ensure the direct release of the merozoites into the host bloodstream. In *P. ovale* and *P. vivax* liver infections, not all sporozoites that infect the hepatocytes maintain the developmental pattern and immediately progress through schizonts into merozoites. Some sporozoites remain dormant in the liver cells for a year or more in the form of hypnozoites. Hypnozoites are later reactivated to resume development and are responsible for malaria relapse many months after an apparent initial cure of the disease (Lee & Vythilingam, 2013; Tuteja, 2007; Antinori *et al.*, 2012). Liver-stage infection is asymptomatic and produces no disease condition (Derbyshire *et al.*, 2011).

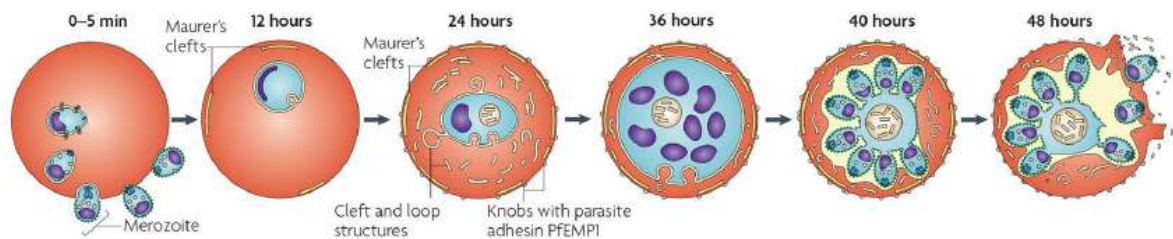


Figure 1.3. Developmental stages of *P. falciparum* in the erythrocyte. The *P. falciparum* merozoite attaches to, reorients and invades erythrocytes, and develops a parasitophorous vacuole (PV) around itself. Once inside, the parasite develops through the ring- (0–24 hours), trophozoite- (24–36 hours) and schizont-stages (40–48 hours). In the mature forms of the parasite (>24 h), different proteins are produced and exported to the cytoplasm and membrane of the erythrocyte, causing knobby deformations to appear on the erythrocyte membrane. The infected erythrocyte and the mature schizont rupture after approximately 48 hours, releasing 16–32 daughter merozoites into the blood. Hemozoin crystals, formed as a result of hemoglobin degradation, are deposited in a digestive vacuole. PfEMP1, *Plasmodium falciparum* erythrocyte membrane protein 1. Taken and modified from (Maier *et al.*, 2009).

While in the bloodstream, merozoites burst to release hepatic merozoites which use a complex acto-myosin motor system to invade erythrocytes and initiate a second phase of asexual multiplication called erythrocytic schizogony (Cox, 2010; Tuteja, 2007; Antinori *et al.*, 2012; Collins & Jeffery, 2007; Gerald *et al.*, 2011). Erythrocyte invasion is complex and involves several steps; i) initial recognition and reversible attachment of merozoite to the erythrocyte plasma membrane, ii) merozoite reorientation, irreversible attachment and the formation of the parasitophorous vacuole stimulated by the release of signal compounds from the rhoptry and the microneme organelles, iii) invagination of erythrocyte membrane around the attached merozoite with the loss of the merozoite surface coat and iv) closing of the parasitophorous vacuole and the erythrocyte membrane around the merozoite (Cowman *et al.*, 2012; Tuteja, 2007; Garcia *et al.*, 2006). *P. falciparum* merozoites can infect all age classes of erythrocytes but *P. vivax* and *P. ovale* preferentially infect the reticulocytes while *P. malariae* prefers old erythrocytes (Kerlin & Gatton, 2013; McQueen & McKenzie, 2004). Once inside the erythrocyte, the merozoite goes through several different stages of development that includes the early trophozoite or ring (1n), trophozoite (1n) and the schizont (1n) (Figure 1.3). The early trophozoite is uninucleated and has a characteristic ring-shaped

morphology. A ring is small in size and grows by feeding on hemoglobin from the normal size host erythrocyte. The ring later differentiates into a mature trophozoite by increased metabolism through the glycolytic consumption of large amounts of imported glucose. The ring also digests hemoglobin into constituent amino acids for protein synthesis and detoxifies free heme as hemozoin (Tuteja, 2007; Garcia, 2010; Mohandas & An, 2012). The mature trophozoite subsequently increases in size and also modifies the infected erythrocyte in many ways. Consequently, the infected erythrocyte loses its normal discoid shape and its membrane becomes more rigid and more permeable. Numerous proteins are produced by the parasite at this stage and are exported into the cytoplasm or to the surface of the infected erythrocyte. Some of these proteins such as the *P. falciparum* erythrocyte membrane protein 1 (PfEMP1) and the knob-associated histidine-rich protein (KAHRP) play a central role in parasite cytoadhesion (Tuteja, 2007; Mohandas & An, 2012; Ganguly *et al.*, 2015). The changes to the host cell also facilitate the survival of the parasite and are responsible for the severity of malaria (Mohandas & An, 2012). The period from the infective mosquito bite to the appearance of the first trophozoites in the erythrocytes is called the prepatent period. This period is about 8-25 days in *P. falciparum* (8-27 days in *P. vivax*, 15 days in *P. malariae*, 9-17 days in *P. ovale* and 15-30 in *P. knowlesi*) (Tuteja, 2007; Antinori *et al.*, 2012).

The trophozoite-stage is completed with four to five asynchronous nuclear divisions without cytokinesis resulting in the formation of the multinucleate plasmodial schizont (Lee & Vythilingam, 2013; Tuteja, 2007; Gerald *et al.*, 2011). Between 8 and 36 new merozoites are produced per erythrocytic schizont. The merozoites are released into the bloodstream upon rupture of the schizont and the infected red blood cell, thus completing one cycle of erythrocytic schizogony (Cox, 2010; Tuteja, 2007; Antinori *et al.*, 2012; Gerald *et al.*, 2011). The characteristic symptoms of malaria are all associated with blood-stage development of the parasite with the classical fevers coinciding with the release of merozoites (Cox, 2010; Lee & Vythilingam, 2013; Tuteja, 2007; Antinori *et al.*, 2012; Gerald *et al.*, 2011). Although some of the merozoites are arrested by the host immune system, others survive and immediately invade new healthy erythrocytes to begin another cycle of erythrocytic schizogony (Garcia, 2010; Garcia *et al.*, 2006; Gerald *et al.*, 2011). The time needed to complete one cycle of erythrocytic schizogony is 48 hours in *P. falciparum*, *P. ovale* and *P. vivax* (72 hours in *P. malariae* and 24 hours in *P. knowlesi*) (Lee & Vythilingam, 2013; Tuteja, 2007). After several recurrent cycles of erythrocytic schizogony, some young merozoites are stimulated to differentiate into micro- or macrogametocytes (haploid male and female sexual forms respectively) after infecting a new erythrocyte in a process called gametocytogenesis (Cox, 2010; Lee & Vythilingam, 2013; Antinori *et al.*, 2012; Garcia, 2010). The gametocytes are highly specialized cells, the development of which is controlled by over 250 genes (Bousema & Drakeley, 2011). Five morphologically distinguishable gametocyte developmental stages occur during which the cell enlarges and elongates to occupy most of the space in the infected erythrocyte (Fig 1.4). These stages, I-V, take between 10-12 days to complete development. Stage I gametocytes are indistinguishable from asexual trophozoites. At stage II, gametocytes begin to elongate and are D-shaped. The subpellicular-microtubules, which are involved in gametocyte structure and motility, also begin to form. Stage III gametocytes are further elongated with rounded ends and also contain proliferating mitochondria and Golgi bodies. Stage IV gametocytes are more elongated but now have pointed ends. In the macrogametocytes, osmiophilic bodies and an extensive rough

endoplasmic reticulum develop. In stage V, gametocytes assume their characteristic crescent form and the macrogametocytes which are more elongated and curved with a prominent nucleolus are distinguishable from the thicker microgametocytes. Only the mature stage V gametocytes circulate in peripheral blood of the host because erythrocytes that contain the early-stage gametocytes are usually found sequestered (Dixon *et al.*, 2012; Bousema & Drakeley, 2011; Schwank *et al.*, 2010; Josling & Llinás, 2015). During *P. falciparum* infection, mostly ring stages and stage V gametocytes are normally detected in the peripheral blood circulatory system of the host.

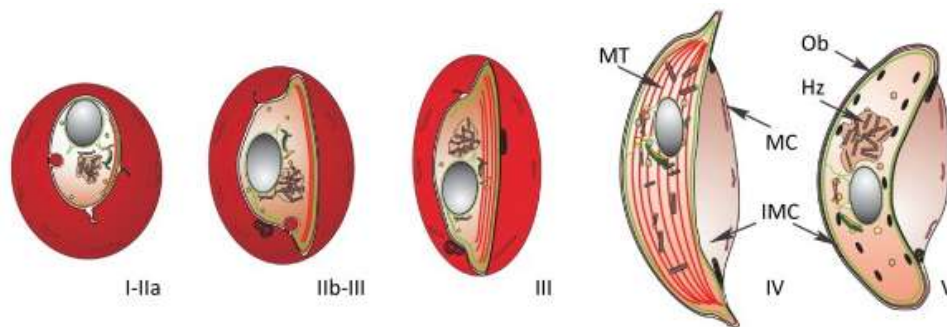


Figure 1.4. Schematic representation of the morphological stages of *P. falciparum* gametocytes. *P. falciparum* gametocytes develop through five distinct morphological stages. Early gametocytes (stage I and IIa) are almost indistinguishable from trophozoites. In stage IIb–III the parasite elongates and adopts a D-shaped morphology with rounded ends. Stage IV gametocytes are further elongated, have pointed ends adopting a curvature to conform to the confines of the host erythrocyte which is now reduced to a thin layer around the parasite. Hemozoin crystals are seen to be dispersed in the microgametocyte. In the final-stage (V), the ends of the gametocyte become more rounded. Hemozoin crystals in the macrogametocyte are seen to be partly aggregated. N, nucleus, Hz, hemozoin crystals, MC, the Maurer's clefts, Ob, osmiophilic bodies, IMC, inner membrane complex, and MT, microtubules. A male-stage IV and a female-stage V gametocyte are depicted. Taken and modified from (Dixon *et al.*, 2012).

The highly modified erythrocytes that host the mature trophozoite or schizonts are sticky and adhere to the endothelial lining of the small capillaries of organs. Adhered erythrocytes normally do not appear in the host's blood circulation (Cox, 2010; Bousema & Drakeley, 2011; Garcia, 2010).

Male and female gametocytes are ingested when the female *Anopheles* mosquito takes a blood meal from an infected person, an activity that is vital to the transmission of malaria (Cox, 2010; Lee & Vythilingam, 2013; Tuteja, 2007; Collins & Jeffery, 2007). Both physical (heat, moisture and visual) and chemical cues (characteristic odours) play an important role leading the mosquito to the vertebrate host (Antinori *et al.*, 2012). It takes between 2-3 days for circulating mature gametocytes (still in the erythrocyte) to be infectious to the mosquito. If infectious gametocytes are not injected by the mosquito, they only survive for a short period (5-12 hours) in blood circulation before they are degraded (Tuteja, 2007; Bousema & Drakeley, 2011; Antinori *et al.*, 2012). In the lumen of the mosquito mid-gut, the macrogametocytes are released by the rupture of the erythrocyte and mature within 5 min into mature macrogametes (1n) whereas the microgametocytes go through the process of exflagellation. This process involves division of the nucleus (20 min) of the microgametocyte

and subsequent differentiation of the cell into 8 haploid flagellated microgametes (1n) which are liberated from the erythrocyte to fertilize the macrogametes (Cox, 2010; Antinori *et al.*, 2012; Garcia, 2010; Garcia *et al.*, 2006; Collins & Jeffery, 2007). Still in the lumen of midgut, a microgamete penetrates a macrogamete in the process of fertilization to form the diploid zygote (2n) which subsequently differentiates into a motile ookinete. Several parallel fertilizations can occur concurrently depending on the number of gamete pairs available in the midgut of the mosquito (Garcia *et al.*, 2006). The ookinete (4n) is invasive and undergoes meiosis to generate a cell with four haploid nuclei (Garcia *et al.*, 2006; Gerald *et al.*, 2011). The ookinete then actively penetrates the wall of the midgut, positioned under the basal membrane of the midgut and differentiates into the oocyst. An oocyst is capable of undergoing sporogony, generating thousands of sporozoites (1n) through the process of mitosis (Lee & Vythilingam, 2013; Garcia *et al.*, 2006; Collins & Jeffery, 2007; Gerald *et al.*, 2011). When the mature oocyst ruptures, about a quarter of the sporozoites are released into the hemocoel of the mosquito. From there, they are able to actively migrate through the haemolymph to the salivary glands (Collins & Jeffery, 2007). After about a day of maturation in the salivary glands, sporozoites become highly infective to the vertebrate host when the mosquito takes the next blood meal (Antinori *et al.*, 2012). Depending on the ambient temperature, mature sporozoites normally appear in the mosquito's salivary glands between 10-18 days after the mosquito acquired the male and female gametocytes. The mosquito remains infectious for 1-2 months (Lee & Vythilingam, 2013; Tuteja, 2007; Collins & Jeffery, 2007).

1.1.4. Morphology and metabolism of *P. falciparum*

Morphologically, *Plasmodium* species share a variety of traits with other unicellular eukaryotes of the phylum Apicomplexa. Examples of these traits include an apicoplast and an apical complex comprising rhoptries, micronemes and the apical polar rings. The rhoptries and micronemes secrete proteins that are crucial in mobility, adhesion, host cell invasion and the formation of the parasitophorous vacuole. The apical polar rings are one of several microtubule-organizing centers in the parasites (Garcia *et al.*, 2006; Morrissette & Sibley, 2002; Aikawa, 1977; Preisera *et al.*, 2000). The *Plasmodium* parasite is also surrounded by the pellicle, which is a structure formed from the plasma membrane and the closely apposed internal membrane complex. The pellicle is closely associated with a cytoskeletal complex made up of actin, myosin, microtubules and other filament-like elements (Morrissette & Sibley, 2002; Olshina *et al.*, 2015; Cowman *et al.*, 2012). Even though the different developmental stages of *Plasmodium* share morphological traits, substantial structural differences, both in architecture and number of organelles, are clearly evident when the erythrocytic, exoerythrocytic and mosquito stages of the malaria parasite are compared. These differences are an indication of the adaptation of the parasite to the different environments in which the parasite resides and develops. For instance, the food vacuole is very evident in the ring- and trophozoite-stages and inconspicuous in the sporozoite- and merozoite-stages (Dooren *et al.*, 2005; Aikawa, 1977). The components of the apical complex along with the inner pellicular membrane and associated subpellicular microtubules also disappear in the young trophozoites only to reappear later in the schizont-stage (Aikawa, 1977; Dooren *et al.*, 2005).

Of particular interest is the apicoplast, a multi-membrane bound non-photosynthetic plastid organelle which is found in very close association with the mitochondrion in *Plasmodium* species (Sherman, 1979; Dooren *et al.*, 2006; Aikawa, 1971; Lim & McFadden, 2010). This essential organelle is semi-autonomous with its own genome and gene expression machinery comparable to plant chloroplasts. It, however, also imports numerous nuclear-encoded proteins, which are usually tagged with apicoplast-targeting signal sequences (Tuteja, 2007; Sherman, 1979; Bannister *et al.*, 2000; Gardner *et al.*, 2002). The apicoplast is thought to be derived from a red algae that entered into a secondary endosymbiotic partnership with another eukaryotic host cell (Bannister *et al.*, 2000; Lim & McFadden, 2010; Waller & McFadden, 2005). Though the exact cellular role of the apicoplast is still elusive, it is known to play an important role in the synthesis of lipids, heme and isoprenoids (Yeh & DeRisi, 2011). Along with many other parasite biochemical pathways, the plant-like metabolic processes of this organelle are (potential) targets for drug discovery against malaria (Lim & McFadden, 2010; Bannister *et al.*, 2000; Jomaa *et al.*, 1999).

Biochemical studies of the malaria parasite have generally been restricted to the asexual blood stages of the life cycle because of the challenges of obtaining workable quantities of material from the other stages. As mentioned above, the merozoite differentiates into the trophozoite, which lies in the parasitophorous vacuole and begins to ingest host cell cytoplasm through its cystostomes. As it develops, the trophozoite produces and exports different types of proteins into the parasitophorous vacuole and into the cytosol of the erythrocyte. Some of these proteins are incorporated into the host plasma membrane making it more permeable to sugars and other solutes from the external environment (Mohandas & An, 2012; Sherman, 1979; Bannister & Mitchel, 2003; Staines *et al.*, 2006). The intraerythrocytic stages of the parasite possess no glycogen or other polysaccharides and therefore depend on the simple sugars for growth and development (Sherman, 1979). Glucose and sometimes maltose were identified to support parasite growth in cell culture (Sherman, 1979). Early biochemical studies on carbohydrate utilization by the malaria parasite established that, glucose is the preferred source of energy and that parasitized erythrocytes consume up to 75 times more glucose compared to uninfected erythrocytes (Sherman, 1979; Dooren *et al.*, 2006). It is now known that the sustenance of this high glucose demand by parasitized erythrocytes is through an increased permeability of the infected erythrocyte, which is itself a consequence of parasite infection (Sherman, 1979). The transport of glucose from the cytosol of the infected erythrocyte into the cytosol of the parasite is mediated by the parasite hexose transporter (PfHT) (Tjhin *et al.*, 2013). Once inside the cell, mechanisms for the breakdown of glucose in *Plasmodium* species are similar to those used by many other eukaryotic organisms. Among other products, it has also been established that the major end-product of glucose metabolism in the parasite is L-lactate, which is produced by the anaerobic glycolytic pathway (Sherman, 1979; Dooren *et al.*, 2006; Ginsburg, 2016). This pathway involves the initial hydrolysis of glucose to pyruvate and then the anaerobic conversion of pyruvate to lactate (Ginsburg, 2016; Gardner *et al.*, 2002). All genes involved in the glycolytic pathway have been identified in the malaria parasite and it has also been suggested that, the parasite's glycolytic pathway is up to 100 times more active than that of the host erythrocyte (Gardner *et al.*, 2002; Ginsburg, 2016). Intense glycolytic metabolism leads to the spontaneous formation of toxic methylglyoxal from the 3-carbon intermediates of glycolysis. To prevent the accumulation of this toxic intermediate, methylglyoxal is detoxified by the glyoxalase system of the parasite

leading to the production of D-lactate. In most eukaryotes, pyruvate from glycolysis is metabolized aerobically in the mitochondria to store energy in the form of ATP, using tricarboxylic acid (TCA) cycle and a protein gradient that is formed by the electron protein chain. However, only an unconventional TCA cycle occurs in the asexual stages of *Plasmodium* species. Even though all the enzymes of the conventional TCA pathway have been identified in the parasite, the localization of major enzymes in the cell suggests that the pathway found in the parasite may play an alternative role rather than its usual role of full oxidation of products of glycolysis (Ke *et al.*, 2015; Gardner *et al.*, 2002). Pyruvate dehydrogenase and malate dehydrogenase identified in the parasite seem to localize to the apicoplast and cytosol respectively instead of the mitochondrion (Gardner *et al.*, 2002).

Malaria parasites acquire amino acids for protein bio-synthesis by degrading hemoglobin in the parasite food vacuole. The *P. falciparum* food vacuole is a lysosome-like organelle that is formed by fusion of small vesicles that pinched off from the base of the cystostome at the ring-stage of parasite development (Lamarque *et al.*, 2008; Dluzewski *et al.*, 2008). The parasite is able to degrade about 60 – 80% of the hemoglobin contained in the host cytoplasm as it grows. Proteolysis of hemoglobin in the parasite leads to the release of heme and amino acids (Francis *et al.*, 1997; Liu *et al.*, 2006). While the amino acids are incorporated into proteins or probably used in energy metabolism, the heme group is not metabolized further and is polymerized into hemozoin crystals and safely stored within the food vacuole (Liu *et al.*, 2006; Francis *et al.*, 1997; Garcia, 2010). Hemoglobin metabolism is an essential catabolic process in *Plasmodium* parasites and involves two families of proteolytic enzymes called plasmepsins and falcipains in *P. falciparum* (Liu *et al.*, 2006). Most of the amino acid requirements of *Plasmodium* parasites are acquired from hemoglobin catabolism since the parasites have a limited ability to produce amino acids *de novo*. However, hemoglobin is a poor source of methionine, cysteine, glutamine and glutamate and contains no isoleucine at all. Thus, for normal healthy growth, the parasite also depends on exogenous acquisition of amino acids, most especially isoleucine, for growth (Liu *et al.*, 2006; Francis *et al.*, 1997). It has been reported that more amino acids are generated from breakdown of hemoglobin than is needed for protein synthesis, resulting in the diffusion of some hemoglobin-derived amino acids into the host cell. This phenomenon has led to the suggestion that the catabolism of hemoglobin may also play other functions in the cell (Liu *et al.*, 2006; Francis *et al.*, 1997; Mohandas & An, 2012; Tuteja, 2007; Garcia, 2010).

1.2. Control of malaria

1.2.1. Prevention of transmission

Control of malaria can be viewed as an attempt to control the proliferation of the malaria parasite in two moving organisms, man and mosquito. Humans and mosquitoes can host, multiply and distribute the parasite from place to place. Depending on the target of the specific method, malaria transmission can be controlled by employing one or a combination of three strategies: i) preventing the mosquitoes from biting humans through vector control, ii) administration of drugs to suppress infection and prevent disease through chemoprevention or chemoprophylaxis and, iii) the administration of antimalarial vaccines.

For vector control, the insecticide dichlorodiphenyltrichloroethane (DDT) has been a front-liner in the fight against the mosquito vector for decades. DDT was very instrumental in achieving eradication of malaria in the United States of America and was also very important in the fight against the disease in many parts of the globe. For the past decades, however, there have been increasing reports of the emergence of DDT-resistant *Anopheles* mosquitoes in many parts of the world (WHO, 2006). The insecticide has also been implicated as a danger to both humans and environment (Bouwman *et al.*, 2011). As a result, DDT use has been banned in many countries and is now only restrictedly used to fight malaria in regions where mosquitoes are still sensitive (Corin & Weaver, 2005; WHO, 2009). The use (sleeping under) of insecticide-treated mosquito nets (ITNs) is currently one common, easy and inexpensive way to prevent humans from being bitten by mosquitoes in many malaria endemic regions of the world. Among several insecticides used to impregnate mosquito nets, permethrin solution (or other pyrethroids) is now one of the most effective insecticides used in the field today (Garcia, 2010; Hemingway *et al.*, 2016; WHO, 2016b). Indoor residual spraying (IRS) is the third strategy employed to control the insect vector. It involves the application of the effective insecticide on walls and surfaces of indoor human-dwelling places where mosquitoes would normally rest (WHO, 2016b; Hemingway *et al.*, 2016; Shiff, 2002). As effective as ITNs and IRS may be, these methods only target mosquitoes that bite and settle indoors. Outdoor resting mosquito populations are also very significant in the transmission and spread of malaria. Personal protection by wearing protective cloths and application of mosquito repellent creams while outdoor is an effective method of controlling this form of parasite transmission (Gueye *et al.*, 2016). Environmental management that involves drainage of water bodies that breed mosquitoes and improved house design to keep mosquitoes out are also important malaria control methods. In some places, larval source-management strategies have been adopted. The introduction of larvivorous fish or larviciding agents into water bodies to kill mosquito larvae has been a supplementary vector control strategy in many areas (WHO, 2016b; Gueye *et al.*, 2016).

Strategies to suppress malaria infection and prevent disease before or after exposure to the parasite include the example of intermittent preventive treatment of malaria. This strategy is especially effective for vulnerable groups (pregnant women and children under 5 years) living in malaria endemic regions and has helped to reduce malaria cases and severity in these groups (WHO, 2016b). Chemoprevention also involves the monthly administration of malaria treatment to coincide with peaks of transmission. The target group is again children under 5 years and pregnant women, and it has been shown to be an effective in some parts of Africa (Hemingway *et al.*, 2016). A similar approach is chemoprophylaxis which involves the administration of antimalarial drugs every week or everyday to individuals traveling from malaria free zones to endemic areas. Mefloquine, doxycycline, atovaquone-proguanil (Malarone), and to some extent primaquine are principle drugs that are regularly used as chemoprophylaxis for *P. falciparum* malaria (Schwartz, 2012).

The development of an effective vaccine against malaria has been a major research focus for many years. But so far, no vaccine candidate with a high efficacy has yet been produced (Hemingway *et al.*, 2016; Shiff, 2002). RTS,S, a pre-erythrocytic vaccine that should prevent clinical *P. falciparum* malaria in children, is the only vaccine to successfully pass through phase III of clinical trials. The trials, performed on African children, however, protected only 50% and 30% of children between 5-17 months and infants respectively from clinical malaria

(Hemingway *et al.*, 2016; WHO, 2016b). Clearly, a better vaccine or a combination of vaccines (which ideally should produce a much higher efficacy, protect against disease and prevent transmission of several *Plasmodium* species) is vital to control malaria.

1.2.2. Diagnosis of malaria

Malaria is diagnosed using a combination of results from physical examinations, patient records and laboratory diagnostic tests (Amir *et al.*, 2018). Detection of parasites in Giemsa-stained thin and thick peripheral blood smears using light microscopy has been the gold standard for laboratory diagnosis of human malaria for many years (Garcia, 2010; Lee & Vythilingam, 2013). Performing blood smears is simple, rapid and cheap. For a thick blood smear, a drop of blood is dried, fixed in methanol and stained on a glass-slide for microscopic examination. Thin blood smears involve spreading the drop evenly on the slide before staining. Blood samples for blood smears are preferably taken when the patient's temperature is rising using a syringe and needle or a finger prick. Stained smears are examined under the oil immersion 100x objective (Amir *et al.*, 2018). Thick blood smears are about 10 times more sensitive than thin blood smears (Warhurst & Williams, 1996). For quicker malaria diagnosis, the rapid diagnostic kits (RDTs) are an excellent choice for testing persons already showing signs of malaria and therefore may have high levels of blood parasitemia. The development of molecular tools such as polymerase chain reaction (PCR) has revolutionized malaria diagnosis and is now routinely used to confirm diagnoses. Traditional PCR detects many more cases of malaria than do thick blood films, especially in situations when samples are of low parasitemia (Garcia, 2010; Tavares *et al.*, 2011; Amir *et al.*, 2018). PCR diagnosis is also very valuable in the determination of specific *Plasmodium* species causing infection especially in cases of mixed infections (Garcia, 2010; Lee & Vythilingam, 2013). Nested PCR and real-time PCR are improvements on traditional PCR methods and are more superior in both specificity and sensitivity compared to traditional PCR-based malaria diagnostic methods (Lee & Vythilingam, 2013; Amir *et al.*, 2018).

1.2.3. Drug treatment of malaria

Malaria is generally curable if the appropriate treatment is given adequately and promptly, but most antimalarials are effective only against blood-stage parasites (Derbyshire *et al.*, 2011; Winstanley, 2000; Cui *et al.*, 2015). Quinine and its dextroisomer quinidine have been for a long time the first widely used antimalarial drug especially for the treatment of severe malaria (Petersen *et al.*, 2011; Dronamraju & Arese, 2006; Sinha *et al.*, 2014; Bloland, 2001). These drugs are extracted from the bark of the Andean *Cinchona* tree originally found in South America (Petersen *et al.*, 2011; Tuteja, 2007; Dronamraju & Arese, 2006; Sinha *et al.*, 2014). Chloroquine is the first synthetic quinoline-based drug that was found to be very effective in the treatment of malaria. Following its first syntheses in 1934, chloroquine became one of the most commonly used and most affordable therapeutic drug against malaria for many decades (Petersen *et al.*, 2011; Dronamraju & Arese, 2006). The drug acts by capping developing hemozoin crystals, preventing further biocrystallization of heme. It can also bind

heme forming a cytotoxic complex. This complex, together with toxic heme metabolites, eventually causes autodigestion of the parasite (Petersen *et al.*, 2011; Hempelmann, 2007). Unfortunately, extensive drug use has over time led to the development and spread of resistance to quinine and chloroquine in *P. falciparum* and *P. vivax*, limiting the use of the drugs in many parts of the world (Tuteja, 2007; Winstanley, 2000; Sinha *et al.*, 2014). Chloroquine is, however, still one of the few drugs used for the treatment of *P. vivax* malaria in some parts of Asia (Cui *et al.*, 2015; Petersen *et al.*, 2011). Other synthetic quinoline-based drugs that have been very effective in the treatment of malaria include amodiaquine, mefloquine and primaquine. These drugs all act as inhibitors of heme biocrystallization (Hempelmann, 2007; Petersen *et al.*, 2011). Primaquine is one of the very few drugs that are also potent against liver-stage infection and is principally used to prevent disease relapse in *P. ovale* and *P. vivax* infections (Cui *et al.*, 2015).

Another group of drugs that are effective in the treatment of malaria include the antifolate drugs (Dronamraju & Arese, 2006). Pyrimethamine, proguanil, proguanil and sulfa drugs such as sulfadoxine and dapsona belong to this class of drugs. Antifolate drugs are generally dihydrofolate reductase (DHFR) or dihydropteroate synthase (DHPS) inhibitors that affect DNA and RNA synthesis during cell replication (Petersen *et al.*, 2011; Dronamraju & Arese, 2006; Garcia, 2010; Bloland, 2001). These drugs are usually administered in combinations to increase the synergistic effect on the parasite and also overcome the problem of drug resistances (Dronamraju & Arese, 2006). For instance, Fansidar is a combination drug of pyrimethamine and sulfadoxine.

Lumefantrine, an aryl alcohol, and atovaquone, a hydroxynaphthoquinone, are also effectively used in Africa for the treatment of chloroquine-resistant malaria. Atovaquone acts through the inhibition of the electron transport chain at the cytochrome *bcl* complex that indirectly affects pyrimidine bio-synthesis and replication (Painter *et al.*, 2007; Petersen *et al.*, 2011). To reduce the development of parasite resistance, atovaquone is now administered in combination with proguanil in an antimalarial called Malarone (Bloland, 2001; Garcia, 2010). Artemisinin and its analogues are currently compounds used as the first-line of defense against acute uncomplicated malaria around the world (Petersen *et al.*, 2011; Dronamraju & Arese, 2006; Cui *et al.*, 2015). These compounds that also include artesunate and artemether are extremely effective and rapid acting antimalarial drugs. They are also nontoxic and appear to be safe for treating all classes of patients (Dronamraju & Arese, 2006). Artemisinin is obtained from the Chinese herb *Artemisia annua*, which has been used for centuries for the treatment of parasitic diseases (Petersen *et al.*, 2011; Dronamraju & Arese, 2006). The target of artemisinin is still not confirmed. This drug or its derivatives are commonly used in combination with several slow acting antimalarial drugs such as Fansidar, lumefantrine or mefloquine for the treatment of malaria in many parts of the world (Petersen *et al.*, 2011; Tuteja, 2007; Derbyshire *et al.*, 2011). ACTs are also first line drugs for the treatment of *P. vivax* malaria and for the treatment of chloroquine-resistant, chloroquine-sensitive or multidrug-resistant *P. falciparum* malaria (Dronamraju & Arese, 2006). Tetracycline and its derivative doxycycline are a group of antibiotics that have proven to be very potent against *Plasmodium* species. These compounds can act as apicoplast protein synthesis inhibitors and are therefore potent as malaria chemoprophylaxis. They are also effective in combination with quinine for the treatment of severe malaria (Garcia, 2010; Bloland, 2001; Cui *et al.*, 2015). In

the Sahel subregion of Africa, Fansidar and its combination with amodiaquine are advocated for use as an intermittent preventive therapy against malaria (Cui *et al.*, 2015).

1.2.4. Emergence and implications of drug resistance

Drug-resistant strains of *Plasmodium* species have over the last decades become prevalent for almost all of the few potent antimalarial drugs currently used (Petersen *et al.*, 2011; Cui *et al.*, 2015; Winstanley, 2000). Among the five human *Plasmodium* species, antimalarial drug resistance has been registered mainly in *P. falciparum*, *P. vivax* and *P. malariae* (Dronamraju & Arese, 2006; Sinha *et al.*, 2014). *P. falciparum* has developed resistance to almost all effective malaria drugs currently in use, even though the geographical distribution of resistance to each drug varies (Bloland, 2001). Quinine-resistant parasites have been reported for many years now in parts of East/South-East Asia and some few parts of South America (Dronamraju & Arese, 2006). Resistance to chloroquine, Fansidar, mefloquine and amodiaquine has also been reported in *P. falciparum* across the world. Chloroquine resistance is the most wide-spread, occurring in almost all regions where *P. falciparum* malaria is transmitted except in very few locations of Central America, the Middle East and Central Asia (Dronamraju & Arese, 2006; Bloland, 2001). An increased dependence on Fansidar as a result of the spread of chloroquine resistance also led to the development of resistance to this drug in South-East Asia, South America and most recently in Africa (Dronamraju & Arese, 2006; Bloland, 2001). Mefloquine resistance is also frequently reported in South-East Asia, some parts of Africa and the Amazon region of South America (Bloland, 2001; Sinha *et al.*, 2014). Resistance to amodiaquine, a drug also used (in combination with artesunate) to treat chloroquine-resistant malaria, has also been reported in Tanzania in Africa (Dronamraju & Arese, 2006; Sinha *et al.*, 2014). Cases of resistance of *P. falciparum* to malarone have been reported in some parts of Africa (Dronamraju & Arese, 2006). Upon an official recommendation by the World Health Organization in 2001, artemisinin-based combination therapies (ACTs) are now the first-line treatment especially for *P. falciparum* malaria, and this has generally led to a substantial decline in global cases of malaria (Sinha *et al.*, 2014). However, parasites showing first signs of resistance to artemisinin and its analogues have recently been detected in several parts of Cambodia, Thailand, Myanmar and Vietnam, all in South-East Asia (Petersen *et al.*, 2011; Cui *et al.*, 2015; Sinha *et al.*, 2014).

The mechanisms of parasite resistance are manifold and generally appear to develop through spontaneously occurrence and selection for mutations that lead to reduced sensitivity of the given antimalarial drug or a group of drugs (Dronamraju & Arese, 2006; Bloland, 2001). Resistant mutations may be single or multiple and can occur in a single gene or multiple genes (Dronamraju & Arese, 2006; Bloland, 2001). The mutation may introduce a polymorphism in genes leading to the reduction in drug import or in drug metabolism. Mutation may also alter the structure of a drug-associated enzyme causing drug binding defects (Dronamraju & Arese, 2006). *P. falciparum* resistance to chloroquine is reported to be mediated by a single nucleotide polymorphism (SNP) in the chloroquine resistance transporter gene (*Pfcr*) that causes the increased efflux of the drug out of the food vacuole (Petersen *et al.*, 2011; Bloland, 2001; Cui *et al.*, 2015). SNPs in the autologue of the *P. falciparum* multidrug resistance protein-1 (*Pfmdr1*) gene are also linked to reduced sensitivity of *P. vivax* to chloroquine and quinine (Cui *et al.*, 2015). *P. falciparum* and *P. vivax* resistance

to antifolate antimalarials have also been attributed to single and multiple mutations in the genes coding for DHFR and DHPS (Petersen *et al.*, 2011; Dronamraju & Arese, 2006; Bloland, 2001; Cui *et al.*, 2015). Recent cases of resistance to artemisinin have been attributed to mutations in the propeller domain of the *P. falciparum* kelch (K13) gene located on chromosome 13 (Cui *et al.*, 2015) and resistance to atovaquone has been linked to single-point mutations in the cytochrome *b* (*Pf**cytb*) gene (Petersen *et al.*, 2011; Bloland, 2001; Cui *et al.*, 2015).

Antimalarial drug resistance poses a serious threat to the global fight to control and eliminate malaria. The successes made so far in the fight against the disease are in fear of being reversed by continuous reports of drug resistance especially to ACTs. As the world continues to wait for the arrival of an effective malaria vaccine, the need for the development of novel potent medications and the appropriate use of current antimalarial drugs to prevent the development of parasite resistance remains the cornerstone to the fight against the disease.

1.3. Molecular biology and genetic manipulation of *P. falciparum*

1.3.1. Historical and general aspects

The sequencing and publication of the full *P. falciparum* genome in 2002 provided a good stimulus for increased research into understanding the cellular and molecular mechanisms of the malaria parasite. Over 5500 genes that control most aspects of the functioning of the parasite have been identified (Gardner *et al.*, 2002; Conway, 2015). These genes are encoded by an approximately 23 Mb haploid genome on 14 different chromosomes, 81% of which is A-T in composition (Conway, 2015; Tuteja, 2007; Gardner *et al.*, 2002). The parasite also contains a 35 kb circular apicoplast genome encoding about 57 genes and a 6 kb mitochondrial genome (Gardner *et al.*, 2002; Tuteja, 2007; Wilson & Williamson, 1997).

An improved understanding of the complex biology of the malaria parasite is necessary to facilitate the identification and characterization of new drug targets, strategies for vaccine development and the molecular basis of resistance to current drugs. Molecular manipulation of the parasite offers a major window to understanding parasite gene functions and usually involves genetic alteration of the parasite genome using gene knockout or editing strategies (Koning-Ward *et al.*, 2015; Cowman & Crabb, 2005). The establishment of cell culture systems for some of the *Plasmodium* species including the asexual blood stages of *P. falciparum* (Trager & Jensen, 1976) has made genetic manipulation of the parasite genome more feasible and achievable. Customized vectors carrying foreign genetic material are more easily introduced into cultured parasites through the process of transfection, and can possibly lead to modification of the parasite genome. A major hindrance to genetic manipulation of *Plasmodium* species, however, is the inefficiency of the transfection process. This is particularly a problem in *Plasmodium* species because the parasites are intracellular for most of their life cycle and the introduced plasmid must cross multiple membrane barriers of the host-parasite unit before a successful transfection is achieved (Cowman & Crabb, 2005; Goonewardene *et al.*, 1993). Electroporation greatly improves the transfection efficiency of *Plasmodium* parasites compared to the few other methods available for getting plasmids into the parasite nucleus (Lee *et al.*, 2014; Waterkeyna *et al.*, 1999). Infected erythrocytes

synchronized at ring- or schizont-stages of development are usually electroporated in *P. falciparum* transfection (Koning-Ward *et al.*, 2015; Lee *et al.*, 2014). However, transfection efficiency is much more improved when uninfected erythrocytes are first electroporated (preloaded) with the transfection DNA before infection, usually by mixing with infected erythrocytes that are synchronized at the schizont-stage (Cowman & Crabb, 2005; Deitsch *et al.*, 2001).

Transfection vectors (plasmids) are usually generated through a series of cloning steps and routinely contain reporter or selectable marker genes to allow selection for transgenic parasites once a successful transfection is achieved. For studies that involve gene knockout or editing, the vectors also contain DNA sequences (homology regions) complementary to portions of the target gene on the parasite genome to allow for one or both forms of homologous recombination: single cross-over recombination and double crossover recombination (Cowman & Crabb, 2005). Single cross-over recombination results in plasmid DNA insertion into the native genome whereas double crossover recombination events result in the replacement of DNA sequences in the native genome by a template sequence from a donor DNA.

The first report of genetic manipulation of *Plasmodium* parasites was in 1993 by Goodwardene *et al.* They described the successful transfection of gametes and zygotes of the avian malaria parasite *P. gallinaceum* with a transient vector and the expression of the firefly luciferase gene in transgenic parasites (Koning-Ward *et al.*, 2015; Goonewardene *et al.*, 1993). Shortly after, transient and stable transfections were also achieved for the blood-stage forms of *P. falciparum* and *P. berghei* by several different groups (Koning-Ward *et al.*, 2015; Cowman & Crabb, 2005; Carvalho & Ménard, 2005). Following these earlier reports, there has been a speedy progression of the development of other technologies including efficient gene knockout and genome editing approaches for *P. falciparum*, *P. berghei* and other *Plasmodium* species (Koning-Ward *et al.*, 2015). Transient transfection has been a molecular tool for studying gene expression of *Plasmodium* species. Traditionally, this tool has been used to characterize DNA elements essential for gene expression in many eukaryotic cells (Cowman & Crabb, 2005; Morrissette & Sibley, 2002). Episomal plasmids used in transient transfection normally contain a reporter gene flanked by the DNA segments under study. Commonly used reporter genes include chloramphenicol acetyltransferase, firefly luciferase and green fluorescent protein (GFP) (Corin & Weaver, 2005). Stable transfection on the other hand is used for functional analysis of parasite genes as occurs in knockout or gene editing studies. It is also used for the expression of fluorescent chimeric transgenes allowing for direct visualization of protein trafficking to subcellular and extracellular locations in the host-parasite unit (Cowman & Crabb, 2005; Hempelmann, 2007; Ghorbal *et al.*, 2014). Plasmid vectors used in stable transfections (or parts of them) ultimately get integrated into the parasite genome through one of the two forms of homologous recombination (Cowman & Crabb, 2005). The plasmids are also designed to carry positive and or negative drug-selectable marker(s). Positive selection helps to select for parasites that pick up the episomal plasmid after transfection (and single cross over events) whereas negative selection selects for parasites that have lost a vector, for example because of a double crossover event after transfection. To facilitate a clean double crossover event in gene knockout or editing studies, transfection plasmids are designed so that the positive drug-selectable marker is flanked by two homology regions. Examples of commonly used positive drug-selectable markers in *P.*

falciparum and *P. berghei* are the mutated form of *Toxoplasma gondii* dihydrofolate reductase-thymidylate synthase (*dhfr-ts*) and human DHFR which confer resistance to pyrimethamine and WR99210, respectively (Cowman & Crabb, 2005; Bousema & Drakeley, 2011; Crabb *et al.*, 2004).

An important prerequisite for genome editing strategies is the requirement of a double strand break (DSB) (Lee *et al.*, 2014). In *Plasmodium* species, DSBs in DNA are naturally repaired by the precise homologous recombination because the parasite does not encode the more common alternative error-prone nonhomologous end-joining (NHEJ) pathway. An atypical *Plasmodium* specific NHEJ pathway is, however, identified and reported in *Plasmodium* parasites for the repair of DSBs (Singer *et al.*, 2015; Singer & Frischknecht, 2017; Koning-Ward *et al.*, 2015; Lee *et al.*, 2014; Reinke & Troemel, 2015; Crawford *et al.*, 2017). The inclusion of homology regions on the episomal plasmid therefore facilitates repair of targeted DSBs on the parasite genome.

Traditional stable transfections in *P. falciparum* take several months of cell culture for gene knockout or editing to occur through a random homologous recombination event (Lee & Fidock, 2014; Duraisingh *et al.*, 2002). The culture process usually involves several weeks of positive selection to maintain the plasmid in the parasite, and then several months of drug on- and off-selection regimes to allow for the integration of the plasmid into the parasite genome and selection of integrants (Koning-Ward *et al.*, 2015; Cowman & Crabb, 2005; Duraisingh *et al.*, 2002; Maier *et al.*, 2006). Unintegrated plasmids are rapidly lost in the absence of the drug but integrated plasmids persist (Koning-Ward *et al.*, 2015; Cowman & Crabb, 2005; Maier *et al.*, 2006). This chance-dependent strategy, though used successfully to manipulate some genes, was generally inefficient and time-consuming among other disadvantages (Cowman & Crabb, 2005; Duraisingh *et al.*, 2002; Maier *et al.*, 2006). The introduction of negative selection which selected for rare double-crossover homologous recombination events improved the process of genome editing a bit in *P. falciparum* (Cowman & Crabb, 2005). Negative selection helped remove circular episomal plasmids and the backbone of integrated plasmids. This decreases the time to obtain transgenic parasites during genome editing (Koning-Ward *et al.*, 2015; Lee *et al.*, 2014; Maier *et al.*, 2006). Nevertheless, double crossover events, similar to single crossovers, depend on the rare stochastic strand breaks in genomic DNA and are therefore also time consuming and inefficient (Lee *et al.*, 2014). Recently, more sophisticated stable transfection-based genome-editing tools have been developed for eukaryotic cells. These include zinc-finger nuclease (ZFNs)-mediated genome-editing, transcription activator-like type II effector nucleases (TALENs) and the clustered regularly interspaced short palindromic repeats (CRISPR) – CRISPR-associated protein 9 (Cas9) (CRISPR-Cas9) systems (Singer *et al.*, 2015; Lee *et al.*, 2014). Specialized endonucleases incorporated in these systems are directed to cause the needed DSBs at specific target loci in the target genome. These enzymes include endonuclease FokI in ZFN-mediated genome-editing and TALENs systems, and Cas9 endonuclease of the CRISPR-Cas9 system. DSBs are then repaired by homologous recombination using the homologous regions (HR) which reside on the plasmid or linear DNA (Koning-Ward *et al.*, 2015; Lee *et al.*, 2014; Lee & Fidock, 2014; Crawford *et al.*, 2017). The principle behind these strategies involves exploiting and directing the non-specific endonucleases to target sequences in the genome via association with protein or RNA (Lee *et al.*, 2014). To date, only ZFNs and the CRISPR-Cas9 system have been successfully used to achieve genome-editing in *P. falciparum* (Koning-

Ward *et al.*, 2015; Lee *et al.*, 2014). Though both systems have been shown to generate transgenic parasites within a few weeks of transfection, the CRISPR-Cas9 system has recently been shown to be more workable with *P. falciparum* (Lee *et al.*, 2014; Koning-Ward *et al.*, 2015; Lee & Fidock, 2014).

1.3.2. The CRISPR-Cas9 genome-editing strategy

The CRISPR-Cas9 genome-editing strategy is based on the CRISPR-Cas system present in many bacteria and most archaea. In these organisms, the system plays the main role of providing adaptive immunity and confers protection against exogenous viruses and plasmids (Barrangou & Marraffini, 2014). CRISPR-mediated immunity is acquired when bacteria pick up DNA fragments from invading viruses and plasmids and orderly integrate the fragments into the genomic CRISPR loci (Barrangou & Marraffini, 2014; Westra *et al.*, 2014). Upon subsequent reinfection, relevant complementary DNA portions (CRISPR spacers) of the CRISPR loci are transcribed and processed into small interfering crRNAs that guide endonucleases by complementary base-pairing to cleave and destroy the invading elements (Barrangou & Marraffini, 2014; Westra *et al.*, 2014). The CRISPR loci thus contain short partially palindromic DNA repeats that occur at regular intervals (CRISPR repeats) and alternate with the variable CRISPR spacers. Each locus is immediately flanked by a short 'leader' DNA sequence and accompanying CRISPR associated (*cas*) genes (Barrangou & Marraffini, 2014; Westra *et al.*, 2014). The DNA sequence of the invading element that is complementary to the unique CRISPR spacer sequence is called the protospacer. One to four nucleotides away, the protospacer is flanked by a system-specific highly conserved 2-5 nucleotide CRISPR motif called protospacer adjacent motif (PAM) (Barrangou & Marraffini, 2014). The PAM sequence of *Streptococcus pyogenes* protospacer is NGG where N can be any of the four nucleotides of the genetic code (Lee & Fidock, 2014; Zhang *et al.*, 2014). PAM sequences can occur at the 3' or 5' end of the protospacer depending on the type of system (Barrangou & Marraffini, 2014) and have been implicated in both sampling for which exogenous DNA fragment is taking up as a spacer unit, and in directing for targeted strand cleavage (Barrangou & Marraffini, 2014; Barrangou, 2015b).

CRISPR-Cas systems are diverse and are classified into three major types: type I, type II and type III mainly by the nature of the *cas* genes they encode (Barrangou & Marraffini, 2014; Barrangou, 2015b, 2015a). Among the three, the type II system (Fig 1.5) requires the least complex *cas* machinery for immunity and typically encodes the Cas9 gene (Barrangou & Marraffini, 2014; Barrangou, 2015a). In the biogenesis of the interfering crRNAs, the type II system employs a *trans*-encoded CRISPR RNA (*tracrRNA*) which is a small RNA that shares partial complementarity with the CRISPR repeats and whose gene is also located in the CRISPR locus (Barrangou & Marraffini, 2014). Pairing between *tracrRNA* and processed crRNA (transcribed from relevant spacer) leads to recruitment of the Cas9 protein (Barrangou & Marraffini, 2014; Westra *et al.*, 2014; Barrangou, 2015a; Zhang *et al.*, 2014). The spacer sequence of the mature crRNA (CRISPR guide RNA) is also called the guide sequence and usually consists of the first 20 nucleotides at the 5' end. The guide sequence determines the specificity of the system by being homologous to the target (Lee & Fidock, 2014).

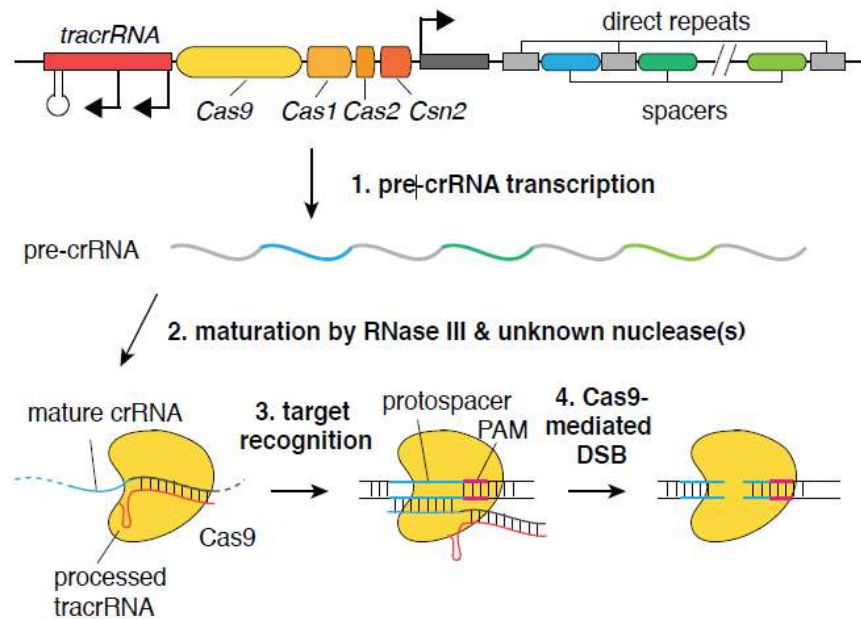


Figure 1.5. Scheme of type II CRISPR-mediated DNA double-strand breaks. A typical type II CRISPR system occurs in *Streptococcus pyogenes*. The type II CRISPR locus contains genes common to other CRISPR types such as *Cas1* and *Cas2* as well as unique genes like the *Cas9* gene. It also contains the two non-coding elements *tracrRNA* and the CRISPR repeats which alternate with variable CRISPR spacers. Each spacer is complementary to the protospacer on the foreign genetic material from which it (spacer) was acquired. The spacers together with the associated PAM direct the Cas9 protein to cleave the foreign genetic material upon subsequent encounter. In the Type II CRISPR system, the process of achieving a targeted double-strand break (DSB) is initiated by the transcription of the pre-crRNA array and *tracrRNA*. The pre-crRNA is transcribed from one of the CRISPR spacer sequences. The transcribed *tracrRNA* hybridizes with processed pre-crRNA (mature crRNA) and Cas9 protein. The mature crRNA also contains the guide sequence which gives specificity to Cas9 endonuclease to incise the target DNA within the protospacer sequence of the target DNA sequence. An upstream PAM is required for the incision to occur. Taken and modified from (Cong *et al.*, 2013).

To initiate the cleavage step, the mature CRISPR guide RNA complexes with the *tracrRNA* and drives conformational changes in the single large multi-domain Cas9 protein leading to the incision of DNA in a gene sequence that must also contain an upstream PAM sequence. The Cas9 protein contains two independent nuclease domains, HNH and RuvC, each of which cleaves one strand of the DNA helix generating blunt ends (Barrangou & Marraffini, 2014; Barrangou, 2015a; Zhang *et al.*, 2014).

The engineered CRISPR-Cas9 genome editing strategy of *P. falciparum* is based on the type II CRISPR-Cas system of *Streptococcus pyogenes* (Barrangou & Marraffini, 2014; Barrangou, 2015a). In principle, the requirements for targeted DNA cleavage by Cas9 in the type II CRISPR-Cas system (*tracrRNA* and crRNA) are engineered into a chimeric RNA guide, also called single-guide RNA (sgRNA) (Koning-Ward *et al.*, 2015). A guide sequence of 20 nucleotides can then be designed for each target using special molecular tools to generate a workable system. The first report of a CRISPR-Cas9 strategy for *P. falciparum* was by Ghorbal and colleagues in 2014 (Ghorbal *et al.*, 2014). The group demonstrated in their ground-breaking study the versatility of the CRISPR-Cas9 approach for genetic manipulation of the parasite. In a record time of 3 weeks post-transfection, they were able to generate transgenic parasites with a gene disruption or single-nucleotide edited gene (Ghorbal

et al., 2014; Lee & Fidock, 2014). Ghorbal *et al.* used two plasmids (Fig 1.6) to express the Cas9 protein, transcribe the single-guide RNA (sgRNA) and to deliver the HR for homologous recombination (Ghorbal *et al.*, 2014). The first was the pUF1-Cas9 episome that expressed the human codon-optimized *S. pyogenes* endonuclease Cas9 under the control of plasmodial regulatory elements. The Cas9 gene sequence used was engineered with nuclear localization signals and carried the yeast dihydroorotate dehydrogenase (*ydhodh*) for positive selection with DSM1, a *P. falciparum* dihydroorotate dehydrogenase inhibitor. The second is the pL7 episome for transcription of the sgRNA under the control of *P. falciparum* U6 small nuclear (sn) RNA regulatory elements dependent on RNA polymerase III. For positive selection, the pL7 episome carried the human dihydrofolate reductase (*hdhfr*) that confers resistance to WR99210. Flanking the drug-selectable marker were the homology regions of the target gene. The pL7 episome also carried the suicide fusion gene, yeast cytosine deaminase and uridyl phosphoribosyl transferase (*yfcu*), allowing for negative selection with 5-fluorocytosine. Both plasmids were co-transfected and the Cas9 protein only transiently expressed (Ghorbal *et al.*, 2014; Lee & Fidock, 2014; Lu *et al.*, 2016). Even though the high A-T composition of the *Plasmodium* genome presents a peculiar possibility of off-target activity, Ghorbal and colleagues convincingly showed that the approach is highly efficient and can be used to target potentially every *P. falciparum* locus (with a nearby PAM sequence) for modification.

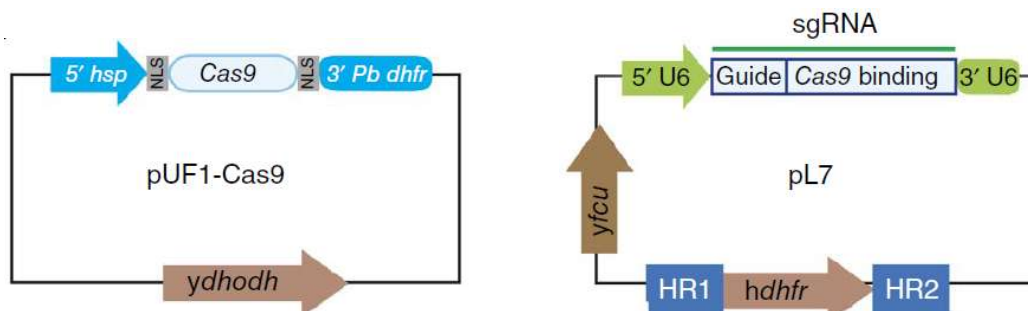


Figure 1.6. Two plasmids for targeted *P. falciparum* genome editing using sgRNA:Cas9. The pUF1-Cas9 expresses the Cas9 endonuclease using plasmodial regulatory elements. The Cas9 protein also bears nuclear localization signals (NLS). The pL7 episome contains the sgRNA-expression cassette and 5' and 3' homologous regions (donor DNA). sgRNA is expressed from the *P. falciparum* U6 snRNA polymerase III promoter (5' U6). The homologous region 1 (HR1) and homology region 2 (HR2) of the gene of interest (GOI) must surround a drug-selectable marker (*hdhfr*) to select for gene disruption. 5' *hsp*, heat shock protein 86 promoter region; 3' *Pb dhfr*, 3' region of *P. berghei dhfr*; *ydhodh*, yeast dihydroorotate dehydrogenase gene. Taken and modified from (Ghorbal *et al.*, 2014).

1.4. The glyoxalase system

1.4.1. History and general aspects

1.4.1.1. History

In 1913, Neuberg working alone and Dakin and Dudley independently discovered an enzymatic activity that converted the 2-oxoaldehyde methylglyoxal into the

hydroxycarboxylic acid lactic acid in a variety of tissues and cell extracts (Silva *et al.*, 2013; Dakin & Dudley, 1913; Racker, 1951; Inoue *et al.*, 2011; Urscher *et al.*, 2011; Deponte, 2013). This discovery laid the foundation for the elucidation of the glyoxalase system and the identification of its components. The key enzyme then, ketonaldehydemutase (now glyoxalase 1) together with methylglyoxal became the focus of the then poorly understood biochemical pathway of glycolysis (Deponte, 2013; Racker, 1951). The accepted model of glycolysis at this time was the split of glucose into two three-carbon sugars that were converted to methylglyoxal and then to lactic acid through the action of glyoxalase 1 (Deponte, 2013). In 1950, building on a previous work by Hopkins and Morgen, Crook and Law reported the presence of a second enzyme (glyoxalase 2) involved in methylglyoxal metabolism.

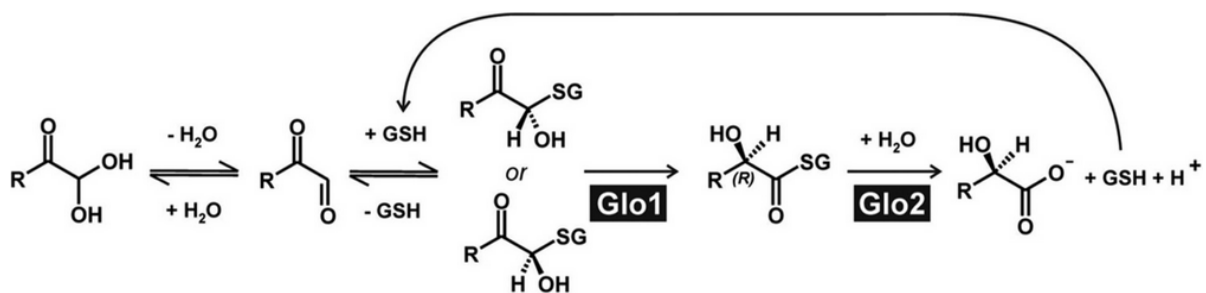


Figure 1.7. The glyoxalase detoxification system. Glo1 isomerizes the spontaneously formed hemithioacetal between toxic dehydrated 2-oxoaldehydes and reduced glutathione (GSH) to the 2-hydroxy thioester. This product is then hydrolyzed by Glo2 to the corresponding less-harmful 2-hydroxycarboxylic acid and GSH. Taken from (Deponte, 2014).

Eventually, a definition of the specific biochemical functions of glyoxalase (Glo1) and glyoxalase 2 (Glo2) were described by Racker who, after combining this new finding with earlier reports of the role of glutathione in methylglyoxal metabolism, attempted to spell out the pathway of present-day glyoxalase system (Racker, 1951; Urscher *et al.*, 2011; Thornalley, 1993; Deponte, 2013). Racker did not only demonstrate the basis of the first enzymatic assay of glutathione but later also showed that the lactic acid produced from methylglyoxal metabolism was actually D-lactate (Deponte, 2013; Racker, 1951), a finding that dismissed the physiological role of methylglyoxal and the glyoxalase enzymes in the mainstream glycolytic pathway. Having been made orphan by this finding, it took almost another two decades for the physiological relevance of the glyoxalase system as a detoxification pathway for toxic dicarbonyls to be proposed by Mannervik in 1974 (Deponte, 2013). The glyoxalase system is now accepted as a ubiquitous glutathione-dependent (trypanothione-dependent in rare cases) pathway that performs the main task of detoxifying harmful 2-oxoaldehydes to non-toxic 2-hydroxycarboxylic acids (Inoue *et al.*, 2011; Cameron *et al.*, 1997; Ariza *et al.*, 2006; Urscher *et al.*, 2012; Deponte, 2014, 2013). Renewed interest in the glyoxalases and the glyoxalase system has recently helped to identify other potential roles of the pathway, which include the regulation of cellular growth and spermatogenesis (Glo2), signal transduction and assembly of microtubules (Urscher *et al.*, 2011; Thornalley, 1993; Cameron *et al.*, 1997; Urscher *et al.*, 2012; Deponte, 2013). The glyoxalases are also thought to function in the regulation of osteoclastogenesis in mouse macrophages (Kawatani *et al.*, 2008) and the intermediate of the glyoxalase system, S-D-lactylolglutathione (SLG), is

thought to regulate the efflux of potassium in *Escherichia coli* (*E. coli*) (Ferguson *et al.*, 1993; Ozyamak *et al.*, 2010). The generalized glyoxalase system comprises the isomerase Glo1, the thioesterase Glo2, and a catalytic amount of the reduced tripeptide glutathione (GSH) as co-factor (Fig 1.7) (Urscher *et al.*, 2012; Deponte, 2014; Thornalley, 1998). Glo1 catalyzes the virtually irreversible isomerization of the nonenzymatically formed hemithioacetal of GSH and a 2-oxoaldehyde to a 2-hydroxythioester. The latter is then hydrolyzed by glyoxalase 2 (Glo2), with the release of GSH and the corresponding 2-hydroxycarboxylic acid (Deponte, 2013; Thornalley, 1998; Silva *et al.*, 2013; Urscher *et al.*, 2011).

1.4.1.2. Glo1

Glo1 (also known as GloI or Glx1) has been characterized as a metalloenzyme in many organisms, from mammals to plants, yeast, bacteria and protozoan parasites (Deponte, 2013). The enzyme belongs to the vicinal oxygen chelate (VOC) metalloenzyme superfamily whose members contain a $\beta\alpha\beta\beta$ -motif required for metal ion coordination (Deponte, 2013; Urscher *et al.*, 2011). Studies in organisms expressing this enzyme show that it is localized mostly to the cytosol (Marasinghe *et al.*, 2005; Urscher *et al.*, 2010; Deponte, 2013). Structurally, most eukaryotic Glo1 enzymes and the Glo1 of some prokaryotes such as *E. coli* are homodimers with two subunits, each of which contain a pair of the $\beta\alpha\beta\beta$ -motif thought to have originated from a gene duplication event (Iozef *et al.*, 2003; Deponte, 2013; Thornalley, 2003). Each subunit contains two halves of two structurally identical active sites, each of which contains a zinc or nickel metal center necessary for catalysis, and a glutathione-binding pocket located at its interface (Inoue *et al.*, 2011; Thornalley, 1993; Frickel *et al.*, 2001; Deponte, 2013). Two essential glutamate residues at the active site as well as two other residues, which can be glutamine or histidine depending on the organism, exert the acid-base catalyzed isomerization of the diastereomeric hemithioacetals to the single corresponding thioester (Deponte, 2013). Eukaryotic Glo1 enzymes commonly contain zinc whereas nickel is the co-factor in many prokaryotes, even though this is not a strict pattern (Deponte, 2013; Frickel *et al.*, 2001). The glutathione-binding pocket is predominantly composed of basic/polar residues via the γ -glutamyl and glycine moiety (Deponte, 2013). The functional dimeric Glo1 enzyme thus consist of four $\beta\alpha\beta\beta$ -motif contained in two subunits with the N-terminal domain of one subunit interacting with the C-terminal domain of the other (Deponte, 2013). In contrast, Glo1 enzymes of some other prokaryotes, *P. falciparum* and *S. cerevisiae* are monomers with two different structural and functional active sites (Inoue *et al.*, 2011; Deponte, 2014, 2013). The monomeric enzyme is similar in overall structural architecture to the homodimer isoform and is thought to have arisen from a second gene duplication event which occurred sometime in the evolutionary process (Deponte, 2013; Iozef *et al.*, 2003). The catalytic mechanism generally accepted for Glo1 reaction involves base-catalyzed shielded-deprotonation from C-1 of the hemithioacetal that is bound to the active site to form an ene-diolate intermediate that is converted to the thioester product. The role of glutathione is to provide specific binding to the active site and to activate the C-1 residue of the 2-oxoaldehyde by the formation of the hemithioacetal. The role of the enzyme is to control and define substrate specificity, the stereoselectivity of the reaction and to provide the base for base catalysis (Thornalley, 1993). Even though Glo1 is often considered ubiquitous, the gene encoding Glo1 is absent in some

organisms including the protozoans *Entamoeba histolytica*, *Giardia lamblia* and *Trypanosoma brucei* (Silva *et al.*, 2013). In other trypanosomatids that express the enzyme, trypanothione-derived hemithioacetal is the preferred substrate for Glo1 instead of a glutathione-derived substrate (Deponte, 2013; Ariza *et al.*, 2006).

1.4.1.3 Glo2

Glo2 (also known as GloII or GlxII) is a monomeric metalloenzyme and has been characterized in a number of organisms including humans, plants, yeast, bacteria and protozoan parasites (Deponte, 2013; Marasinghe *et al.*, 2005). Similar to Glo1, this enzyme is ubiquitous even though some mammals and bacteria are reported to lack the encoding gene (Deponte, 2013). Glo2 enzymes are composed of an N-terminal β -lactamase domain, which contains a single active site and a C-terminal domain with five α -helices. The active site of the enzyme consists of a binuclear metal center and a substrate-binding site which extends over the domain interface. Two Zn^{2+} ions, a Zn^{2+} - Fe^{3+} combination or a combination of other metal ions form the metal center depending on the organism. The ions are coordinated by a highly conserved THxHxDH active site motif and a water molecule (Deponte, 2013). Due to the β -lactamase domain, Glo2 is classified among the diverse group of binuclear metallohydrolases (Deponte, 2013). Some organisms, including *P. falciparum* and *S. cerevisiae*, express two different Glo2 enzymes (Silva *et al.*, 2013; Deponte, 2014). One of these two Glo2 enzymes is cytosolic while the other is localized to the mitochondrion or apicoplast as in *S. cerevisiae* (Glo4) and *P. falciparum* (tGlo2) respectively (Deponte, 2013; Urscher *et al.*, 2010). If multiple isozymes of Glo2 occur in an organism, the different enzymes are mostly encoded by separate genes rather than by a single gene. In humans, however, the two Glo2 isozymes, one localized to the cytosol and the other to the mitochondrion, are both encoded by the same gene (Marasinghe *et al.*, 2005). To date, the actual function of the additional Glo2 isoenzymes localized to mitochondrion or apicoplast is still to be determined even though the catalytic activity of mitochondrial Glo2 is suggested to direct one of several routes through which glutathione is made available to the mitochondrion (Urscher & Deponte, 2009; Cordell *et al.*, 2004). Similar to Glo1, Glo2 is generally specific to glutathione thioesters. As an exception, the Glo2 of trypanosomatids, as expected, specifically hydrolyses *S*-*D*-lactoyltrypanothione (Silva *et al.*, 2013). In the proposed reaction mechanism, the substrate first binds to the enzyme at the domain interface, with its glycine and cysteine residues hydrogen-bonding with the conserved substrate binding-site of the enzyme (Deponte, 2013). The reaction then proceeds with a nucleophilic attack by a hydroxide ion (OH^-) on the C1 atom (carbonyl carbon) of the substrate to form a negatively charged tetrahedral intermediate that may be stabilized by coordination to the nearest metal ion. The C-S bond of the substrate subsequently breaks while glutathione is protonated. The catalytic products of reduced glutathione and lactic acid then diffuse out of the active site of the free enzyme to be replaced by a water molecule (Urscher & Deponte, 2009; Cameron *et al.*, 1999). Binding of the active site residues to the two metal ions is thought to generate the nucleophile (the deprotonation of water at physiological pH) at the metal center (Deponte, 2013; Thornalley, 1993; Cameron *et al.*, 1999). Histidine residues as well as an aspartate residue are important in metal ion binding in the active site of the enzyme (Deponte, 2013).

1.4.1.4. 2-Oxoaldehydes

The primary 2-oxoaldehyde substrate of the glyoxalase system appears to be methylglyoxal, the metabolism of which leads to the production of D-lactate through the formation of the thioester *S*-D-lactoylglutathione (Cameron *et al.*, 1999; Urscher *et al.*, 2011). Other physiological and artificial substrates of the glyoxalase systems include glyoxal, phenylglyoxal, hydroxy-pyruvaldehyde, 3-phosphohydroxy-methylglyoxal, kethoxal and 4,5-dioxovalerate (Silva *et al.*, 2013; Thornalley, 1998; Akoachere *et al.*, 2005). The products and intermediate metabolites produced in the course of the metabolism of these other substrates are different from those produced during the metabolism of methylglyoxal. For instance, glyoxal is metabolized through a glycolylglutathione thioester to the 2-hydroxycarboxylic acid glycolate (Thornalley, 1998). In living cells, the 2-oxoaldehydes can be generated from multiple different sources (Urscher *et al.*, 2011). Methylglyoxal is considered the most important 2-oxoaldehyde because it is mainly produced as a spontaneous intermediate of the glycolytic pathway in all cells and organisms (Silva *et al.*, 2013; Urscher *et al.*, 2011; Thornalley, 1998). The compound is produced by the non-enzymatic (and to some extent by the enzymatic) elimination of a phosphate group from phosphate-ene-diolate of dihydroxyacetone-phosphate (DHAP) and glyceraldehyde-3-phosphate (GAP), the three-carbon intermediates of glycolysis (Silva *et al.*, 2013; Urscher *et al.*, 2011; Thornalley, 1998, 1996; Cooper, 1984). Methylglyoxal is also formed by the oxidation of acetone by cytochrome P450, by the oxidation of aminoacetone formed in the catabolism of L -threonine, by the oxidation of ketone bodies by myeloperoxidase and by lipoperoxidation reactions (Silva *et al.*, 2013; Thornalley, 1996). Some bacteria such as *E. coli* can also use the enzyme methylglyoxal synthase to produce methylglyoxal from DHAP as an important bypass of glycolysis, usually under conditions of limited inorganic phosphate (Urscher *et al.*, 2011; Thornalley, 1996; Cooper, 1984). Methylglyoxal synthase is also present in yeast, but concerning other eukaryotes, there has been till date only one reported isolation of the enzyme from goat liver (Silva *et al.*, 2013; Vander Jagt *et al.*, 1990).

In general, most 2-oxaldehydes including glyoxal and hydroxypyruvaldehyde found in many organisms, seem to be unwanted by-products of the biochemical pathways mentioned above (Silva *et al.*, 2013; Urscher *et al.*, 2011; Akoachere *et al.*, 2005). Nevertheless, the 2-oxoaldehydes are also thought to have several functions in the living cell. For instance, methylglyoxal is reported to function in osmoregulation and transcription regulation in yeast (Maeta *et al.*, 2004; Inoue *et al.*, 2011). Some studies also suggest a direct involvement of some 2-oxoaldehydes in cellular regulatory processes and in signal transduction. Methylglyoxal for example, has been implicated in the regulation of the co-repressor mSin3A in kidneys of diabetic mice (Deponte, 2014, 2013). Methylglyoxal-derived glycation of α -crystallin and hsp27 has also been demonstrated to enhance the function of these two chaperones. The same effect has been reported for glycation of hsp26 and hsp71/72 of yeast (Silva *et al.*, 2013). Some level of glycation caused by the 2-oxoaldehydes therefore seems to be physiologically beneficial to the living cell.

The major reason why the 2-oxoaldehydes have been a centre of recent studies is, however, because of their high spontaneous reactivity to important cellular molecules leading to their modification and damage (Urscher *et al.*, 2011). Owing to their adjacent carbonyl groups, the 2-oxoaldehydes are strong electrophiles, making them potentially cytostatic at low

concentrations, and cytotoxic and mutagenic at high concentrations (Urscher *et al.*, 2011; Cameron *et al.*, 1997; Urscher *et al.*, 2012; Deponte, 2013). They can react irreversibly with nucleophiles in proteins, membrane lipids and nucleic acids leading to the formation of so-called advanced glycation endproducts (AGE) both *in vivo* or *in vitro* (Urscher *et al.*, 2011; Thornalley, 1996; Deponte, 2013). The accumulation of AGE in cells is thought to lead to many disease conditions such as cancer, diabetes, renal failure and neurological disorders (Thornalley, 1996; Deponte, 2013; Akoachere *et al.*, 2005). The activation of the receptor to AGE (RAGE) by AGE, which initiates downstream activities in the AGE-RAGE system for example, is believed to be involved in the pathogenesis of diabetes (Inoue *et al.*, 2011). 2-Oxoaldehydes react reversibly and irreversibly with arginine, lysine and cysteine residues of proteins under physiological conditions and concentrations (Thornalley, 1996; Lo *et al.*, 1994). This reactivity can cause fatal cross-linking, conformational changes and inactivation of enzymes and other important proteins. It can also lead to the endocytosis and degradation of important proteins by monocytes and macrophages (Thornalley, 1996; Lo *et al.*, 1994). The 2-oxoaldehydes also react with cytosine, adenine and predominantly guanine residues of DNA and RNA leading to mutations and inter-strand cross-links in these macromolecules. These are mostly irreversible changes in nucleic acids that can cause apoptosis (Thornalley, 1998; Akoachere *et al.*, 2005; Thornalley, 1996; Marasinghe *et al.*, 2005). The glyoxalase system is therefore thought to play the very important physiological role detoxifying the 2-oxoaldehydes and keeping AGE concentrations at healthy levels in the living cell (Urscher *et al.*, 2011; Deponte, 2014). The system is particularly thought to act at the Amadori product level by preventing the glycation cascade in the early steps of the Maillard reaction (Silva *et al.*, 2013). Glo1 and or Glo2 have thus gained attention as potential drug targets in several parasitic protozoans and cancer cells that are known to have elevated glycolytic fluxes leading to increased formation of methylglyoxal (Urscher & Deponte, 2009). In cancer cells in particular, higher levels of expression of the glyoxalases are observed (Silva *et al.*, 2013). Inhibition of the detoxification pathway in these cells may therefore lead to cellular damage (Silva *et al.*, 2013; Urscher & Deponte, 2009). In fact, experimental support for this observation in some cells and organisms has led to the development of glutathione-based and nonglutathione Glo1 and Glo2 inhibitors including *S-p*-bromobenzylglutathione diesters, curcumin and methyl-gerfelin (Urscher *et al.*, 2011; Ariza *et al.*, 2006). Some of these inhibitors have been identified to exhibit antimalarial and antitrypanosomal properties (Urscher *et al.*, 2011; Ariza *et al.*, 2006; Urscher *et al.*, 2012; Thornalley, 1998).

1.4.1.5. Other pathways of methylglyoxal metabolism

In the trypanosomatids and *S. cerevisiae*, other pathways of 2-oxoaldehyde metabolism have been described over the years. Two of such additional pathways are known in the trypanosomatids; NADPH-dependent aldose reductase metabolizes methylglyoxal to hydroxyacetone and D-lactaldehyde, while the NADPH-dependent methylglyoxal reductase reduces methylglyoxal to L-lactaldehyde through a reduction/oxidation system (Silva *et al.*, 2013; Thornalley, 1996). A similar route of detoxification of methylglyoxal to L-lactic acid is found in *S. cerevisiae* involving the enzymes methylglyoxal reductase and lactaldehyde

dehydrogenase (Inoue *et al.*, 2011). Again in the yeast *Hansenula mrakii*, the enzyme aldehyde reductase converts methylglyoxal to acetol (Inoue *et al.*, 2011).

1.4.2. Glyoxalase system of the human erythrocyte

The glyoxalase system of human cells comprises two enzymes: glyoxalase 1 (hGlo1) and glyoxalase 2 (hGlo2) (Table 1.1) (Cordell *et al.*, 2004; Thornalley, 1993). hGlo1 has been purified from many human tissues including pancreas, lung, liver, brain and blood (Thornalley, 1993). As stated above, hGlo1 is a homodimer with two structurally identical active sites (Ariza *et al.*, 2006; Urscher *et al.*, 2011). The enzyme is encoded by a diallelic gene located on chromosome 6 with a translational product of 184 amino acids and is transmitted in an autosomal codominant manner. There are thus three different allozymes (Glo1a-a, Glo1a-b and Glo1b-b) of hGlo1, all of which are present in the erythrocytes of heterozygotes (Thornalley, 1993; Urscher *et al.*, 2011; Aronsson *et al.*, 1979; Thornalley, 2003).

Table 1.1. Summary of properties of the glyoxalases in the host/parasite unit.

Protein name(s)	<i>Plasmodium falciparum</i> glyoxalases				<i>Homo sapiens</i> glyoxalases	
	<i>Pf</i> Glo1 (GloI, GlxI)	<i>Pf</i> cGlo2 (cGloII, GlxIIb)	<i>Pf</i> tGlo2 (tGloII, GlxII)	<i>Pf</i> GILP	<i>h</i> GloI	<i>h</i> GloII (HAGH, GlxII)
Accession number	PF110145 ^a or AF486284 ^b	PFD0311w ^a or AY494055 ^b	PFL0285w ^a or AF486285 ^b	PFF0230c ^a	L07837 ^b	NM001040427 & NM005326 ^c
Gene locus	Chr. 11	Chr. 4	Chr. 12	Chr. 6	Chr. 6p21.3-p21.1	Chr. 16p13.3
mRNA length	1071 bp	792 bp	969 bp	924 bp	623 bp	783 bp & 927 bp
Authentic Mw/pI	42441/ 5.75	30528/ 7.64	38414/ 8.71	35838/ 8.59	20720/ 5.24	28860/6.86 33806/8.34
His-tagged Mw/pI ^{d,e)}	43,708/ 6.10	31,795/ 8.10	32,940/ 6.94	34,782/ 8.06	-	30544/ 7.01
Subcellular localization/N-terminal signal sequence	Cytoplasm/ none	Cytoplasm/ none	Apicoplast/ yes	Apicoplast?/ yes	Cytoplasm/ none	Cytoplasm & mitochondrial matrix/ none & yes
Activity/Protein superfamily	Isomerase/ Vicinal oxygen chelate metallo-enzyme	Hydrolase/ Binuclear metallo-hydrolase	Hydrolase / Binuclear metallo-hydrolase	Inactive?/ Vicinal oxygen chelate metallo-enzyme?	Isomerase/ Vicinal oxygen chelate metallo-enzyme	Hydrolase/ Binuclear metallo-hydrolase
Structural motives	Four $\beta\alpha\beta\beta$ motifs/domains	N-term. metallo- β -lactamase fold and C-term. α -helical domain	N-term. metallo- β -lactamase fold and C-term. α -helical domain	Four putative $\beta\alpha\beta\beta$ motifs/domains	Two $\beta\alpha\beta\beta$ motifs/domains	N-term. metallo- β -lactamase fold and C-term. α -helical domain
Quaternary structure / Active sites	Monomer/ A + B	Monomer-dimer equilibrium/A&A+A'	??	?/A + B?	Dimer/ A + A'	Monomer (dimer ?)/A (& A + A' ?)
Metal ion	Zn ²⁺	Zn ²⁺	Zn ²⁺	none?	Zn ²⁺	Zn ²⁺
Catalytic mechanism	Two conformations and allosteric coupling	Theorell-Chance acid-base mechanism	Regular Michaelis-Menten kinetics?	No activity with MG and GSH	Regular Michaelis-Menten kinetics?	Regular Michaelis-Menten kinetics?

^aPlasmodium genome database annotation (<http://plasmodb.org>); ^bGenBank annotation; ^cNCBI Reference Sequence; ^dRecombinant protein sizes; ^eCalculated molecular weight (average) and isoelectric point (<http://www.expasy.org/tools>). Taken and modified from (Urscher *et al.*, 2011).

The allozymes have a molecular weight of approximately 44 kDa (the molecular weight of each subunit measuring approximately 22 kDa) but have different charge densities and molecular shapes (Thornalley, 1993; Thornalley, 2003). The physiological substrate of hGlo1 is thought to be the hemithioacetal formed spontaneously from the unhydrated form of methylglyoxal and reduced glutathione (Thornalley, 1993; Cameron *et al.*, 1999). The reaction of the enzyme generally follows the Michaelis-Menten kinetics that effects the metal ion-dependent isomerization of the substrate glutathione hemithioacetal to a glutathione thioester (Thornalley, 1993).

Human Glo2 (hGlo2) activity has been detected in the cytosol and mitochondrion of human liver, brain and red blood cells (Thornalley, 1993; Uotila, 1973; Board, 1980). The gene (hydroxyacylglutathione hydrolase, *HAGH*, gene) that encodes the cytosolic hGlo2 is located on chromosome 16 and adopting an alternative exon usage, this gene is also able to encode the mitochondrial hGlo2-isoform which carries a mitochondrion targeting sequence. Only the cytosolic form of 260 amino acids is found in mature human erythrocytes (Cordell *et al.*, 2004; Urscher *et al.*, 2011). Genetic polymorphism of *HAGH* is extremely rare but occasionally, expression of a second form of the gene is detected among Japanese and Micronesian people. Inheritance of the alleles of the *HAGH* gene also proceeds in an autosomal codominant manner (Urscher *et al.*, 2011; Board, 1980; Thornalley, 1993). hGlo2 is a monomer consisting of two domains (Thornalley, 1993; Cameron *et al.*, 1999) with a molecular mass in the range of 23-29 kDa (Thornalley, 1993; Uotila, 1973; Cameron *et al.*, 1999). Though the enzyme is known to have a broad substrate specificity for glutathione thiol esters, its physiological substrate in the cytosol is *S*-D-lactyoglutathione (Cordell *et al.*, 2004; Thornalley, 1993; Cameron *et al.*, 1999). The rate of reaction of hGlo2, as in hGlo1, follows the Michaelis-Menten kinetics leading to the hydrolysis of *S*-D-lactyoglutathione to D-lactate in the cytosol (Thornalley, 1993; Allen *et al.*, 1993). About 95% of hGlo2 activity is found in the cytosol while the rest (5%) is detected in the mitochondrion (Cordell *et al.*, 2004). Even though the specific role of the mitochondrial hGlo2 enzyme is not determined yet, it is possible this enzyme hydrolyses *S*-D-lactoylglutathione that has diffused or is transported into the mitochondrion from the cytosol (Scire` *et al.*, 2000). hGlo2 is inhibited by reduced glutathione, the hemethioacetal formed from methylglyoxal and reduced glutathione, and several anions (Uotila, 1973).

1.4.3. Glyoxalase system and methylglyoxal metabolism in *P. falciparum*

The genome of *P. falciparum* encodes four glyoxalases: a cytosolic Glo1 (*PfGlo1*), two Glo2 isozymes (a cytosolic protein, *PfcGlo2*, and an apicoplast-localized protein, *PftGlo2*), and a Glo1-like protein (*PfGILP*) that also carries an apicoplast targeting signal (Table 1.1) (Deponte, 2014; Urscher *et al.*, 2010). *PfGlo1*, *PfcGlo2* and *PftGlo2* are functional enzymes but recombinant *PfGILP* till date is reported to be inactive in standard enzyme assays (Deponte, 2014; Urscher *et al.*, 2011). Localization studies have revealed a cytosolic glyoxalase system of *P. falciparum* comprising the cytosolic enzymes *PfGlo1* and *PfcGlo2* (Deponte, 2014; Urscher *et al.*, 2010).

PfGlo1 belongs to the subgroup of large monomeric Glo1 proteins which consist of highly homologous N- and C-terminal amino acid sequences with two different active sites (Deponte *et al.*, 2007). This is in contrast to the smaller homodimer subgroup to which the human Glo1

enzyme belongs (Deponte, 2013; Urscher *et al.*, 2011; Akoachere *et al.*, 2005). The two halves of *PfGlo1* are also homologous to each of the 2-domain subunits of hGlo1 (Iozef *et al.*, 2003; Akoachere *et al.*, 2005). Both halves of recombinant *PfGlo1* have been produced in *E. coli*, and the C-terminal half was shown to yield a stable protein that formed an enzymatically active dimer. This result supports the hypothesis that the enzyme was generated by an evolutionary subunit fusion (Iozef *et al.*, 2003). Similar to Glo1 enzymes of most eukaryotes, *PfGlo1* uses Zn^{2+} as a co-factor. The active site of *PfGlo1* also consists of the binding sites for glutathione, Zn ions and a catalytic loop. With the exception of a few residues, almost all the amino acid residues representing these three parts of the active sites are also conserved in *PfGlo1* as in hGlo1, resulting in a similar enzymatic action (Deponte *et al.*, 2007). The two active sites of the monomeric *PfGlo1* have similar turnover numbers but significantly different substrate affinities (Urscher *et al.*, 2012; Deponte *et al.*, 2007). Both active sites also adopt two distinct conformations and are allosterically coupled in a substrate concentration-dependent manner. This means that *PfGlo1* exists in a high affinity-conformation at low substrate concentrations and a high activity-conformation at high substrate concentrations (Urscher *et al.*, 2012; Deponte *et al.*, 2007). Allosteric coupling points to a possible adaptation of the parasite to growth in the environment of variant methylglyoxal fluxes as occurs during the vertebrate and mosquito stages of the parasite (Urscher *et al.*, 2011; Deponte, 2014; Deponte *et al.*, 2007). The two active sites of *PfGlo1* may also reflect and adaptation to alternative substrates or even play regulatory functions by allowing signal molecules to bind to one site, leading to the control of the overall enzyme activity or stimulating interaction with other effector molecules (Urscher *et al.*, 2011; Deponte, 2014).

PfcGlo2 is a monomeric thioesterase and the first member of this class of binuclear metallohydrolases for which acid-base catalysis was described (Urscher *et al.*, 2011; Urscher & Deponte, 2009). The Zn^{2+} /metal binding motif THxHxDH as well as two additional histidine residues essential for Zn^{2+} and or Fe^{2+} binding are conserved to a large extent in *PfcGlo2*, pointing to a comparable catalytic pathway to that which occurs in hGlo2 (Akoachere *et al.*, 2005). The metal ions (Zn^{2+} and or Fe^{2+}) of *PfcGlo2* are thought to activate water and to generate the nucleophile (OH^-) at the reaction centre (Urscher & Deponte, 2009). As in hGlo2, substrate binding is revealed to be through the highly conserved glutathione-mioety (Urscher & Deponte, 2009; Urscher *et al.*, 2011). Even though most Glo2 enzymes are functional monomers, cross-linking experiments with glutaraldehyde and disuccinimidyl substrate revealed that recombinant *PfcGlo2* can also form dimers in solution and the enzyme usually exists in rapid monomer-dimer equilibrium. There is as yet no experimental evidence of dimer occurrence *in vivo* but dimer formation may play regulatory functions in the cytosol. In addition, a role of dimer formation in signal transduction was suggested (Urscher *et al.*, 2011). Dimerization has also been reported in hGo2 and is expected to occur in Glo2 enzymes of other organisms (Urscher *et al.*, 2010).

PfGILP is only present and highly conserved in *Plasmodium* species. An apicoplast targeting sequence located at the N-terminus of *PfGILP* suggests that the protein is localized to the apicoplast (Akoachere *et al.*, 2005). As mentioned above, *PfGILP* is inactive and this is most likely due to the fact that the enzyme lacks the essential highly conserved active site residues found in all Glo1 enzymes (Urscher *et al.*, 2011; Deponte, 2013). The physiological substrate of *PfGILP*, if any, is yet to be determined.

*Pf*Glo2 is the first experimentally confirmed plastid glyoxalase (Urscher *et al.*, 2010). As in *Pf*GILP, *Pf*Glo2 also carries an apicoplast targeting sequence located at the N-terminus (Urscher *et al.*, 2010; Akoachere *et al.*, 2005). The Zn²⁺/metal binding motif THxHxDH as well as other amino acid residues essential for metal binding are conserved in *Pf*Glo2 as in *Pfc*Glo2. The catalytic properties of the enzymes are therefore thought to be similar to those of hGlo2 and *Pfc*Glo2 (Urscher & Deponete, 2009; Akoachere *et al.*, 2005). Even though *Pf*Glo2 has been found to be active *in vitro*, its actual physiological function as well as the source and structure of its substrate are still unknown (Urscher *et al.*, 2011). Localization of triosephosphate isomerase (TIM) in the apicoplast was confirmed experimentally in apicomplexan parasites (Fleige *et al.*, 2007) suggesting that the production of methylglyoxal in the apicoplast is possible (Urscher *et al.*, 2011). There is, however, no confirmation of the existence of a functional apicoplast-targeted Glo1 (tGlo1). The most probable candidate in this regard is *Pf*GILP which, however, does not exhibit a typical Glo1 activity (Urscher *et al.*, 2011; Silva *et al.*, 2012). The extent to which GSH is imported into or utilized in the apicoplast is also unclear (Urscher *et al.*, 2011). Thus, the existence of a functional apicoplast glyoxalase system is still to be discovered (Urscher *et al.*, 2011; Akoachere *et al.*, 2005).

Concerning expression profiles of the glyoxalases of the malaria parasite, reports suggest a constitutive expression of the encoding genes during the erythrocytic cycle and gametogenesis. Only the levels of mRNA of *Pf*Glo2 and *Pf*GILP seem to slightly increase in the late trophozoite and early schizont blood stages of the parasite (Urscher *et al.*, 2011). Protein mass spectrometric data has also confirmed that mRNAs encoding the four glyoxalases are translated in the blood-stage parasites (though only a few *Pf*GILP mRNAs) (Urscher *et al.*, 2011).

1.4.4. Glyoxalase systems of the host-parasite unit as a potential drug target

P. falciparum and all other *Plasmodium* species develop and proliferate in the anucleated, nutrient-rich and relatively safe intracellular environment of the erythrocyte, which is also devoid of all cellular organelles (Urscher *et al.*, 2011; Acharya *et al.*, 2017). In the erythrocyte, the parasite encapsulates itself within the parasitophorous vacuole but communicates to the external host cytosol using intricate membranous extensions that include the Maurer's clefts and the tubulovascular network (Acharya *et al.*, 2017; More & Vince, 2009). Two D-lactate producing glyoxalase systems are found in the host-parasite unit of the *P. falciparum*-infected erythrocyte: one in the cytosol of the erythrocyte and the other in the parasite cytosol (Fig 1.8) (Urscher *et al.*, 2011). The apicoplast of the parasite also harbours a functional Glo2 isozyme and a highly mutated Glo1-protein (Urscher *et al.*, 2011). The erythrocyte-parasite unit has been shown to consume more glucose than uninfected erythrocytes (Sherman, 1979; Vander Jagt *et al.*, 1990; Deponete, 2014). The consequence of this high glucose demand is the increased level of methylglyoxal and other intermediates of glucose breakdown in the host-parasite unit (Urscher *et al.*, 2011; Vander Jagt *et al.*, 1990). Results from two studies confirmed that the high influx of glucose in the (infected) erythrocyte indeed leads to elevated levels of methylglyoxal in the cell (Vander Jagt *et al.*, 1990; Thornalley, 1988). Since neither the erythrocyte nor the parasite harbour methylglyoxal synthase activity, the source of methylglyoxal in the host-parasite unit is suggested to be

parasite glyoxalase system using parasite-specific Glo1 and Glo2 inhibitors. In the first approach, the exceptionally high glycolytic fluxes in parasitized erythrocytes, coupled with the fact that the parasite consumes more glucose than the host erythrocytes (Sherman, 1979; Vander Jagt *et al.*, 1990), could make the host-parasite unit more sensitive to glyoxalase inhibition compared to unparasitized erythrocytes. Treatment with inhibitor concentrations that should normally be save for uninfected erythrocytes could therefore be disruptive to the unit leading to parasite death. Since the erythrocyte lacks *de novo* protein bio-synthesis, moderate inhibitor concentrations may inactivate key redox enzymes leading to the development of redox imbalances in the cell and presenting a hostile environment for the parasite to survive. The second approach is based on the fact that the kinetic properties and quaternary structures of the parasite glyoxalases are different from those of the host (Urscher *et al.*, 2011; Vander Jagt *et al.*, 1990). Novel *PfGlo1*- or *PfcGlo2*-specific inhibitors can thus be used to induce selective toxicity to the parasite.

One strategy that can be employed to investigate the essentiality of glyoxalases of the host-parasite unit is to generate glyoxalase knockout of lines of the parasite. To date, there are no reports of knockout lines for any of the *P. falciparum* glyoxalases. The relevance of the host glyoxalase system for parasite development is also unknown. Concerning the latter, a couple of important questions need to be addressed. Firstly, does the parasite import host glyoxalase enzymes to cope with elevated 2-oxoaldehyde concentrations? Enzyme import is plausible as *P. falciparum*, for example, imports human peroxiredoxin 2 for peroxide detoxification (Koncarevic *et al.*, 2009). Secondly, does the parasite export methylglyoxal to the host? The answers to the above questions will help address the relevance of the host glyoxalase system to parasite development.

A number of compounds have already been investigated as potential inhibitors of the *P. falciparum* glyoxalases (Urscher *et al.*, 2012; Thornalley *et al.*, 1994; Kawatani *et al.*, 2008; Thornalley *et al.*, 1996). Curcumin, methyl-gerfelin and glutathione-derived compounds such as *S-p*-bromobenzyl glutathione have been tested against recombinant *PfGlo1* or *P. falciparum* blood-stage parasites and are reported to exhibit promising but variant degrees of potency. Curcumin was reported to act on only one active side of recombinant *PfGlo1* while methylgerfelin was shown to act on both sites and is also more potent in cell culture (Urscher *et al.*, 2012). *S-p*-bromobenzylglutathione ethylester has also been shown to have antimalarial properties against *P. falciparum* culture with an IC_{50} value of approximately 5 μ M after 6 h of exposure (Iozef *et al.*, 2003; Thornalley *et al.*, 1994). A few not-so impressive *PfcGlo2* glutathione-based inhibitors were also described (Akoachere *et al.*, 2005). The common theme of these early *P. falciparum* glyoxalase inhibitor studies is the fact that, almost all have IC_{50} values in the lower micromolar concentration range (Urscher *et al.*, 2011). Furthermore, two potent glutathione-based yeast Glo1 inhibitors were tested with *PfGlo1*. These inhibitors, compounds 1 and its gamma-glutamyltranspetidase (γ -GT)-resistant derivative, compound 2, were found to be specific and to inhibit both active sites of *PfGlo1* regardless of the enzyme conformation. Both compounds were reported to be non-competitive tight-binding inhibitors with K_i^{app} values in the nanomolar range (Urscher *et al.*, 2012). A major issue concerning some of the tested *P. falciparum* glyoxalase inhibitors is, however, the question of whether the compounds specifically target the parasite glyoxalase, the host enzymes or both (Silva *et al.*, 2013). In summary, the glyoxalases of the host parasite-unit are hypothesized as potential drug targets for the development of new antimalarials. Even though a number of potential

inhibitors have already been identified, the suitability of the glyoxalases of *P. falciparum* as drug targets should be investigated by reverse genetics.

1.5. Inhibitory effects of standard pro- and antioxidants on *P. falciparum*

Malaria manifests when *Plasmodium* parasites infect and multiply in the red blood cells of the human host (Schofield & Grau, 2005). It is also known that, even upon blood invasion, most cases of infection in malaria-endemic regions are clinically silent, reflecting the ability of the host immune system to prevent disease (Schofield & Grau, 2005). In individuals with insufficient immunity, however, blood infection normally leads to overt disease with life threatening consequences if antimalarial treatment is not administered appropriately (Schofield & Grau, 2005; Gazzinelli *et al.*, 2014). The redox metabolism of the host-parasite unit has been suggested to play a key role in the parasite survival and clearance (Becker *et al.*, 2004; Goyal *et al.*, 2012). Sources of redox agents in the host-parasite unit may be endogenously produced or from exogenous sources such as antimalarial drugs (Goyal *et al.*, 2012; Jortzik & Becker, 2012). For instance, the metabolism of hemoglobin in the digestive vacuole has been proposed as a major endogenous source of reactive oxygen species that affects parasite survival. Endogenous oxidative stress is also suggested to be exerted on the parasite-host unit by the host immune system in reaction to immunogens from lysed erythrocytes (Goyal *et al.*, 2012; Jortzik & Becker, 2012). Furthermore, genetic traits such as sickle-cell haemoglobin and glucose-6-phosphate dehydrogenase deficiency are suggested to affect parasite survival by generating oxidative stress in the erythrocytes (Jortzik & Becker, 2012). Hemoglobin S trait in particular is suggested to be able to reduce cytoadhesion of infected erythrocytes by generating redox agents that affect the actin cytoskeleton of the cell (Cyrklaff *et al.*, 2016). It is also known that chloroquine and quinacrine, among other quinolone drugs, work by inhibiting the heme detoxification system of the parasite (Petersen *et al.*, 2011; Goyal *et al.*, 2012). In principle, oxidative stress has been defined as a prolonged redox imbalance that results in the accumulation of oxidized and damaged molecules (Sies, 1986). A major question that needs to be address is whether redox agents and oxidative stress really play a physiological role in parasite survival or clearance by the host system. While numerous studies point to the physiological relevance of the redox state of the host-parasite unit to parasite survival and host immune response, mechanistic insights in support of the diverse hypotheses on oxidative stress are surprisingly scarce. Data regarding specific effects of standard redox agents on the parasite survival are also limited. There is, in particular, a lack of IC₅₀ values for these agents for parasite survival in culture. This lack is remarkable especially on the account that some redox agents have already been used as adjuvants in clinical trials (Isah & Ibrahim, 2014; Charunwatthana *et al.*, 2009). A common approach to test the relevance of oxidative stress on the development of the malaria parasite is to challenge infected erythrocytes *in vitro* with bolus amounts of standard pro- and antioxidants.

1.6. Hypothesis and aims of the study

Deletion of the genes coding for the *P. falciparum* glyoxalases is expected to lead to the accumulation of methylglyoxal and the depletion of glutathione in the parasite-host unit and may cause growth impairment or death of the parasite (Vander Jagt *et al.*, 1990; Urscher *et al.*, 2011). Disruption of each of the four glyoxalase genes or their combination could generate transgenic parasites, 3D7 Δ *glo1*, 3D7 Δ *cglo2*, 3D7 Δ *tglo2* and 3D7 Δ *gilp*, that should have no activity for *P. falciparum* enzymes *PfGlo1*, *PfcGlo2*, *PftGlo2* and *PfGILP* respectively. This would lead to an abolished or impaired parasite glyoxalase system and the accumulation of toxic 2-oxoaldehydes in the parasite. If disruption of any of the genes is lethal to the parasite, it would point to their essentiality, thereby signifying their use as antimalarial drug targets. This hypothesis is plausible considering that chloroquine, one of the few potent antimalarials, works by targeting a detoxification system of the parasite (Urscher *et al.*, 2011). The main objective of this project was to determine whether knockout of one or more of the glyoxalase genes of the malaria parasite *P. falciparum* impairs parasite growth or is even lethal. In this study, the CRISPR/Cas9 system gene knockout strategy (Ghorbal *et al.*, 2014) was employed to attempt the deletion of each of the four *P. falciparum* glyoxalase-encoding genes and to investigate whether the enzymes are essential for the blood-stage development of the parasite. Viable transgenic parasites were characterized phenotypically using microscopy and biochemical methods.

A second objective of the thesis was to investigate the relevance of the host glyoxalase system for the survival of the parasite in the host-parasite unit. To address this aspect, known Glo1-specific tight-binding inhibitors were employed to inactivate the glyoxalase system of erythrocytes. The treated erythrocytes were subsequently used to culture purified *P. falciparum* parasites. Since there are no glyoxalase knockout erythrocytes available, this strategy allowed for an indirect assessment of the contribution the host Glo1 to parasite growth and survival in the host-parasite unit of the *P. falciparum*-infected erythrocyte.

A third objective of the thesis was to investigate the effects of standard pro- and antioxidants on the survival of the chloroquine-sensitive 3D7 strain of *P. falciparum* as a way of addressing the relevance of oxidative stress on the development of the parasite. Specifically, IC₅₀ values for hydrogen peroxide (H₂O₂), *N*-acetyl-L-cysteine (NAC), ascorbate and dithiothreitol (DTT) were determined for *in vitro* cultures of the malaria parasite using SYBR green-based growth assays. The growth analysis of *P. falciparum* 3D7 parasites which were treated with different concentrations of ascorbate was also performed. Results from these investigations might serve as a guideline to manipulate the redox state of the host-parasite unit and the use of redox agents in the management of malaria.

2. MATERIALS

2.1. Technical equipments

Equipment	Company, Design
Agarose gel running system	Bio-Rad, Mini-sub cell GT [®]
Agarose gel documentation system	Herolab, UVT-28 MV, Easy syst, Hama 390 UV filter
Autoclave	Systec, VX-95
Automated pipette controller	Brand GmbH + CO KG, accu-het [®] <i>pro</i>
Automatic film processor	LiCOR, JP-33
Balances and scales	Sartorius, Entris-124-1S, Kern & Sohn, 440
Blotting system	Peqlab Sedec M, PerfectBlue apparatur
Bunsen burner	Labogaz, 470
Centrifuges	Beckmann, J2-21M centrifuge, Heraeus, multifuge 1 S-R
Electroporation system	Bio-Rad, Gene Pulser II
Fridges -20°C, -80°C fridge	Liebherr, labor freezers, Kleinfeld, Labortechnik
Hemocytometer	Marienfeld, superior CE
Glass cuvettes	Hellma Analytics, OS blue quartz
Incubator (Bacterial)	Heraeus, B5050 E
Incubator (CO ₂)	Mytron, BS250/S
Incubator shaker	Infors HT, triple stack
Light microscope	Carl-Zeiss, Axio scope.A1 Pol
Microfuge	Eppendorf, 5417R
Microplate reader	BMG Latech, stapel machine stacker
Microwave	AEG, micromat FX 175 Z
Molten glass pipette	Lenz Laborglasinstrumente,
Multichannel pipette	Abimed, discovery comfort
NanoDrop	Thermo Scientific, ND-1000 spectrophotometer
Orbital shaker	Ratek, RPM5
Overhead shaker	Heidolph, duomax 1030
pH meter	Sartorius, PY-P10
Rotator mixer	Grant-Bio, PTR-30
Red light	Petra electric, IR 10
SDS-PAGE system	Bio-Rad, mini-protean tetra electrophoresis cell
Sterile bench-Bacterial culture	Gelaire [®] , BSB 3A
Sterile bench- <i>Plasmodium</i> culture	Thermo Fischer Scientific, Herasafe [™] KS
Thermoblocks	Eppendorf, thermomixer comfort
Thermal cycler	Eppendorf, mastercycler gradient
Ultrasonic laboratory homogenizer	Bandelin, electronic sonopuls HD 2070
UV/vis-Photomer	Jasco, V-550 UV-vis spectrophotometer
Magnetc cell separator	Miltenyi Biotec, SEVarioMACS [™] Separator
Vortex mixer	Heidolph instruments, reax2000

Water bath

Fischer Scientific, Isotemp 210

2.2. Chemicals, Consumables and kits

Company	Chemical, consumable, kit
Abcam	Anti-AGE antibody, anti- <i>P. Berghei</i> heat shock protein 70
Amersham	ECL Western blotting detection reagent
Bio-Rad	Goat anti-rabbit IgG (H+L)-HRP conjugate, HRP-conjugated goat anti-mouse, coomassie brilliant blue R-250
Carl Roth	Giemsa solution, Akasolv aqua care, phenol/chloro-form /isoamylalcohol solution, milk powder
c.c.pro	Gentamycin, hypoxanthine,
Clontech	In-Fusion HD cloning kit, stellar competent cells
Fischer Scientific	Culture tubes
Fischer-Sehner	Super RX-N film, fujifilm
Fermentas	dNTPs
GE Healthcare Life Sciences	Whatman paper, Nitrocellulose blotting membrane Protran BA85
Gibco/Life Technologies	Kanamycin, RPMI 1640
Greiner Bio-One, cellstar	2 mL cryovial, 15 and 50 mL Falcon tubes, culture dishes and flasks, 96 well plates, black fluotrac microplates, 15 and 50 mL centrifuge buckets
Infors HT	Incubator shaker
Invitrogen	TOPO-TA cloning kit, SYBR green 1 solution
Life technologies GmbH	Albumax II
Metabion	Primers
Millex GV	0.22 µm filter
New England Biolabs	<i>Taq</i> DNA polymerase, ThermoPol Taq-buffer, 6X purple gel loading dye, 1kb and 100 bp Quick-Load DNA ladder, restriction enzymes, T4 ligase and ligase buffer
Nippon Genetics	Midori green advance DNA stain
Novagen	<i>E. coli</i> NovaBlue
Pierce	SulfoLink resin
Pineda Antibody Service	Peptide synthesis and antibody production
Promega Corporation	Wizard Gel and PCR clean-up system
Qiagen	Plasmid maxi kit
Roche	Protease inhibitor, proteinase K

Sarstedt	0.5, 1.5 and 2 mL micro tubes, 1, 5, 10 and 25 mL, serological pipettes, disposable cuvettes, TEMED
Serva	Agar, LB agar, bovine serum albumin Ampicillin, isopropanol, absolute ethanol
Sigma-Aldrich	Parafilm, methanol, ethanol, isopropanol, D-sorbitol, 5-fluorocytosine, saponin, SDS, DNase-free RNase, chloroform, 2-mercaptoethanol, Ponceau S-stain, Tris Tween-20, GSH, S-D -lactylolglutathione, methylglyoxal, glyoxal, phenylglyoxal, ascorbate, dithiothreitol, hydrogen peroxide, N-acetyl-L-cysteine
Simax	2L, 3L culture flasks
Steinbrenner	Pipette tips
Ted Pella, Inc	Glass chamber with a lid
Thermo Sci./Menzel-Glaezer	Frosted-end microscope glass slides

All other chemicals and reagents not listed above were obtained in analytical grade from certified distributors including Carl Roth, Merck, Sigma-Aldrich, Serva, Bio-Rad and AppliChem, or prepared using tested standard protocols in the laboratory.

2.3. Plasmids, Primer and Strains

Table 2.1. Table of plasmids used.

Plasmid	Properties/application	Reference
pQE30 <i>GLO1</i>	Amp ^R , Expression of wild-type <i>PfGlo1</i> , N-term. His-tag	(Iozef <i>et al.</i> , 2003)
TOPO-TA	Kan ^R , Amp ^R , Single 3'-thymidine overhang for TA Cloning, Topoisomerase I	Invitrogen
pUF1- <i>Cas9</i>	Expression of Cas9 protein in <i>P. falciparum</i> , 5'hsp : 3' <i>Pb dhfr</i> regulatory elements. NLS, <i>ydhodh</i> - positive selection.	(Ghorbal <i>et al.</i> , 2014)*
pL6	Expression of sgRNA in <i>P. falciparum</i> , 5' U6 : 3' U6 regulatory elements <i>hdhfr</i> - positive selection, <i>ycfu</i> - negative selection.	(Ghorbal <i>et al.</i> , 2014)*
pL7- <i>PFGLO1</i>	pL6 containing guide sequence and HR for generation of <i>PfGlo1</i> knockout strains	This thesis
pL7- <i>PFcGLO2</i>	pL6 containing guide sequence and HR for generation of <i>PfcGlo2</i> knockout strains	This thesis
pL7- <i>PfGLO2</i>	pL6 containing guide sequence and HR for generation of <i>PfGlo2</i> knockout strains	This thesis
pL7- <i>PfGILP</i>	pL6 containing guide sequence and HR for generation of <i>PfGILP</i> knockout strains	This thesis

* Kindly provided by Dr Jose-Juan Lopez-Rubio, Montpellier, France.

Table 2.2. Oligonucleotides used.

Primer No.	Primer Name	Sequence 5' → 3'
P1	<i>PfGlo1</i> /5'fragKO/s:(SacII)	GATCCCGCGGATTGCACAAGAAATATCAAATTTAG

P2	<i>Pf</i> Glo1/5'fragKO/as:(XbaI)	GATC <u><i>CTAGAC</i></u> CCAATAATTATTAGGATCTAAAGC
P3	<i>Pf</i> Glo1/3'fragKO/s:(EcoRI)	GATC <u><i>GAATTC</i></u> CAATGATTAGGGTTAAGAACCC
P4	<i>Pf</i> Glo1/3'fragKO/as:(NcoI)	GATC <u><i>CCATGG</i></u> TTTGCAATAAATGAAGTGTCCC
P5	<i>Pfc</i> Glo2/5'fragKO/s:(SacII)	GATC <u><i>CCGCGG</i></u> TAGCCATGCGCACAAGTAC
P6	<i>Pfc</i> Glo2/5'fragKO/as:(XbaI)	GATC <u><i>CTAGAT</i></u> TGGTTCATATGCTGATCCGAC
P7	<i>Pfc</i> Glo2/3'fragKO/s:(EcoRI)	GATC <u><i>GAATTC</i></u> CGACGGTCAAATTATACGTTTAG
P8	<i>Pfc</i> Glo2/3'fragKO/as:(NcoI)	GATC <u><i>CCATGG</i></u> TAAAGGGTATACTCATGTCCGC
P9	<i>Pft</i> Glo2/5'fragKO/s:(SacII)	GATC <u><i>CCGCGG</i></u> GAGGAAGGTATTGTTGTTGATC
P10	<i>Pft</i> Glo2/5'fragKO/as:(XbaI)	GATC <u><i>CTAGAT</i></u> TCGAGTGTATATTCATGACCAC
P11	<i>Pft</i> Glo2/3'fragKO/s:(EcoRI)	GATC <u><i>GAATTC</i></u> CCCATTCCTAAGATGTGATCAG
P12	<i>Pft</i> Glo2/3'fragKO/as:(NcoI)	GATC <u><i>CCATGG</i></u> TGTCACACTATAATCTATTAACTC
P13	<i>Pf</i> GILP/5'fragKO/s:(SacII)	GATC <u><i>CCGCGG</i></u> GATGGTATAGAATATAAGGTCC
P14	<i>Pf</i> GILP/5'fragKO/as:(XbaI)	GATC <u><i>CTAGAC</i></u> GACTTCAATTCATAACCATC
P15	<i>Pf</i> GILP/3'fragKO/s:(EcoRI)	GATC <u><i>GAATTC</i></u> CCTACGTCAACAAAAGATGCTC
P16	<i>Pf</i> GILP/3'fragKO/as:(NcoI)	GATC <u><i>CCATGG</i></u> TAAACATTATATCCGTCTAGGTC
P17	<i>Pf</i> Glo1/guideRNA/s	TAAGTATATAATATTA <i>AAAGATCCAATCAAGTAAA</i> GTTTTAGAGCTAGAA
P18	<i>Pf</i> Glo1/guideRNA/as	TTCTAGCTCTAAAAC <i>TTAACTTGATTGGATCTTT</i> AATATTATATACTTA
P19	<i>Pfc</i> Glo2/guideRNA/s	TAAGTATATAATATTT <i>ACTTTCTCGTTACACCTG</i> GTTTTAGAGCTAGAA
P20	<i>Pfc</i> Glo2/guideRNA/as	TTCTAGCTCTAAAACC <i>AGGTGTAAACGAGAAAAGTA</i> AATATTATATACTTA
P21	<i>Pft</i> Glo2/guideRNA/s	TAAGTATATAATATTT <i>CAAGTAATGTAGGAACAGT</i> GTTTTAGAGCTAGAA
P22	<i>Pft</i> Glo2/guideRNA/as	TTCTAGCTCTAAAAC <i>ACTGTTCTTACATTACTTGA</i> AATATTATATACTTA
P23	<i>Pf</i> GILP/guideRNA/s	TAAGTATATAATATTT <i>GAGAGCGACAAATTAGATA</i> GTTTTAGAGCTAGAA
P24	<i>Pf</i> GILP/guideRNA/as	TTCTAGCTCTAAAAC <i>TATCTAATTTGTGCTCTC</i> AAATATTATATACTTA
P25	3D7/Cas9/s	CTCTTGGAGA <i>ACTCGCTGATCTG</i>
P26	hDHFR s	CATGGTTCGCTAA <i>ACTGCATC</i>
P27	hDHFR as	CCTTTCTCCTCCT <i>GGACATC</i>
P28	<i>Pf</i> Glo1_5'UTR s	GTGAGTATAGATCCTCATAACA <i>ACTTA CG</i>
P29	<i>Pf</i> Glo1_3'UTR as	CATTGAATAATTGTGCATATATGATATA <i>CACAC</i>
P30	<i>Pfc</i> Glo2_5'UTR s	CGAGGATATGATTTCTTTATTTTATA <i>ACC</i>
P31	<i>Pfc</i> Glo2_3'UTR as	AATCCTTATAAACAGTGACACATT <i>ACAC</i>
P32	3D7/Cas9/as	ACCGAGATTACCCTGGCCA <i>ACG</i>
P33	MCS1 primer pL6	CAAAATGCTTAAGTCC <i>TCCAC</i>
P34	MCS2 primer pL6	AACATTTGCTTTCTTGAA <i>ACGG</i>

P35	SP6 primer	ATTTAGGTGACACTATAGAA
P36	guideRNA Rev	TTATGGTAGCCTTAAAACTTC
P37	<i>Pf</i> Glo2 5'UTR s	ATTATAAAGGCTTGTTACAATTGTGGAATG
P38	<i>Pf</i> Glo2 3'UTR as	TTACAAGAATATATGGAAATAGGGTTACAG
P39	<i>Pf</i> GILP 5'UTR s	TTAAGCCACTTTAATATCAATCC
P40	<i>Pf</i> GILP 3'UTR as	GCTAGCTATTCATAATTTTCATAAC

Introduced restriction sites are underlined; guide sequence and its complementary sequence are capitalized and italicized respectively.

Table 2.3. Table of bacterial and *P. falciparum* strains used.

Strain	Genotype/Description	Reference
<i>E. coli</i> XL 1-Blue	<i>recA1 endA1 hsdR17 supE44 thi-1 recA1 gyrA96 relA1 lac</i> [F' <i>proAB lacIq</i> Δ <i>M15Tn10</i>] (Tet ^R)	Qiagen
NovaBlue	<i>endA1 hsdR17</i> ($\Gamma_{K12}^- m_{K12}^+$) <i>supE44 thi-1 recA1 gyrA96 relA1 lacF'</i> [<i>proA+B+</i> <i>lacI^f</i> Δ <i>M15::Tn10</i>] (Tet ^R)	Novagen
Stellar	<i>F</i> ⁻ , <i>endA1, supE44, thi-1, recA1, relA1, gyrA96, phoA, Φ80d lacZΔ M15, Δ (lacZYA - argF) U169, Δ (mrr - hsdRMS - mcrBC), ΔmcrA, λ</i> ⁻	Clontech
<i>P. falciparum</i> 3D7	Clonal line derived from NF54 (isolated from a person in Amsterdam, The Netherlands)	(Rosario, 1981; Walliker <i>et al.</i> , 1987)*
<i>P. falciparum</i> 3D7Δ <i>glo1</i>	<i>Pf</i> Glo1 knockout clone	This thesis
<i>P. falciparum</i> 3D7Δ <i>glo2</i>	<i>Pfc</i> Glo2 knockout clone	This thesis

*kindly provided by Prof. Dr. M. Lanzer, Heidelberg

3. METHODS

3.1. Design of strategy for *P. falciparum* glyoxalase gene disruption

The gene maps and complete open reading frames of the four *P. falciparum* glyoxalases, *PfGlo1*, *PfcGlo2*, *PftGlo2* and *PfGILP*, were obtained from the *Plasmodium* genomic resource PlasmoDB (PlasmoDB.org) with the gene identification numbers PF3D7_1113700, PF3D7_0406400, PF3D7_1205700 and PF3D7_0604700 respectively. *PFGLO1*, *PFcGLO2*, *PfTgLO2* and *PFGILP* are located on chromosomes 11 (529493 - 530563), 4 (332,043 - 333,856), 12 (253155 - 254123) and 6 (204,640 - 206,207) respectively. The length of the full coding sequence of *PFGLO1*, *PFcGLO2*, *PfTgLO2* and *PFGILP* are 1071 bp, 1814 bp, 969 bp and 1568 bp respectively. Regions within the coding sequences of the genes or areas just extending outside the 3' or 5' untranslated regions were selected as areas to be amplified by PCR for the cloning of the HRs (Table 3.1). The selected regions were areas that had the lowest A-T content in order to avoid non-specific homologous recombination. JustBio (JustBio.com), an online bioinformatics tool, was used to 'clean' gene sequences and to identify restriction sites for fragment selection and cloning.

Table 3.1. 5' and 3' HRs and primers used for PCR amplifications.

Gene locus	Fragment	Primer set	Size of amplicon
<i>PFGLO1</i>	5'	P1 & P2	~ 477 bp
	3'	P3 & P4	~ 521 bp
<i>PFcGLO2</i>	5'	P5 & P6	~ 642 bp
	3'	P7 & P8	~ 442 bp
<i>PfTgLO2</i>	5'	P9 & P10	~ 467 bp
	3'	P11 & P12	~ 640 bp
<i>PFGILP</i>	5'	P13 & P14	~ 612 bp
	3'	P15 & P16	~ 625 bp

3.2. Design and purification of peptide antibodies

For the production of antibodies against *PfGlo1* and *PfcGlo2*, the synthetic peptides NH₂-CLKYQTDEDYENFKQSWEPV-CONH₂ and NH₂-CSAYEPTPGVNEKVYDGGQ-CONH₂ were respectively generated and used to immunize rabbits by Pineda Antibody Service, Berlin, Germany. The two antibodies were subsequently purified from sera of the immunized animals by affinity chromatography according to previously described protocols. Antibody purification and testing were performed by Linda Liedgens. Briefly, the peptides were reduced by 25 mM borohydride in 50 mM Tris/HCl, 5 mM EDTA, pH 8.5 overnight at 4°C. The reduced peptides were coupled for 45 min to 1 ml SulfoLink resin (Pierce, Bonn, Germany). Unspecific binding sites were blocked by 50 mM cysteine solution in 50 mM Tris, 5 mM EDTA, pH 8.5. Chromatography and elution were performed according to the manufacturer's protocol. Antibody-containing eluate fractions were identified on a coomassie-stained 15% sodium dodecyl sulphate (SDS)-gel. Approximately 2*10⁷ purified malaria parasites were analyzed per lane on a SDS-gel followed by western blotting using

preimmune serum (PS), serum (S) and purified antibody (Ab) for decoration of the membrane.

3.3. Plasmid constructs

3.3.1. Cloning strategy of knockout plasmids

The Cas9-encoding plasmid (pUF1-Cas9) and the pL6 plasmid containing the single guide RNA (sgRNA) that carries only the Cas9 binding sequence were generously supplied by Jose-Juan Lopez-Rubio (Ghorbal *et al.*, 2014). pL7 transfection plasmids containing the full complement of the sgRNA expression-cassette (including the 20 bp guide sequence) and the 5' and 3' homologous regions of *PFGLO1*, *PFcGLO2*, *PFtGLO2* and *PFGILP* were generated by multiple cloning steps into the pL6 plasmid. The 3' and 5' homologous regions of each gene were first cloned one-after-the-other into the empty pL6 plasmid to generate plasmids pL6-*PFGLO1*, pL6-*PFcGLO2*, pL6-*PFtGLO2* and pL6-*PFGILP* respectively. The specific guide sequence for each gene was then cloned into the pL6-*PFGLO1*, pL6-*PFcGLO2*, pL6-*PFtGLO2* and pL6-*PFGILP* plasmids to generate the respective pL7 plasmids.

3.3.2. PCR amplification of homologous regions

The 5' and 3' homologous regions of *PFGLO1* were amplified by PCR from the pQE30/*PFGLO1* plasmid (Urscher *et al.*, 2012). The homologous regions of *PFcGLO2*, *PFtGLO2* and *PFGILP* were amplified from genomic DNA (gDNA) of *P. falciparum* 3D7 wild-type strain. All PCR-generated homologous regions were initially sub-cloned into the pCRII-TOPO vector as single entry fragments before they were excised and re-cloned into the pL6 vector. A summary of the sizes of the 5' and 3' fragments together with the primers used for the amplifications PCR is shown in table 3.1. Primers used in this project were ordered from Metabion International AG, Germany, in 100 μ M concentrations as listed in table 2.2. *Taq* DNA polymerase was used for all fragment PCR amplifications in order to generate the 3' deoxyadenosine (A) overlap required for TOPO cloning. All PCRs contained 100 ng (0.5 μ L) of genomic DNA in a reaction mixture with 2 μ L of dNTPs (0.4 mM), 5 μ L ThermoPol *Taq*-buffer, 1 μ L *Taq* DNA polymerase and 0.5 μ L of each primer (1 μ M) in 40.5 μ L of Millipore water. The cycler program used was: 94°C for 3 min, followed by 30 cycles of 94°C 45 s, 58°C 45 s and 68°C 60 s, and then a final extension at 68°C for 2 min and hold at 4°C. PCR reactions were performed in an Eppendorf mastercycler gradient thermal cycler. To analyze the PCR products, 8 μ L of the product was added and mixed with 2 μ L of gel loading dye that was supplemented with Midori green advance DNA stain. Two (2) μ L of Midori green solution was added to the original 1 mL volume of the loading dye, purple 6X (NEB). The samples were then loaded on a 2% agarose gel along with 5 μ L of 100 bp DNA ladder to estimate the length of the PCR products. To enhance ladder-band clarity, the original Quick-Load 100 bp DNA ladder vial (NEB) of 1.25 mL was also supplemented with 2 μ L Midori green advance DNA stain. The gel was ran at 100 V for 30 min in 1x Tris-acetate-EDTA

(TAE) buffer in a Bio-Rad agarose gel running system. To produce the 2% agarose gel, 8 g of agarose powder was heated to melt in an AEG Micromat at 100% for 3 min. The gel was viewed on a gel documentation system transilluminator/ UV and a picture was taken with a camera fitted with a Hama 390 UV filter.

1x TAE buffer 40 mM Tris (pH 7.6)
 20 mM acetic acid
 1 mM EDTA

3.3.3. TOPO cloning of homologous regions

Positive HR PCR products were cloned into TOPO-TA vectors using the TOPO-TA cloning kit from Invitrogen according to the manufacturer's protocol. Briefly, 4 μ L of positive PCR product was mixed with 1 μ L each of salt solution and linearized TOPO vector to give a final reaction volume of 6 μ L. The reaction was incubated at room temperature (22-23°C) for 5 min and then after stored on ice or at -20°C pending transformation. The TOPO reaction was used to transform commercial Novablue chemical competent cells following the manufacturer's protocol. Briefly, 1 μ L of the reaction was gently mixed with 20 μ L of thawed Novablue chemical competent cells and the mixture was stored on ice for 5 min. The mixture was heat-shocked at 42°C for 30 s on a heating block and immediately returned to ice for 2 min. Eighty (80) μ L of room-temperature super optimal broth with catabolite repression (SOC) was added and gently mixed. To regenerate the cells, the mixture was incubated whilst shaking at 37°C (250 rpm, orbital shaking) for 30 min. Fifty (50) and 150 μ L of the transformed cell suspension were plated and selected on kanamycin agar overnight at 37°C in a laboratory incubator after sealing the plates with parafilm. Plates with grown colonies were removed and stored at 4°C pending plasmid expansion, extraction and purification.

3.3.4. Plasmid miniprep preparation from *E. coli* cells

TOPO-TA plasmid DNA was extracted and purified by miniprep preparation of plasmid DNA based on alkaline lysis of transformed *E. coli* cells (Birnboim & Doly, 1979). Briefly, several single colonies from each plate were picked and used to inoculate sterile glass test tubes containing 3 mL of autoclaved lysogeny broth (LB) medium that was supplemented with ampicillin to a final concentration of 100 μ g/mL. The cultures were transferred to an Inforts triple stack shaker and incubated overnight at 37°C whilst shaking (130 rpm, orbital shaker). Bacterial cells were harvested by the step-wise transfer of each of the overnight cultures into a 2 mL microtube and centrifugation at 16 000 g in a microfuge for 30 s at 4°C. After discarding the supernatant, the cell pellets were thoroughly dried and completely resuspended in 100 μ L of ice cold buffer 1. To lyse the cells, 200 μ L of room-temperature buffer 2 was added to the cell suspensions and gently mixed by inverting the tube five times. The mixtures were incubated at room temperature for 5 min to ensure complete cell lysis. One hundred and fifty (150) μ L of ice cold buffer 3 was added to each mixture to neutralize the pH and precipitate the genomic DNA and proteins. After mixing by gently inverting the tube 3 times,

the suspensions were centrifuged at 16 000 g in a microfuge for 10 min at 4°C. The clear supernatants were decanted into a 1.5 mL micro tubes and the plasmid DNA precipitated by adding 600 µL of room-temperature isopropanol. The tubes were inverted 3 times and the suspensions were centrifuged at 16 000 g for 5 min at 4°C to pellet the plasmid DNA. Note was taken of the position of the formed DNA pellets for each preparation and the supernatants was gently removed by aspiration using a molten glass pipette. Six hundred (600) µL of 70% ethanol (-20°C) was added and the tubes inverted 3 times to wash the pellets. The suspensions were again centrifuged at 16 000 g for 5 min at 4°C and the supernatants completely removed by aspiration. The plasmid DNA pellets was finally dried under red light for 10 min, dissolved in 30 µL of autoclaved Millipore water and stored at -20°C. To analyze the extracted TOPO-TA plasmids for integration of the 5' and 3' fragments of each gene, 4 µL of each plasmid suspension was digested with the restriction enzyme *EcoRI* (NEB) according to NEB recommendations and ran on a 1% agarose gel. Positive plasmids were checked for the fidelity of the integrated 5' and 3' fragments by Sanger sequencing (GATC Biotech, Cologne Germany) using the GATC Biotech SP6 TOPOTA plasmid negative sense primer, P23. A 1:4 dilution of plasmid in a total volume of 20 µL was sent for sequencing. Positive plasmids of high sequence fidelity were stored at -20°C pending pL6 cloning.

Buffer 1	10 mM EDTA, pH 8.0 50 M Tris 0.1 mg/ml RNase A (store Buffer 1 at 4°C)
Buffer 2	1% (w/v) SDS 200 mM NaOH (store Buffer 2 at room temperature)
Buffer 3	60 ml 3 M potassium acetate 11.5 ml glacial acetic acid 28.5 ml millipore water (store Buffer 3 at 4°C)

3.3.5. Cloning of homologous regions into the pL6 plasmid

To generate the pL6-*PFGLO1*, pL6-*PFcGLO2*, pL6-*PFtGLO2* and pL6-*PFGILP* plasmids, the pL6 plasmid was first amplified. This was achieved by transforming home-made XL1-Blue chemical competent cells with the plasmid following the protocol described above but with slight changes. Briefly, 3 µL of plasmid was mixed with 50 µL of competent cells and stored on ice for 30 min. The suspension was then heat-shocked at 42°C for 90 s in a heating block and transferred to ice for 5 min. Five hundred (500) µL of room-temperature LB medium was added to the suspension and incubated at 37°C while shaking at 500 rpm on a heating block for 1 hr. Fifty (50) and 150 µL aliquots were plated on ampicillin selection agar and grown overnight at 37°C in a laboratory incubator. Plasmid expansion, extraction and purification were achieved through minipreparation as described above for TOPO-TA plasmid. For the cloning steps, the 3' and 5' fragments were excised from the TOPO-TA vector using double restriction digestion according to NEB protocol. Restriction enzyme-pairs used to excise the 5' and 3' fragments from the TOPO-TA plasmids were *SacII/XbaI* (NEB)

and *EcoRI/NcoI* (NEB) respectively. pL6 plasmids were also step-wise double digested with the enzymes *EcoRI/NcoI* for cloning-in the 3' fragment and *SacII/SpeI* for cloning-in the 5' fragments. Digested TOPO-TA and pL6 plasmids were run on 2% and 0.8% agarose gels respectively. Gel portions containing the fragments and linearized pL6 plasmid were cut out and collected in 2.0 mL microtubes. The gel pieces were purified using the Wizard SV gel and PCR clean-up system (Promega Corporation) according to the manufacturer's instructions and stored at -20°C. Ligation of the fragments and the linearized plasmid was performed according to NEB protocol. Briefly, 1 µL of purified plasmid, 4 µL of purified fragment, 2 µL of T4 ligase buffer (NEB) and 1 µL T4 ligase (NEB) were adjusted to a total reaction volume of 20 µL with autoclaved Millipore water in a 0.5 mL micro tube. The reaction was incubated overnight at 16°C and then heated to 65°C for 10 min in a heating block to inactivate the ligase. Eight (8) to 15 µL of the ligation mixture was used to transform 50 µL of home-made XL1-Blue competent cells as described above. Transformed cells were plated and selected on ampicillin agar that was subsequently incubated overnight at 37°C in a laboratory incubator. Plasmid expansion, extraction and purification were achieved as described above. The integration of the 3' and 5' fragments into the plasmid was controlled by PCR and Sanger sequencing. For the PCR control, the primer sets P1/P33, P5/P33, P9/P33 and P13/P33 were used to check for 5' fragment integration on the pL6-*PFGLO1*, pL6-*PFcGLO2*, pL6-*PFtGLO2* and pL6-*PFGILP* plasmids respectively (Table 2.2). To check for the 3' fragment integration, the primer sets P3/P34, P7/P34, P11/P34 and P15/P34 were used for the pL6-*PFGLO1*, pL6-*PFcGLO2*, pL6-*PFtGLO2* and pL6-*PFGILP* plasmids respectively (Table 2.2). The PCR conditions and cyler program followed the same parameters used to amplify fragments as described above. Primers P33 and P34 were also used to respectively sequence the integrated 5' and 3' fragments of all four plasmids (Table 2.2).

3.3.6. Cloning of guide sequence into the pL6 plasmid

To generate plasmids pL7-*PFGLO1*, pL7-*PFcGLO2*, pL7-*PFtGLO2* and pL7-*PFGILP*, the *BtgZI*-adaptor on the sgRNA of the pL6-*PFGLO1*, pL6-*PFcGLO2*, pL6-*PFtGLO2* and pL6-*PFGILP* plasmids was replaced by the guide RNA (gRNA) using the In-Fusion HD cloning kit from Clontech following the manufacturer's protocol. In-Fusion HD cloning procedure employs a special In-Fusion enzyme to join complementary 15 bp overlaps on the pL6 plasmid and on specially designed 50 bp primers that also carry the specific guide sequence (gRNA) of each target gene. Twenty- (20)-base gRNAs for each target were designed flanked with the 15 bases (necessary for In-Fusion cloning) using the Protospacer software and ordered as two complementary oligonucleotides (guide sequence primers). The guide sequence primer pairs for cloning of the pL7-*PFGLO1*, pL7-*PFcGLO2*, pL7-*PFtGLO2* and pL7-*PFGILP* were P17/P18, P19/P20, P21/P22 and P23/P24 respectively (Table 2.2). The modified pL6 vectors were first amplified, extracted and purified, as described above, to obtain enough plasmid DNA for the reaction. Ten (10) µL of purified plasmid was digested stepwise with *AvrII* and *BtgZI*. The plasmid was first digested with *AvrII* for 2 hr at 37°C and then *BtgZI* for 2 hr at 60°C. For the cloning procedure, the excised plasmid was separated on a 1% agarose gel and purified using the Wizard SV Gel and PCR clean-up system. The plasmid concentration was subsequently determined on a gel by band intensity analysis. Fifty

(50) μL of each guide sequence primer pair were mixed in a 0.5 mL micro tube, heated at 94°C for 2 min and slowly cooled down to anneal. In the ligation step, approximately 100 ng of purified linearized plasmid and 50 ng of duplex oligonucleotide were mixed with 2 μL of In-Fusion HD enzyme. The mixture was topped up with distilled water to a final reaction volume of 10 μL , incubated for 15 min at 50°C and then placed on ice or stored for longer periods at -20°C pending transformation. In-Fusion reaction products were used to transform Stellar chemical competent cells from Clontech following the producer's directions. Briefly, 5 ng (2.5 μL) of reaction product was mixed with 50 μL of Stellar chemical competent cells. The cell suspension was placed on ice for 30 min and heat shocked for exactly 60 s at 42°C . The suspension was transferred back to ice for 2 min, 450 μL of 37°C pre-warmed SOC was added and then after incubated at 37°C while shaking (225 rpm) for 1 hr on a heating block. Twenty (20) μL , 50 μL and 100 μL of the transformed cell suspension as well as 50 μL of a 1 in 100 dilution in SOC medium were plated and selected on ampicillin plates. The rest of the suspension (about 330 μL) was centrifuged for 5 min at 6000 rpm and plated after 200 μL of the supernatant was discarded. The plates were incubated overnight at 37°C . Plasmid expansion, extraction and purification were achieved by minipreparation as described above for pL6 plasmid. The integration and sequence fidelity of the cloned-in guide sequence of each pL7 plasmid was confirmed by PCR and Sanger sequencing. PCR analyses were performed using the primer pairs P17/P24, P19/P36, P21/P36 and P23/P36 to control the guide sequence integration on the pL7-*PFGL01*, pL7-*PFcGLO2*, pL7-*PFtGLO2* and pL7-*PFGLP* plasmids respectively (Table 2.2). PCR conditions and cycler program followed the same parameters used to amplify the fragments from genomic DNA as described above. Sequencing was done using primer P36 (Table 2.2).

3.3.7. Maxipreparation of pL7 plasmid for transfection

To produce appropriate quantities of pL7 plasmid DNA for the transfection of *P. falciparum* 3D7 wild-type strains, a maxipreparation of controlled plasmids was performed using a Qiagen plasmid maxi kit according to the manufacturer's instructions. Briefly, 2 μL of minipreparation of each plasmid was used to transform 50 μL of home-made XL1-Blue competent cells as described above for the transformation with pL6 plasmids. A single colony from each plasmid plate was picked and used to inoculate a sterile glass test tube of 3 mL starter culture made up of autoclaved LB medium supplemented with ampicillin to a final concentration of 100 $\mu\text{g}/\text{mL}$. The cultures were transferred to an Infors triple stack shaker and incubated at 37°C for 8 hr whilst shaking (130 rpm, orbital shaker). After the incubation, 500 μL of each culture was used to inoculate 500 mL of autoclaved LB medium supplemented with ampicillin to a final concentration of 100 $\mu\text{g}/\text{mL}$ in a 2 liter flask. The cultures were grown while shaking at 300 rpm in a triple stack shaker set at 37°C . Bacterial cells from each culture were harvested after 16 hr of growth and transferred into two 500 mL J10 rotor centrifuge buckets. The cells were pelleted by centrifugation at 6 000 g for 15 min at 4°C in a Beckmann centrifuge using a J10 rotor. Each cell pellet (about 1.7 g) was resuspended in 10 mL of resuspension buffer (P1) and then transferred to a 30 mL J17 rotor centrifuge tube. Cell lysis was performed by the addition of lysis buffer (P2). Suspensions was thoroughly mixed and incubated at room temperature for 5 min to ensure complete cell lysis. Ten (10) mL of ice cold neutralizing buffer (P3) was added and the mixtures were incubated on ice for 20 min to

neutralize the pH and precipitate the genomic DNA and proteins. The mixtures were subsequently centrifuged at 20 000 g for 30 min at 4°C in a Beckmann centrifuge using a J17 rotor. Each plasmid supernatant was promptly transferred into a fresh sterile J17 rotor centrifuge tube and centrifuged again at the same speed and temperature for 15 more min to further clear the supernatant. The clear supernatants were loaded onto different Qiagen-tip 500 column that was already equilibrated with 10 ml of equilibration buffer. After DNA binding to the column resin and after discarding the follow-through, the columns were washed with 60 mL of wash buffer (QC) to remove carbohydrates and other plasmid contaminants. Purified plasmid DNA was then eluted with 15 mL of elution buffer (QF) into fresh sterile J17 rotor centrifuge tubes. Ten and half (10.5) mL of isopropanol at room-temperature was added to each DNA elution and mixed to precipitate the DNA. The mixtures were centrifuged at 15 000 g for 30 min at 4°C in a Beckmann centrifuge using a J17 rotor to pellet the plasmid DNA. Note was taken of the sites of DNA pellet formation on the tubes during centrifugation. After decanting the supernatants, each DNA pellet was washed once with 70% ethanol that was at room-temperature and then centrifuged again for 15 min at the same speed and temperature. The pellets were air-dried for 10 min after carefully decanting the supernatants. The air-dried DNA was finally redissolved in 250 µL of Tris-EDTA (TE) buffer and a 2 µL aliquot of each DNA suspension was taken for determination of the concentration using a Nanodrop spectrophotometer. Pending transfection, the purified plasmid DNA samples were stored at -20°C.

TE buffer 10 mM Tris, pH 8.0 with HCl
 1 mM EDTA

3.4. *P. falciparum* cell culture

3.4.1. *P. falciparum* parasite culture

Culture of *P. falciparum* parasites was performed aseptically on a cell culture sterile bench. Culture media, solutions, flasks, plates, tubes, equipment, pipettes and drugs were sterilized or autoclaved before use to avoid contamination. Parasite cultures were performed using fresh and steril human A⁺ red blood cells which were kindly provided by the laboratory of Prof. Michael Lanzer, Heidelberg. Sterile gloves were worn at all times when working on the sterile bench and handling cell culture materials. After every work day, the sterile bench was sterilized with U-V light for one hour. The sterile bench was then started 15 min before work commences again. The working area and gloves were disinfected with 70% ethanol before beginning every cell culture session. The Isotemp 210 water bath for prewarming media and solutions was cleaned regularly, and the water was replaced with fresh Millipore water that was supplemented with Akasolv aqua care. The parasite incubator and cell culture centrifuge were also kept clean and disinfected at all times.

3.4.2. Thawing and cultivation of parasite strains

Thawing of glycerol frozen stocks of *P. falciparum* strains followed the method of Stanisic *et al.* (Stanisic *et al.*, 2015) with slight changes. Suspension of cells in cryo-protectants such as glycerol and then freezing in liquid N₂ is effective and increases parasite survival in and after long storage (Miyake *et al.*, 2004). To ensure parasite recovery, survival and viability, the thawing process also involves a method of stepwise suspension cells in three sterile solutions of reducing concentrations of sodium chloride (NaCl). The general effect of the serial application of these solutions is to gradually reconstitute isotonicity of the parasite after the thawing process (Diggs *et al.*, 1975).

A culture of erythrocyte-stage *P. falciparum* 3D7 wild-type strains or transgenic parasite strains was started from a frozen glycerol stock that was previously stored in liquid nitrogen (N₂) in a 2 mL cryovial. The cryovial was removed from the nitrogen tank with a pair of tweezers and quickly thawed for 1 min in a 37°C water bath. The vial was then disinfected and taken to the sterile bench where the content was transferred into a 15 mL Falcon tube using a 1 mL serological pipette. A small volume of solution A (0.2 volumes) that was sterile-filtered with a 0.22 µm filter and prewarmed at 37°C was added drop-wise to the infected erythrocytes while swirling to allow osmosis to occur. The cell suspension was incubated for 2 min to allow the removal of glycerol from the cells. Ten (10) volumes of prewarmed and sterile-filtered solution B was next added drop-wise to the suspension using a 10 mL serological pipette while swirling. The erythrocytes were pelleted by centrifugation at 1198 rpm (300 g) in the Heraeus multifuge for 5 min at room temperature and the supernatant was discarded. The cell pellet was then resuspended in 10 volumes of sterile-filtered solution C and centrifuged again at 300 g for 5 min at room temperature. Most of the supernatant was again discarded and the cell pellet was washed once with 10 ml of complete RPMI medium. After a final centrifugation step to pellet the washed infected-erythrocytes, the supernatant was discarded and the cell pellet was resuspended in 8 mL of complete medium. Finally, the cell suspension was transferred to a new 100 x 20 mm culture petri dish or a 250 mL culture flask that already contained 500 µL of fresh, washed human A+ red blood cells (RBCs) in 6 mL of complete RPMI medium. The starting culture volume was thus set at 14.5 mL with a hematocrit of 3.5%. The new culture was resuspended, transferred to a CO₂ incubator and cultured according to the method of Trager and Jensen (Trager & Jensen, 1976). All pipetting steps were performed with sterile 1 mL or 10 mL pipettes to avoid contamination. The incubation conditions were set at 36.5°C, 5% O₂, 5% CO₂ and 80% humidity. Culture medium was replaced every 24 hr with fresh complete RPMI medium. Giemsa-stained blood smears were performed after 48 hr to determine the culture parasitemia by counting and averaging three microscopic fields using a light microscope (Carl-Zeiss). At ≤ 7% ring parasitemia, the culture was split to a desired parasitemia to maintain the parasites well-nourished and healthy.

Solution A	12% NaCl
Solution B	1.6% NaCl
Solution C	0.9% NaCl
	0.2% (v/v) glucose (energy source)

Complete RPMI medium	incomplete RPMI 1640 medium (500 mL)
	0.45% (w/v) albuMAX II
	2.7 µg/mL gentamicin
	0.2 mM hypoxanthine

3.4.3. Splitting the culture

To split a culture to a desired parasitemia, a new culture petri dish or culture flask was set up containing 14 mL of complete culture medium (minus the volume of the original culture to be added to it to make the culture dilution). Four (4) mL of supernatant was removed from the original 14 mL culture to be split and the remaining culture (10 mL) was resuspended. The estimated volume of original culture to make the new parasitemia was pipetted and added to the new petri dish or flask. Five hundred (500) µL of fresh erythrocytes (minus the volume of erythrocytes added from the old culture), was added to the new culture to give a new starting hematocrit of 3.5% in a final culture volume of 14.5 mL. The new culture suspension was mixed, transferred to the incubator and cultured under standard conditions.

3.4.4. Determination of parasitemia and culture viability

The estimation of culture parasitemia and determination of parasite viability were carried out using Giemsa-stained thin blood smears. A portable laboratory Bunsen burner and a lighter were disinfected with 70% ethanol and moved onto the sterile bench along with two microscope glass slides with frosted ends. The culture to be analyzed was also gently moved onto the sterile bench. Using the tip of a 1 mL pipette that was briefly flamed in Bunsen burner fire to create a wider slanting opening, infected erythrocytes were removed from the bottom of the slightly tilted flask and transferred to the upper part of one of the glass slide that was also labeled. With the second slide, the erythrocyte drop was smoothly and gently spread along the labelled slide. The culture was returned to the incubator. The smeared slide was allowed to air-dry and the infected-erythrocytes fixed for 10 seconds in 100% methanol in a glass chamber with a lid. After fixation, the slide was allowed to dry in air before the smear was stained for 30 min in 40 mL of 4% (v/v) Giemsa solution that was freshly prepared in deionised water. Excess stain was washed off both sides of the slide using a strong jet of deionised water. The slide was subsequently dried using a paper towel and analyzed under a light microscope (using the 100 x objective with oil immersion). Employing the incorporated objective grid, the parasitemia was estimated from five (5) to seven (7) random microscope fields (750-1500 erythrocytes). The morphology of the parasites in the erythrocytes was also assessed as one of the signs of parasite viability.

3.4.5. Synchronization of parasite growth

The method of synchronization proceeded as described by Lambros and Landerberg (Lambros & Vanderberg, 1979) but with slight modification. To obtain synchronized cultures,

parasites were treated with 5% (v/v) D-sorbitol. Sorbitol treatment causes selective destruction of trophozoites and schizonts in a mixed-stage *P. falciparum* culture (Lambros & Vanderberg, 1979). A Giemsa-stained thin blood smear was thus first performed to confirm that the culture to be synchronized contained mostly parasites at the young ring-stage of development. To proceed with synchronization, the culture was resuspended in the old medium with a 10 mL pipette on the sterile bench and transferred to a 15 mL Falcon tube. Infected erythrocytes were pelleted by centrifugation of the suspension at 300 g in a Heraeus multifuge for 5 min at room temperature. After discarding the supernatant back on the sterile bench, the pellet was thoroughly resuspended in 10 volumes of sterile-filtered 5% D-sorbitol that was pre-warmed to 37°C. The suspension was incubated for 5 min at room temperature and then after centrifuged at 300 g for 5 min at room temperature to pellet the treated infected-erythrocytes. To remove residual D-sorbitol, the pellet, after discarding the supernatant, was washed in 10 mL of pre-warmed complete RPMI medium and centrifuged at 300 g for 5 min. The supernatant was again discarded. The washed cell pellet was finally resuspended in 14 mL of prewarmed complete medium, transferred into a new culture petri dish and maintained under standard culture conditions as above.

3.4.6. Cryopreservation of *P. falciparum* parasites

Long-term storage of wild-type and mutant strains of *P. falciparum* was achieved by suspending parasites in a freezing solution that contains 28% (v/v) glycerol following the method described by Stanissic and colleagues (Stanissic *et al.*, 2015). A Giemsa-stained blood smear was first performed to confirm that the cultured parasites to be frozen were in the ring-stage of development and have a parasitemia of more than 3%. The sterile-filtered freezing solution was prewarmed to 37°C and transferred to the sterile bench. A 2 mL sterile cryovial was also transferred to the sterile bench and labeled. The ring-stage culture (14.5 mL) was first resuspended in the old medium, transferred to a 15 mL Falcon tube and centrifuged at 300 g in the Heraeus multifuge for 5 min at 23°C. After discarding the supernatant back on the sterile bench, the cell pellet was resuspended in 500 µL of freezing solution. The freezing solution was added drop-wise while swirling after each drop. The cell suspension (about 1 mL) was then transferred into the labeled cryovial. The vial was tightly closed, snap-frozen in a Dewar vessel for 1 minute and then transferred with a pair of tweezers to a liquid nitrogen tank for long-term storage.

Freezing solution	28% (w/v) glycerol
	0.65% (w/v) NaCl
	3% (w/v) sorbitol

3.5. Transfection and selection of transgenic parasites

Transfection of *P. falciparum* parasites was performed using the erythrocyte pre-load method of electroporation and involved an indirect and consecutive introduction of the pUF1-Cas9 and pL7 plasmids into the parasite (Deitsch *et al.*, 2001; Hasenkamp *et al.*, 2012).

Transfection of parasites with the pUF1-Cas9 plasmid was performed first. Transgenic parasites expressing the *Cas9* gene were then transfected with the different pL7 plasmids.

3.5.1. Transfection of the pUF1-Cas9 plasmid

Transfection of *P. falciparum* 3D7 wild-type strain with the pUF1-Cas9 plasmid proceeded as described below. Hundred (100) μg of plasmid DNA ($\approx 900 \text{ ng}/\mu\text{L}$) in a 2 mL micro tube was prepared for transfection by adding a volume of 3 M (pH 5) sodium acetate to make a final concentration of 0.3 M. Total volume of the plasmid DNA suspension was adjusted with autoclaved Millipore water to 200 μL . Five hundred (500) μL of absolute ethanol that was stored at -20°C was added to precipitate the DNA and the suspension was vortexed for 3 min. To enhance the precipitation of the plasmid DNA, the suspension was incubated at -20°C for 30 min. The plasmid DNA was subsequently pelleted by centrifugation at 20 800 g for 30 min at 4°C . After discarding the supernatant, the DNA pellet was washed in 500 μL of 70% ethanol that was stored at -20°C and centrifuged at 20 800 g for 15 min at 4°C . The supernatant was discarded and the washed plasmid DNA pellet was air-dried on the sterile bench for 10 min after which it was resuspended in 30 μL of TE (Tris-EDTA) buffer, pending transfection. In addition, fresh and sterile erythrocytes were washed in preparation for electroporation. Two (2) mL of the red blood cells were suspended in 6 mL of cold sterile-filtered incomplete cytomix (transfection medium) in a 15 mL Falcon tube. The suspension was centrifuged at 800 g for 2 min. After discarding the supernatant, the wash step was repeated and the supernatant was discarded.

For the transfection process, the parasitemia of a 14 mL schizont-stage synchronized culture of *P. falciparum* 3D7 wild-type parasites was estimated by Giemsa-stained thin blood smears. The culture was then resuspended in old medium and diluted to 1% parasitemia in a new petri dish with appropriate volumes of sterile, fresh erythrocytes and complete medium. The diluted culture was resuspended, transferred to a sterile 15 mL Falcon tube and centrifuged at 300 g for 5 min at 23°C . After discarding the supernatant, 100 μL of the infected erythrocytes were aliquoted into a new flask and resuspended in 8 mL of complete culture medium.

The prepared plasmid DNA (30 μL) was next resuspended in the 2 mL micro tube together with 400 μL each of cold transfection medium and fresh, sterile and washed erythrocytes. Approximately 400 μL of the mixture was transferred to each of two pre-cooled transfection cuvettes and incubated on ice for 5 min. Electroporation was executed for each cuvette at a voltage of 0.3 KV and a capacitance of 950 μF using a Bio-rad electroporation system. The cuvettes were incubated on ice for 5 min after electroporation, and aseptically moved back to the sterile bench. The electroporated erythrocytes were resuspended in 2 x 4 mL of transfection medium and transferred into a 15 mL Falcon tube. After centrifugation at 800 g for 2 min at 23°C , the supernatant was discarded and the cell pellet was resuspended in 6 mL of prewarmed complete RPMI medium. The cell suspension was transferred into the culture flask containing 8 mL of infected red blood cell (RBC) suspension that was prepared earlier. The new 14.5 mL culture of 3.5% hematocrit and a starting parasitemia of approximately 0.2% was returned to the incubator and maintained under standard conditions.

For the selection of parasites expressing *yDHODH* and *Cas9*, atovaquone (Sigma-Aldrich) was administered at a final culture concentration of 100 nM 20 hr post-transfection. From the second to the sixth day post transfection, drug and medium were renewed every 24 hr. After the first week, drug and medium were renewed every other day. Seventy (70) μ L of fresh erythrocytes were also added to the culture once every week until resistant parasites were detected by Giemsa-stained thin blood smears. Transgenic parasites were immediately split and cultured in several plates to be used later to prepare parasite glycerol freeze-downs and to extract gDNA for PCR control of plasmid uptake. Transgenic confirmed by PCR to be *Cas9*-expressing parasites were cultured and transfected with the pL7 plasmids.

Incomplete cytomix 120 mM KCl, 0.15 mM CaCl₂, 2 mM EGTA, 5 mM MgCl₂,
10 mM K₂HPO₄, 10 mM KH₂PO₄, 25 mM Hepes, pH 7.6 at RT

3.5.2. Transfection of the pL7 plasmid

For the second step of transfection, 100 μ g of the pL7-*PFGLO1*, pL7-*PFcGLO2*, pL7-*PfGLO2* or pL7-*PFGILP* plasmids was used to transfect *Cas9*-expressing transgenic strains following the preload method described above. Briefly, fresh and washed human A⁺ cells were preloaded with each of the four different pL7 constructs. Four hundred (400) μ L of preloaded erythrocytes were subsequently washed and mixed with 100 μ L of erythrocytes infected with *Cas9*-expressing transgenic parasites. The new 14.5 mL transfection culture of about 3.5% hematocrit and a starting parasitemia of approximately 0.2% was subsequently maintained under standard culture conditions. Positive selection for *hdhfr* integration and expression with WR99210 (WR) (Courtesy of David Jacobus, *Jacobus Pharmaceuticals*, Priston, NJ) commenced 20 hr post-transfection at a final concentration of 2.7 nM. The drug treatment regime proceeded as described above for atovaquone until transgenic parasites that were resistant to WR were detected in Giemsa-stained blood smears. As soon as transgenic parasites were detected, cultures were split into several plates to generate enough parasites for freeze-storage and to proceed with negative selection. Negative selection against unintegrated pL7 plasmid or single-crossover events was achieved with 40 μ M 5-fluorocytosine (5-FC) (Sigma-Aldrich) for 9 days while maintaining WR pressure. Transgenic mixed-culture parasites detected by Giemsa-stained thin blood smears after negative selection were split into several plates and amplified for further freeze-storage and genomic DNA analysis. Parasites from plates that were confirmed by preliminary PCR analysis to contain knockout strains were cultured further and used to perform a limiting dilution for the generation of single clone knockout parasites.

3.5.3. Limiting dilution and generation of single knockout clones

Generation of single clone knockout parasites from a mixed-population of transfectants followed the method described by Butterworth and colleagues (Butterworth *et al.*, 2011) with slight modifications. The dilution was performed from a 14.5 mL transgenic *P. falciparum* parasite culture that was sorbitol-synchronized at the trophozoite-stage. The parasitemia of the

culture was first estimated by Giemsa-stained thin blood smears. The culture was subsequently resuspended in old culture medium on the sterile bench, mixed well and a 200 μL aliquot was removed into a 1.5 mL micro tube. Fifteen (15) μL of the well-mixed aliquot was used to estimate the RBC concentration per mL of culture using a hemocytometer. Using the estimated parasitemia and erythrocyte concentration, the original trophozoite culture was diluted in a 15 mL Falcon tube with prewarmed complete culture medium and washed fresh erythrocytes. The dilution was to obtain a cell suspension that contained approximately one parasite or less per 200 μL of culture and a hematocrit of 2%. 200 μL of the diluted culture was dispensed after resuspension into each of the 24 wells of rows A & B of a 96 well culture plate. 1/10 and 1/100 dilutions of the original dilution were also made in separate 15 mL Falcon tubes. 200 μL of these further diluted cultures were also dispensed into each of the 24 wells of rows C & D and rows E & F for 1/10 and 1/100 dilutions respectively. 200 μL of an erythrocyte culture of 2% hematocrit but with no parasites was dispensed into the 24 wells of rows G & H to serve as negative control wells. The plate was incubated at standard culture conditions. On days 4, 7, 11, 14, 17 and 21, 140 μL of the culture medium was replaced using a 20-200 μL multichannel pipette. Giemsa-stained blood smears were performed to check for growth on days 14 and 21. As soon as parasites appeared in any of the wells, the culture of those wells was amplified into 14.5 mL cultures. Preference was given to the clones from the wells that contained a lower dilution of parasites. Amplified clone cultures were subsequently split and recultured to extract gDNA for control PCRs and for parasite freeze-downs when confirmed positive for glyoxalase gene disruption.

3.6. Genome and western blot analyses of clonal knockout lines

3.6.1. Saponin lysis of infected erythrocytes and purification of parasites

Saponin lyses the membranes of infected and uninfected red blood cells. It also damages the Maurer's cleft and the membrane of the parasitophorous vacuole without affecting the parasite or its membrane (Heiber & Spielmann, 2014). Saponin is therefore a convenient reagent for the isolation of intact parasites for protein and genomic analyses. Depending on the analysis to be performed with the purified parasites, different procedures of saponin lysis were followed. For the extraction of parasite genomic DNA, erythrocytes were lysed with 0.05% (w/v) saponin in modified Ringer solution (lysis buffer) following the method by Elandalloussi and Smith, and others (Elandalloussi & Smith, 2002 ; Doolan, 2002) with slight modification. Briefly, a 14 mL culture of late schizont or early ring-stage at $\geq 5\%$ parasitemia was resuspended in old medium and transferred into a 15 mL Falcon tube. The suspension was centrifuged at 755 g in a Heraeus multifuge for 5 min at 23°C. After completely discarding the supernatant, the cell pellet was resuspended in 10 mL of ice-cold lysis buffer and incubated on ice for 10 min. The erythrocyte cell lysate was centrifuged at 1800 g for 10 min at 23°C to pellet the parasites. After discarding the lysed erythrocyte supernatant, the parasite pellet was resuspended in 1.5 mL of modified Ringer solution, transferred into a 2 mL micro tube and centrifuged again at the same speed and temperature for 10 min. The supernatant was again discarded and the wash step repeated. The parasite pellet was subsequently resuspended in 190 μL of room temperature TE-buffer pending gDNA isolation.

For the extraction of parasite proteins for western blot analysis, erythrocytes were lysed with 0.1% (w/v) saponin in phosphate buffered saline (PBS) following the method of Hsiao and colleagues (Hsiao *et al.*, 1991) with slight modification. Briefly, a 35 mL trophozoite-stage culture of $\geq 5\%$ parasitemia was resuspended in old medium and transferred to a 50 mL Falcon tube. The suspension was centrifuged at 1000 g in a Heraeus multifuge for 5 min at 23°C. After completely discarding the supernatant, the erythrocyte pellet was resuspended in 9 mL of ice-cold PBS. 1 mL of 1% saponin solution in PBS was added to the cell suspension and mixed well. Erythrocyte lysis was allowed to progress for 60 s on ice after which the lysate was centrifuged at 2000 g for 10 min at 4°C. The supernatant was removed and the parasite pellet was washed two times with 10 mL of ice-cold PBS. The pellet was resuspended in 1 mL of ice-cold PBS/Protease inhibitor (Roche) (PBS/PI) solution and transferred to a 1.5 mL micro tube for a last wash at 20800 g for 1 min at 4°C. The protease inhibitor neutralized the effect of released proteases. After discarding the supernatant, the parasite pellet was immediately processed to extract parasite proteins or snap-frozen and stored in liquid N₂ pending future parasite protein analysis.

Modified ringer solution	115 mM NaCl, 10 mM KCl, 1.2 mM CaCl ₂ , 0.8 mM MgCl ₂ , 5.5 mM glucose, 1.0 mM NaH ₂ PO ₄ , 10 mM HEPES pH 7.1 at 37 °C
PBS	1.84 mM KH ₂ PO ₄ , 10 mM Na ₂ HPO ₄ , 137 mM NaCl, 2.7 mM KCl, pH 7.4 at 24°C
PBS/PI	1 tablet of protease inhibitor cocktail/50 ml PBS

3.6.2. Isolation and purification of genomic DNA of knockout strains

The method of isolation and purification of parasite genomic DNA was adopted from a technique used by Denise L. Doolan (Doolan, 2002). Proteinase K solution was added to the parasite cell suspension from saponin lysis (above) to a final concentration of 20 µg/mL. To remove parasite membrane, 20% SDS solution was also added to make a final concentration of 0.5%. The cell suspension was gently inverted several times in the tube and incubated overnight at 55°C in a heating block to liberate the gDNA from the lysed cells and neutralize all liberated parasite proteins. After incubation, the lysate was allowed to cool down to room temperature. DNase-free RNase (Sigma-Aldrich) solution was added to the cooled lysate to a final concentration of 60 µg/mL and the lysate was again incubated for 1 hr at 37°C to destroy all RNA contamination. After the lysate was allowed to cool down to room temperature, 400 µL of phenol/chloroform/isoamylalcohol solution (Carl-Roth) was added to trap debris of cell lysis including proteins. The suspension was mixed by slowly rotating the micro tube on programmable rotator mixer (Grant-Bio) for 10 min. gDNA was isolated from the trapped cell debris by centrifugation at 14000 g at room temperature in a microfuge. The upper aqueous layer containing the gDNA was transferred to a new micro tube using a cut pipette tip to avoid damage to the DNA. The isolation step was repeated one more time and subsequently 200 µL of absolute chloroform was added to the removed upper aqueous layer. The

suspension was slowly mixed on a programmable rotator mixer for 5 min and then centrifuged at 14000 g for 5 min at room temperature. The upper aqueous layer was carefully transferred without contamination into a new 1.5 mL micro tube. DNA-bound proteins were further removed by adding 1/10 volume of ice-cold sodium acetate buffer to the suspension. gDNA was precipitated by adding 2.5 volumes of absolute ethanol stored at -20°C. The suspension was mixed by inverting the micro tube several times and then centrifuged at 14000 g for 10 min at 4°C in a microfuge to pellet the gDNA. After discarding the supernatant, the gDNA pellet was washed with 1 mL of 70% ethanol that was stored at -20°C and the centrifugation step repeated. The gDNA pellet was dried for 10 min in red light after discarding the supernatant. The dried pellet was then resuspended in 50 µl of 10 mM Tris buffer and incubated over night at 65°C. gDNA concentration was determined by a NanoDrop spectrophotometer and the purity checked by 0.5% agarose gel analysis. Extracted gDNA was stored at 4°C pending use for PCR analysis.

3.6.3. Genotyping of wild-type parasites and clonal knockout lines

pUF1-Cas9 uptake or targeted-gene disruption and *hdhfr* integration in case of the pL7 transfection, was verified in gDNA of transgenic parasites by PCR using *Taq* DNA polymerase. The primer set P25/P32 (Table 2.2) was used at a final concentration of 1 µM to detect pUF1-Cas9 uptake in gDNA of transgenic parasites that were resistant to atovaquone. The expected amplicon size for the pUF1-Cas9 uptake PCR was 695 bp. A summary of the primers used for the analytic PCRs of gDNA of pL7-*PFGLO1*, pL7-*PFcGLO2*, pL7-*PFtGLO2* and pL7-*PFGILP* transfectants as well as the expected amplicon sizes is shown in table 3.2. For each of these transfectant-gDNA sample, three different sets of primers were used to target i) the whole locus, ii) the 5' untranslated region (UTR), and iii) the 3' untranslated region (UTR) of each gene. Genomic DNA from the *P. falciparum* 3D7 wild-type strain served as a negative control to all the PCR cycles. All PCR reactions contained 100 ng (0.5 µL) of genomic DNA in a reaction mixture with 2 µL of dNTPs (0.4 mM), 5 µL ThermoPol Taq-buffer (NEB) and 1µL Taq DNA polymerase in 40.5 µL of Millipore water. The cycler program used for the pUF1-Cas9 control PCR was: 94°C for 2 min, followed by 30 cycles of 94°C 45 s, 65°C 45 s and 72°C 1.5 min, then a final extension at 72°C for 3 min and hold at 4°C. The cycler program used for the gene disruption control PCR was: 94°C for 2 min, followed by 30 cycles of 94°C 30 s, 57°C 45 s and 60°C 5 min, then a final extension at 60°C for 10 min and hold at 10°C. Due to the high A-T content of the target loci, a reduced extension temperature ensure a more reliable DNA replication (Su *et al.*, 1996). The reaction was performed in an Eppendorf mastercycler gradient thermal cycler. All PCR products were analyzed on agarose gels as described above (Section 3.3.2). Products of the pUF1-Cas9 control PCR were analyzed on a 0.8% agarose gel using a 100 bp DNA ladder. The products of the gene disruption control PCR were analyzed on 1% or 2% agarose gel using a 1kb DNA ladder.

Table 3.2. Summary of primers used and expected amplicon sizes: PCR analysis of knockout and wild-type gDNA.

gDNA template	Region of amplicon	PCR #	Primer set	Amplicon
3D7 wild-type	<i>PFGLO1/5'UTR - PFGLO1/3'UTR</i>	1	P28 & P29	2203 bp
	<i>PFGLO1/5'UTR - HDHFR insert</i>	2	P27 & P28	-
	<i>HDHFR insert - PFGLO1/3'UTR</i>	3	P26 & P29	-
3D7 Δ <i>glo1</i>	<i>PFGLO1/5'UTR - PFGLO1/3'UTR</i>	1	P28 & P29	4295 bp
	<i>PFGLO1/5'UTR - HDHFR insert</i>	2	P27 & P28	2525 bp
	<i>HDHFR insert - PFGLO1/3'UTR</i>	3	P26 & P29	2290 bp
3D7 wild-type	<i>PFcGLO2/5'UTR - PFcGLO2/3'UTR</i>	1	P30 & P31	1991 bp
	<i>PFcGLO2/5'UTR - HDHFR insert</i>	2	P27 & P30	-
	<i>HDHFR insert - PFcGLO2/3'UTR</i>	3	P26 & P31	-
3D7 Δ <i>cgl2</i>	<i>PFcGLO2/5'UTR - PFcGLO2/3'UTR</i>	1	P30 & P31	4127 bp
	<i>PFcGLO2/5'UTR - HDHFR insert</i>	2	P27 & P30	2588 bp
	<i>HDHFR insert - PFcGLO2/3'UTR</i>	3	P26 & P31	2061 bp
3D7 wild-type	<i>PFtGLO2/5'UTR - P FtGLO2/3'UTR</i>	1	P37 & P38	2556 bp
	<i>PFtGLO2/5'UTR - HDHFR insert</i>	2	P27 & P37	-
	<i>HDHFR insert - P FtGLO2/3'UTR</i>	3	P26 & P38	-
3D7 Δ <i>tglo2</i>	<i>PFtGLO2/5'UTR - P FtGLO2/3'UTR</i>	1	P37 & P38	4588 bp
	<i>PFtGLO2/5'UTR - HDHFR insert</i>	2	P27 & P37	3072 bp
	<i>HDHFR insert - P FtGLO2/3'UTR</i>	3	P26 & P38	2037 bp
3D7 wild-type	<i>PFGILP/5'UTR - PFGILP/3'UTR</i>	1	P39 & P40	1752 bp
	<i>PFGILP/5'UTR - HDHFR insert</i>	2	P27 & P39	-
	<i>HDHFR insert - PFGILP/3'UTR</i>	3	P26 & P40	-
3D7 Δ <i>gilp</i>	<i>PFGILP/5'UTR - PFGILP/3'UTR</i>	1	P39 & P40	3764 bp
	<i>PFGILP/5'UTR - HDHFR insert</i>	2	P27 & P39	2463 bp
	<i>HDHFR insert - PFGILP/3'UTR</i>	3	P26 & P40	1818 bp

3.6.4. SDS-PAGE and western blot analyses of wild-type parasites and knockout lines

The protocol for preparation of parasite samples for western blot analysis followed the methods of Southworth and colleagues, and of Heiber and Spielmann (Heiber & Spielmann, 2014; Southworth *et al.*, 2011). SDS-PAGE and western blot analysis of knockout parasites was performed by Linda Liedgens. Purified parasites from saponin lysis (see above) were resuspended in an appropriate volume ($\approx 150 \mu\text{L}$) of PBS/PI solution and disrupted by the 4x freeze-thaw cycles comprising 5 min freezing in liquid nitrogen, 1 min in a water bath set at 37°C and 30 s of vortexing. An equal volume of 2x laemmli buffer supplemented with 30% 2-mercaptoethanol was added to the lysate and boiled at 95°C for 5 min to denature and reduce the release proteins. Twenty (20) μL of lysate ($\approx 2.0 \times 10^7$ parasites) was loaded into each well of a small SDS-PAGE gel and electrophoresis was performed according to the method of Laemmli (Laemmli, 1970). The gel was run for 1.5 hr in a Bio-rad electrophoresis chamber at an electric current of 35 mA. For the detection of cytosolic *PfGlo1* and *PfcGlo2* proteins, a 15% gel was used. For the analysis of AGE, a 10% gel was used. All gels were precast with two parts: a shorter stacking gel part where samples were loaded and brought to the same front, and a longer resolving part in which sample proteins were separated according to their molecular weight. Gels were set using protein electrophoresis equipment from Bio-rad. Separated proteins were transferred from the gel onto a nitrocellulose blotting membrane

using the semi-dry blotting method according to standard protocol (Towbin *et al.*, 1979). Blotting was performed using an Apparatur PerfectBlue blotting device. Appropriately sized Whatman paper pieces served as a clean support for the delicate gel and membrane. The pieces of Whatman paper, gel and membrane were incubated in 100 mL of transfer buffer to enhance homogeneity in pH and conductivity, and to enable effective elution and transfer of proteins from the gel to the membrane. The set up of the blotting step was as follows: Anode (+), five soaked Whatman paper pieces, soaked membrane, incubated gel, five soaked Whatman paper pieces and cathode (-). Air bubbles were gently removed from the Whatman papers, membrane and gel by gently rolling a cut 25 mL serological pipette over the set up. Excess buffer from the blotting set up was dried up using a paper towel. Removal of air bubbles and excess water before blotting helps to produce a more efficient transfer. The blot was run at a constant electric current of 100 mA for 1.5 hr. Efficiency of the blotting was checked by staining the membrane in 20 mL Ponceau staining solution for 5 min on an overhead shaker. Excess stain was gently washed away with small volumes of deionised water until the protein bands were clearly visible. Complete destaining of the membrane was later done by 40 mL of tris buffered saline (TBS) for 15 min while shaking on an overhead shaker. The parts of the membrane carrying no transferred protein were blocked with 40 mL of 5% milk powder in TBS buffer for 1 hr at room temperature, after which the membrane was rinsed once with TBS. The blocked membrane was incubated with appropriate primary antibodies diluted in 40 mL of 5% milk/TBS at 4°C overnight on a shaker. For the detection of *PfGlo1*, *PfcGlo2*, and AGE, the antibodies α *PfGlo1*, α *PfcGlo2* and Anti-AGE (Ab23722, Abcam) were used in the dilutions 1:500, 1:1000 and 1:500 respectively. As loading controls, cut sections of the membranes for the analyses of *PfGlo1* and *PfcGlo2*, corresponding to protein band size of ≈ 70 kDa, were decorated with 20 mL 1:800-dilution of anti-*P. berghei* heat shock protein 70 (*PbHsp70*) primary antibody. For AGE analysis, a blotted membrane of a gel ran parallel with the test gel was decorated with 40 mL 1:800-dilution of anti-*PbHsp70* primary antibody to serve as a loading control. After overnight incubation, the primary antibody was removed and stored at -20°C for future use, while the membrane was washed five times for 10 min each with 40 mL of TBS-T (0.1% Tween) and once with 40 mL of TBS for 10 min. The membrane was incubated with 40 mL of secondary antibody for 45 min on a shaker at room temperature. The secondary antibody used for *PfGlo1*, *PfcGlo2* and AGE detection was a 40 mL dilution (1:10000) of goat anti-Rabbit IgG (H+L)-HRP conjugate antibody (Bio-rad) in 5% milk/TBS Buffer. The anti-*PbHsp70* antibody was detected with a 30 mL dilution (1:10000) of HRP-conjugated goat anti-mouse secondary antibody in 5% milk/TBS. The secondary antibody solution was discarded after incubation and the membrane washed five times with 40 mL TBST-T (0.1% Tween, 0.2% Triton) for 10 min each and once with 40 mL of TBS for 10 min. Secondary antibodies bound to target proteins were detected on Super RX-N film (Fujifilm) using a LiCOR scanner after activation with detection reagents. Five hundred (500) μ L each of reagents 1 and 2 were mixed and used per membrane. The AGE western blot was repeated five more times.

2x Laemmli buffer	50 mM Tris/HCl pH 6.8
	10% (w/v) SDS
	25% (v/v) glycerol
	0.1% (w/v) bromophenol blue

	30% (v/v) β -mercaptoethanol
10x Transfer buffer	200 mM tris 1.5M glycine 0.2% SDS
1x Transfer buffer	700 mL Millipore water 100 mL 10x transfer buffer 200 mL methanol
TBS	10 mM tris 0.9% NaCl, pH 7.4 at room temperature

3.7. Growth and morphological analyses of knockout strains

3.7.1. Growth analysis

The growth phenotype of confirmed *PFGLO1* and *PFeGLO2* knockout clones (*3D7 Δ glo1* and *3D7 Δ cglo2*) was analyzed in comparison with the control 3D7 wild-type strain by generating growth curves of asynchronous cultures (Djuika *et al.*, 2017). Growth curves were generated for three *PFGLO1* and two *PFeGLO2* clonal knockout lines. Briefly, a 14.5 mL asynchronous culture was set up for each clone at a starting parasitemia of 0.1% and a hematocrit of 3.5% at standard culture conditions as above. Cultures were maintained for six days, changing the medium once every 24 hr for the first three days and thereafter twice every 24 hr. The parasitemia of each culture was assessed every day until the sixth day by counting 7 microscope fields (750-1500 erythrocytes) of Giemsa-stained thin blood smears. The average parasitemia of each clone for each time point was calculated from three independent experiments. Statistical analysis of growth was done by one way ANOVA on SigmaPlot 12.5.

3.7.2. Gametocyte formation assay

Gametocyte formation assays were performed in collaboration with Prof. Gabriele Pradel's laboratory by Alexandra Golzmann. The protocol used is as described in (Wezena *et al.*, 2018). "Wild-type as well as *3D7 Δ glo1* and *3D7 Δ cglo2* knockout parasites were cultured as described above except for the replacement of albumax with 10% inactivated A+ serum as described previously (Wirth *et al.*, 2014). Two days after synchronization with 5% sorbitol, gametocyte commitment was induced by setting up the culture at 2% parasitemia and a hematocrit of 10% in 5 ml of the human A+ medium. The medium was replaced daily and Giemsa-stained blood smears were analyzed 14 days post-induction of gametocyte commitment. The gametocytemia was determined per 1000 red blood cells and the gametocyte stages II-V were counted in triplicate. Data analysis was performed using MS Excel 2010 and GraphPad Prism 5".

3.7.3. Determination of IC₅₀ values for external 2-oxoaldehydes for knockout strains

IC₅₀ values were determined using a SYBR green 1 assay according to established protocols (Smilkstein *et al.*, 2004; Wezena *et al.*, 2017). The parasitemia of a standard culture of each clonal knockout line or the control strain was evaluated by light microscopy of Giemsa-stained thin blood smears. The culture was subsequently transferred to a 15 mL Falcon tube and centrifuged at 300 g for 5 min at room temperature. The supernatant was discarded and cells were adjusted with fresh erythrocytes in complete RPMI medium containing 2x albumax II (0.9% w/v) to a hematocrit of 3% and a parasitemia of 0.5%. Likewise, a suspension containing only uninfected erythrocytes with a hematocrit of 3% was prepared in complete RPMI medium containing 2x albumax II. Albumax-free medium (50 µL) was dispensed in each of the wells of sterile, black 96 well fluotrac microplates (Greiner). The outer wells (including the first column) of each plate were supplemented with 50 µL of the suspension that contained only uninfected erythrocytes. These wells served as parasite- and drug-free controls to determine the background fluorescence at a final culture volume of 100 µL and a hematocrit of 1.5%. Stock solutions of glyoxal, methylglyoxal and phenylglyoxal were freshly prepared in albumax-free RPMI medium and filter-sterilized for the 2-oxoaldehyde susceptibility assays. Aliquots (25 µL) of these stock solutions were pipette into the second column of the microplates. After mixing, 25 µL of the now 75 µL solution in column 2 were transferred to column 3, yielding a 1:3 dilution. This step was repeated for columns 3 to 10 (the 25 µL aliquot from column 10 was discarded). Column 11 served as a drug-free control cultures. Columns 2 to 11 of each plate were supplemented with 50 µL of parasitized erythrocytes yielding a final culture volume of 100 µL, a hematocrit of 1.5% and a parasitemia of 0.5%. Final concentrations of glyoxal, methylglyoxal and phenylglyoxal in the treated wells (columns 2-11) were from 5 mM - 0.38µM, 15 mM - 2.3 µM and 45 mM - 6.9 µM respectively in 1:3 serial dilutions. All microplates were incubated under standard culture conditions for 72 hr. The plates were later removed from the incubator and sealed with parafilm before storage at -80°C. Prior to analysis, the microplates were thawed at room temperature for 1 hr. For each plate, complete lysis buffer was freshly prepared by diluting 1.2 µL of 10,000x SYBR green 1 solution in 10 mL incomplete lysis buffer. The microplates were supplemented with 100 µL of complete lysis buffer per well and immediately covered with aluminium foil. The set up was mixed thoroughly on a horizontal shaker for 2 min and incubated in the dark for 1 hr at room temperature. Fluorescence intensity on each plate was determined using a microplate reader with a gain of 60, an excitation wavelength of 485 nm and an emission wavelength of 535 nm. All data were corrected for the background fluorescence of uninfected erythrocytes, normalized to the growth of control parasites in column 11, and fitted to a sigmoidal dose-response curve using the four parameter Hill function in SigmaPlot 12.5. Each experiment was done in triplicates and was repeated three to seven independent times.

Incomplete lysis buffer	20 mM Tris-HCl, pH 7.5, 5 mM EDTA, 0.08% Triton X-100 0.008% saponin
--------------------------------	---

3.8. Relevance of host cell Glo1 activity for *P. falciparum* growth

Since there are no human glyoxalase knockout erythrocytes, an indirect approach was employed to investigate the contribution of the host glyoxalase system to the parasite's blood-stage development. Tight-binding Glo1 inhibitors were used to inhibit the human Glo1 activity of fresh erythrocytes before using the pretreated erythrocytes to cultivate purified parasites (Figure 4.1 A). To identify the most potent and effective Glo1 inhibitors for this purpose, four glutathione-derived compounds, 1 and 2, and their respective carboxylic *tert*-butyl ester derivatives, compounds 3 and 7 (Figure 3.1) (Wezena *et al.*, 2016), were first tested on fresh erythrocyte cultures. Briefly, five (5) culture plates were set up, each containing 500 μ L of washed fresh erythrocytes resuspended in 14 mL of complete RPMI medium. Four of the plates were each treated with 10 μ M of compound 1, 2, 3 or 7. The fifth plate served as a drug-free control plate. Glo1 and Glo2 activities of the erythrocyte stock used to set up the cultures were determined (see section 3.9), and the erythrocyte cultures were maintained under standard conditions for 96 hr. Every 24 hr, the cultures were resuspended in a 15 mL Falcon tube and centrifuged at 300 g for 5 min at room temperature. A 40 μ L aliquot of erythrocyte pellet was removed from each culture into different 1.5 mL micro tubes for Glo1 and Glo2 enzyme assays (section 3.9.1). The remaining erythrocytes were resuspended in the original medium and recultured. The experiment was repeated with five different blood donors. Analyses of Glo1 and Glo2 activities of the treated erythrocytes revealed compounds 1, 3 and 7 to be the most potent and effective of the four Glo1 inhibitors (Figure 4.1 C). The three compounds were therefore employed to investigate the contribution of the erythrocyte Glo1 to *P. falciparum* blood-stage development.

To perform this investigation, the erythrocyte glyoxalase activity was first inhibited by treating fresh erythrocytes separately with 10 μ M each of compounds 1, 3 and 7 for 96 hr. The erythrocytes were subsequently washed three times with complete RPMI medium to removed residual inhibitor. The washed erythrocytes were used to culture synchronized schizont-stage parasites that were enriched to approximately 98% purity by magnetic cell separation using a VarioMACS™ Separator (Staalsoe *et al.*, 1999). Parasites were cultured under normal conditions for 6 days. The growth rate of parasites in each of the differently treated erythrocytes was averaged every day from 7 microscope fields (750-1500 erythrocytes) by counting Giemsa-stained thin blood smears. Results were calculated from three independent experiments and analyzed statistically in SigmaPlot 12.5 using the one way ANOVA on ranks method.

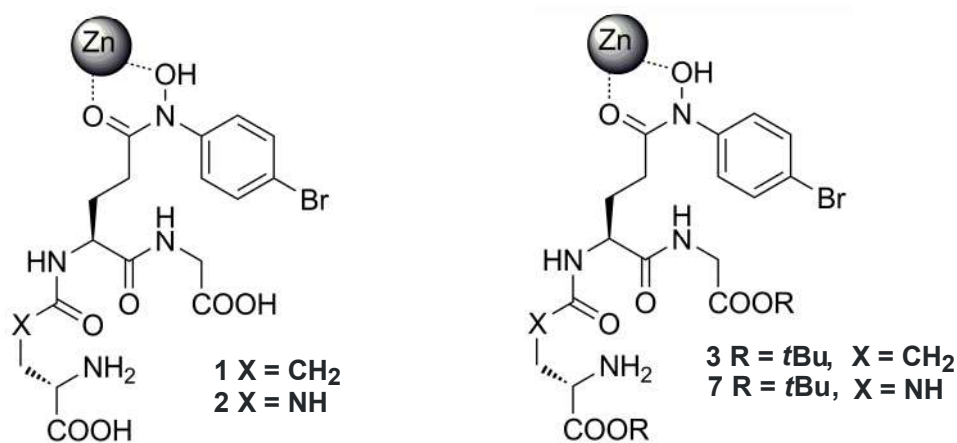


Figure 3.1. Structures of Glo1 inhibitors and their esterified analogues used in inhibition studies. The hydroxamic acid moiety mimics the transition state and interacts with the metal center of Glo1. *t*Bu is the *tert*-butyl ester group. Taken and modified from (Wezena *et al.*, 2016).

3.9. Glyoxalase activity assays of erythrocytes and knockout strains

3.9.1. Preparation of erythrocyte lysate for enzyme assays

Erythrocyte lysate for enzyme assays was prepared by resuspending 40 μ L of treated or untreated (control) erythrocyte pellets in 500 μ l of PBS and centrifuging at 2000 g in a microfuge at 4°C for 5 min. The supernatant was discarded and the wash step was repeated two more times to remove all residual inhibitors and serum contaminants. The washed erythrocytes were subsequently lysed by resuspension in 200 μ L of ice-cold Millipore water for 1 min on an overhead shaker in the cold room to prevent deactivation of enzymes. The lysis step was delayed until all erythrocytes were lysed. The lysate was subsequently transferred on ice and centrifuged at 20000 g in a microfuge for 10 min at 4°C. The supernatant containing erythrocyte enzymes were quickly decanted into a fresh precooled 1.5 mL micro tube and stored on ice for immediate enzyme assays.

3.9.2. Preparation of parasite lysate for enzyme assays

Parasite lysate for enzyme assays was prepared from a 35 mL trophozoite-stage synchronous culture at $\geq 5\%$ parasitemia using a slightly modified saponin lysis and freeze-thaw method (Harwaldt *et al.*, 2002; Akoachere *et al.*, 2005). Briefly, infected erythrocytes were first resuspended in the old culture medium and transferred into a 50 mL Falcon tube. The suspension was centrifuged at 1000 g for 5 min at 23°C after which the supernatant was discarded. The erythrocyte pellet was resuspended for 10 min in 20 volumes of saponin lysis buffer that was prewarmed at 37°C. Following centrifugation of the cell lysate at 2000 g for 3 min at 25°C, the supernatant was discarded and the parasite pellet was washed three times with lysis buffer. The parasites ($\sim 5 \times 10^7$ cells) were subsequently resuspended in 150 μ L of the lysis buffer and disrupted by four cycles of freezing and thawing. The freeze-thaw cycles were composed of 5 min freezing in liquid nitrogen, 1 min in a 37°C water bath and 30 s of

vortexing. The parasite lysate was then cleaned with a spin at 20800 g for 60 min at 4°C. The supernatant was decanted into a fresh precooled 1.5 mL micro tube and stored on ice. The protein content as well as the activities of *PfGlo1* and *PfcGlo2* of the parasite extract were immediately determined.

Lysis buffer 7 mM K₂HPO₄, 1 mM NaH₂PO₄, 11 mM NaHCO₃, 58mM KCl, 56 mM NaCl, 1 mM MgCl₂, 14mM glucose, and 0.02% saponin (pH 7.5 at RT).

3.9.3. Measurement of erythrocyte hemoglobin concentration

The concentration of hemoglobin in the erythrocyte lysate was estimated using a thermostatted Jasco V-550 UV–vis spectrophotometer. Freshly prepared 50 Mm Tris/HCl (pH7.4 at 37°C) was used as a buffer in the hemoglobin absorbance measurements. Measurements of change in absorbance were performed at a fixed-wavelength of 523 nm, which is also the isosbetic point of of Hb (O₂), Hb and Hb (met) (Olsen & Elvevoll, 2011). Briefly, 980 µL of the 50 mMTris/HCl (pH 7.4), pre-warmed to 37°C, was added to a 1 mL disposable plastic cuvette in the spectrophotometer. The assay was set to ‘autozero’ and the baseline absorbance was measured for 30 s. Twenty (20) µL of lysate supernatant was added and the change in absorbance measured for 1.5 min. The measurement was repeated for two more lysate samples. The concentration of Hb (mM or g/L) in the lysate was calculated using the extinction coefficient of $\epsilon_{240nm}=7.12 \text{ mM}^{-1} \text{ cm}^{-1}$ with the formula $[\text{Hb}]=\text{Abs}_{523nm} \times 50 \times 7.12 \text{ [mM]}$ or $[\text{Hb}]=\text{Abs}_{523nm} \times 16.1 \times 50 \times 7.12 \text{ [g/L]}$. All hemoglobin absorbance measurements were performed in triplicates.

3.9.4. Bradford assay

The total protein content of parasite cell lysate was determined by the Bradford assay using bovine serum albumin (BSA) as a standard protein (Bradford, 1976). The assay is based on the shift in absorbance of Coomassie brilliant blue R-250 stain (Bio Rad) with proteins. Coomassie stain is converted from a red form to a blue form as it binds protein and shifts in absorbance wavelength from 465 nm to 595 nm. The increase in absorbance at 595 nm is a measure of protein concentration in the mixture. The assay was performed using a thermostatted Jasco spectrophotometer set at the fixed absorbance wavelength of 595 nm at 25°C. A calibration curve was generated by measuring the absorption of eight disposable plastic cuvettes of serially diluted concentrations of BSA that were thoroughly mixed with Bradford reagent. Briefly, BSA was diluted to a final volume of 800 µL in deionised water and 200 µL Bradford reagent was added. The total volume of reaction in each vial was 1 mL while the known BSA concentrations ranged from 0 – 14 µg/mL. Triplicates of two dilution of the parasite lysate were also made in disposable plastic cuvettes to a final volume of 800 µL in deionised water and mixed well with 200 µL of Bradford reagent. Care was taken that the measured absorbance of lysate (the total protein concentration) fell within the range of the calibration curve. Measurements of absorbance of both the BSA dilutions and lysate dilutions

were done in a manner corresponding to the time interval within which the Bradford reagent was added to each dilution. This helped to eliminate variations in absorbance due to differences in incubation time. A calibration curve was generated by plotting the concentration of BSA (μg) against the measured absorption in Sigmaplot 12.5 using the hyperbolic parameters ($y=a*x/(b+x)$). The mean of the triplicate absorptions of lysate dilutions were projected on the calibration curve to determine the concentration of total protein in the lysate.

3.9.5. Glyoxalase 1 activity assay

*Pf*Glo1 activity in parasite lysate was measured by determining the rate of formation of the S-D-lactoylglutathione (SLG) from the hemithioacetal of methylglyoxal (MG) and glutathione (GSH). Measurements were performed in a thermostatted Jasco spectrophotometer at wavelength of 240 nm and temperature of 25°C following standard protocols (Akoachere *et al.*, 2005; Iozef *et al.*, 2003). The extinction coefficient of $\epsilon_{240\text{nm}} = 2.86 \text{ mM}^{-1} \text{ cm}^{-1}$ was used in the calculation of the enzyme activity. The assay buffers comprising potassium phosphate buffer, buffer 1, (pH 7.0) and 1M potassium chloride, buffer 2, (pH 7.0) were freshly prepared and stored at 4°C. 100 mM GSH and 100 mM MG stock solutions were also freshly prepared in distilled water and stored on ice. The hemithioacetal substrate was formed by mixing 100 μL each of prewarmed buffer 1 and 2, 10 μL of GSH and 20 μL of MG in 740 μL of prewarmed double distilled water in a 1 mL quartz cuvette. The final concentrations of GSH and MG in the assay mixture were 1 mM and 2 mM respectively. The mixture was incubated for 15 min at 25°C. After 14.5 min of incubation, the measurement was set to 'auto zero' and the baseline was recorded for 30 seconds. Thirty (30) μL of parasite lysate supernatant ($\sim 1 \times 10^7$ parasites) was added to the mixture and thoroughly mixed. The change in absorbance at A_{240} was immediately monitored for 1.5 min.

For the determination of human Glo1 activity, measurements were performed at 37°C in 50 mM Na₂HPO₄ (pH 6.6 at 37 °C) assay buffer. GSH and MG stock solutions were both made in the sodium phosphate buffer. The final concentration of GSH and MG in the hGlo1 assays was 2 mM. In the hGlo1 assay, the incubation period for hemithioacetal formation was 10 min (Thornalley, 1988; Arai *et al.*, 2014) while 5 μL of cell lysate was used for the hGlo1 assay. The change in absorbance at A_{240} was also immediately monitored for 1.5 min. The initial rate of change (increase) at A_{240} (dA_{240}/dt)₀ was deduced and the activity of *Pf*Glo1, a_{PfGlo1} , and hGlo1, a_{hGlo1} , were calculated as follows:

$$a_{Glo1} = (dA_{240}/dt)_0 / 2.86 \text{ [mM/min]}.$$

Glo1 activity in parasite and erythrocyte lysates was determined from two-four triplicate measurements. *Pf*Glo1 activities were normalized to corresponding concentration of total parasite lysate protein ($\mu\text{g}/\mu\text{L}$) determine by a Bradford calibration curve and reported in units/mg protein. hGlo1 activities were normalized to hemoglobin concentration of the corresponding erythrocyte lysate. Further statistical analysis of enzyme activities was performed in SigmaPlot 12.5 using the one way ANOVA method.

3.9.6. Glyoxalase 2 activity assay

PfcGlo2 activity in parasite lysate was measured by determining the decrease in absorbance resulting from SLG hydrolysis at 240 nm. The assay was performed at 25°C in a thermostatted Jasco spectrophotometer following to standard protocols. An extinction coefficient of $\epsilon_{240\text{nm}} = 3.1 \text{ mM}^{-1} \text{ cm}^{-1}$ was used in the calculation of the enzyme activity (Iozef *et al.*, 2003; Akoachere *et al.*, 2005). Briefly, 100 mM Tris/HCl (pH 7.4 at 25°C) and 3 mM SLG (in tris buffer) were freshly prepared and stored on ice. The assay set up comprised mixing 500 μL of Tris buffer, 100 μL of SLG (final concentration of 0.3 mM) stock solution and 350 μL of water in a 1 mL quartz cuvette. The measurement was set to 'auto zero' and the baseline measured for 30 seconds. Fifty (50) μL of cell lysate supernatant ($\sim 1.7 \times 10^7$ parasites) was added and mixed thoroughly. The change in absorbance at A_{240} was immediately monitored for 1.5 min.

For the determination of human Glo2 activity, measurements were performed at 37°C in 50 mM Tris/HCl (pH 7.4 at 37 °C) assay buffer. The SLG stock was diluted in the Tris/HCl assay buffer. The final concentration of SLG in the assay buffer was 0.3 mM for the human Glo2 assay (Arai *et al.*, 2014; Thornalley, 1988). Ten (10) μL of cell lysate was used for the human Glo2 assay. The change in absorbance at A_{240} for was immediately monitored for 1.5 min. The initial rate of change (decreases) in A_{240} ($dA_{240}/dt)_0$ was deduced and the activities of *PfcGlo2*, $a_{PfcGlo2}$, and hGlo2, a_{hGlo2} , were calculated as follows:

$$a_{Glo2} = -(dA_{240}/dt)_0/3.10 \text{ [mM/min]}.$$

Glo2 activity in parasite and erythrocyte lysates was determined from two-four triplicate measurements. *PfcGlo2* activities were normalized to corresponding concentration of total parasite lysate protein ($\mu\text{g}/\mu\text{L}$) determine by a Bradford calibration curve and reported in units/mg protein. hGlo2 activities were normalized to hemoglobin concentration of the corresponding erythrocyte lysate. Further statistical analysis of enzyme activities was performed in SigmaPlot 12.5 using the one way ANOVA method.

3.10. Determination of IC₅₀ values for standard pro- and antioxidants for *P. falciparum* 3D7 parasites

IC₅₀ values for H₂O₂, NAc, ascorbate and DTT were determined using a SYBR green 1 assay as described above (Section 3.7.3). Stock solutions of the prooxidant H₂O₂ and antioxidants, NAc, ascorbate and DTT were freshly prepared in albumax-free RPMI medium and filter-sterilized for the assessment of their effects on the growth of *P. falciparum* 3D7 wild-type strain. The final concentrations of H₂O₂, NAc, ascorbate and DTT in the drug wells were set from 1.63 mM - 0.25 mM, 300 mM - 0.05 mM, 300 mM - 0.05 mM and 33.33 mM - 0.01 mM respectively in 1:3 serial dilutions. As the antioxidants ascorbate, N-acetylcysteine and DTT were found to produce a background fluorescence that varied from compound to compound, microplates with unparasitized erythrocytes but with the same compound dilutions were set up in parallel as controls. As above, all data were also corrected for the background fluorescence of uninfected erythrocytes, normalized to the growth of untreated control

parasites and fitted to a sigmoidal dose-response curve using the four parameter Hill function in SigmaPlot 12.5. Each experiment was done in triplicates and was repeated three to seven independent times.

3.11. Growth analysis of ascorbate treated *P. falciparum* 3D7 parasites

To assess the time-dependent growth inhibition of *P. falciparum* 3D7 wild-type strain by ascorbate, a growth curve was generated following the protocol above (see section 3.7.1). Briefly, six 14.5 mL synchronous cultures of *P. falciparum* 3D7 wild-type strain were set up at an initial parasitemia of 0.1% and a hematocrit of 3.5%. Five of the six parasite cultures were treated to final concentrations of 0.05 mM, 0.1 mM, 1 mM, 2.5 mM or 5 mM with aliquots from a sterile-filtered 200 mM ascorbate stock solution that was freshly prepared in complete medium. The sixth plate served as an untreated control parasite culture. The plates were incubated under normal culture conditions. Parasitemia of each culture was monitored for six days by counting 7 microscope fields (750-1500 erythrocytes) of Giemsa-stained thin blood smears. The medium of each flask was replaced every 24 hr. Each culture was retreated after medium replacement with the same concentrations of freshly prepared ascorbate solution as previously. Parasitemia for each data point was averaged from six independent experiments and analyzed as in section 3.7.1 above.

4. RESULTS

4.1. Effect of the host cell Glo1 activity on *P. falciparum* blood-stage cultures

Before the effect of the deletion of a *P. falciparum* glyoxalase can be effectively analyzed in a knockout line, the contribution of the host glyoxalase system to the parasite blood-stage development should be quantified. To date, there are no reports of erythrocyte glyoxalase knockout cells. The use of efficient glyoxalase inhibitors to eliminate the activities of human enzymes in parasite cultures therefore offers an alternative and effective molecular tool to investigate the relevance of the human glyoxalase system to the parasite's development in the host-parasite unit of the infected-erythrocyte.

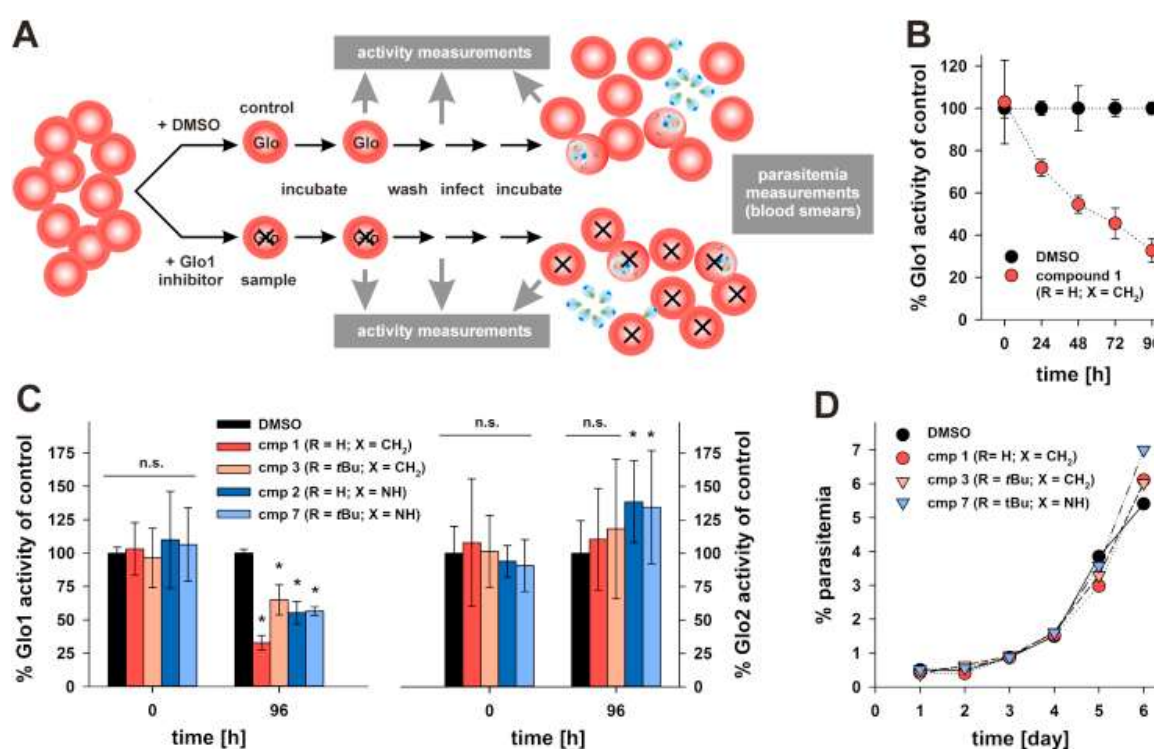


Figure 4.1. Effect of the host cell Glo1 activity on *P. falciparum* blood-stage cultures. (A) Strategy to investigate the contribution of hGlo1 to the blood-stage parasite development. Uninfected erythrocytes were incubated with 10 μ M of compounds 1–3, 7 or DMSO for 96 hr in complete RPMI medium to inhibit the hGlo1 activity. The erythrocytes were washed and subsequently infected with purified schizont-stage parasites in the absence of the tight-binding inhibitors. (B) Representative time course measurement of human Glo1 activity upon treatment of uninfected erythrocytes with 10 μ M of compound 1. (C) Time-dependent effect of 10 μ M of compounds 1–3 and 7 on hGlo1 and hGlo2 activities in uninfected erythrocytes. Stars indicate a p-value of <0.05; n.s., not significant. (D) Growth curve analysis of *P.falciparum* parasites according to the scheme outlined in panel A. Erythrocytes were pre-treated for 96 h with 10 μ M of compounds 1, 3 and 7, washed, and infected with purified parasites (day 0). All data points in panels B–D were averaged from 3–5 independent experiments with different blood donors. Taken from (Wezena *et al.*, 2016).

Compounds 1-3 and 7 were identified earlier as strong tight-binding Glo1-specific inhibitors (More & Vince, 2009). At concentrations of 30 μM and above, the compounds are slightly toxic to the uninfected erythrocyte host cell through hemolysis and the formation of methemoglobin (Wezena *et al.*, 2016). To eliminate the toxic effects, 10 μM of each drug was used to treat uninfected erythrocytes for 96 hr to inhibit host cell Glo1 activity (Figure 4.1 C). Results averaged from five different blood donors revealed the activities of human Glo1 and Glo2 in the DMSO controls to be about 0.154 ± 0.038 and 0.056 ± 0.016 U/mg hemoglobin respectively. These results fitted well with previously reported erythrocyte glyoxalase activities (McLellan *et al.*, 1994). Compound 1 particularly acted quite strongly, though slowly, on uninfected erythrocytes resulting in a three-fold reduction of the Glo1 activity after 96 hr of drug treatment (Figure 4.1 B & C). Treatment of erythrocytes with compounds 3, 7 and 2 also reduced the activity of Glo1 to 60%, 55% and 54% respectively (Figure 4.1 C). Esterification of the carboxylate groups in compounds 3 and 7 did not confer improved pharmacokinetics nor increased the potency of the inhibitors after 96 hr of treatment as compared to the mother compounds, 1 and 2. Surprisingly, the activity of human Glo2 also increased significantly by about 25% after treatment of erythrocytes with compounds 2 and 7 for 96 hr. There was no significant increase in the erythrocyte Glo2 activity after treatment with compounds 1 and 3. Parasite growth was not significantly affected after 6 days of culture in erythrocytes that were pretreated for 96 hr with 10 μM of compounds 1, 3 and 7 (Figure 4.1 D). Inhibition of the erythrocyte Glo1 enzyme with slow acting tight-binding inhibitors did not affect parasite development in the host-parasite unit. The conclusion that can be drawn from these results is that, the human Glo1 appears to be dispensable for the development of *P. falciparum* 3D7 wild-type strain in cell culture.

4.2. pL7-knockout constructs to disrupt the glyoxalase genes in *P. falciparum*

In order to generate clonal knockout lines for the glyoxalase genes of *P. falciparum* 3D7 strain, the recently developed CRISPR-Cas9 gene knockout strategy was employed. This project specifically adopted the *P. falciparum* genome editing method (Figure 4.2 A & B, Figure 4.3 A & B) previously described (Ghorbal *et al.*, 2014). The two plasmids employed for gene disruption by double crossover homologous recombination in this method include the *Cas9*-encoding construct (pUF1-Cas9) and the pL6 plasmid. As the pUF1-Cas9 was acquired ready-to use, only the pL6 plasmid was adapted for specific gene disruption by cloning-in the guide sequence, which directs the Cas9 protein to the target gene, and the flanking HR for homologous recombination. The pL7 plasmids generated from the cloning steps above included pL7-PFGLO1, pL7-PFcGLO2, pL7-PFtGLO2 and pL7-PFGILP which target PFGLO1, PFcGLO2, PFtGLO2 and PFGILP loci respectively. Plasmid pL7-PFGLO1 carried a 477 bp 5' HR and a 521 bp 3' HR. Plasmid pL7-PFcGLO2 carried a 642 bp 5' HR and a 442 bp 3' HR. Plasmid pL7-PFtGLO2 carried a 467 bp 5' HR and a 640 bp 3' HR. And plasmid pL7-PFGILP carried a 612 bp 5' HR and a 625 bp 3' HR. All pL7 plasmids also carried their respective 20 bp guide sequences to direct double strand cleavage of the target genes by the Cas9 protein. Depending on the A-T content and length of the target gene, the 5' and 3' HR both occurred within the coding sequence as in the cases of PFGLO1, PFcGLO2 and PFGILP genes or one HR extended into the untranslated region (UTR) as in the case of

the *PfGLO2* gene (3' region). The cloned-in 5' and 3' HR of the pL7 plasmids flanked the expression cassette for the human dihydrofolate reductase (*hDHFR*) gene that confers resistance to the *P. falciparum* antifolate drug WR9210 (WR) (Fidock & Wellem, 1997),

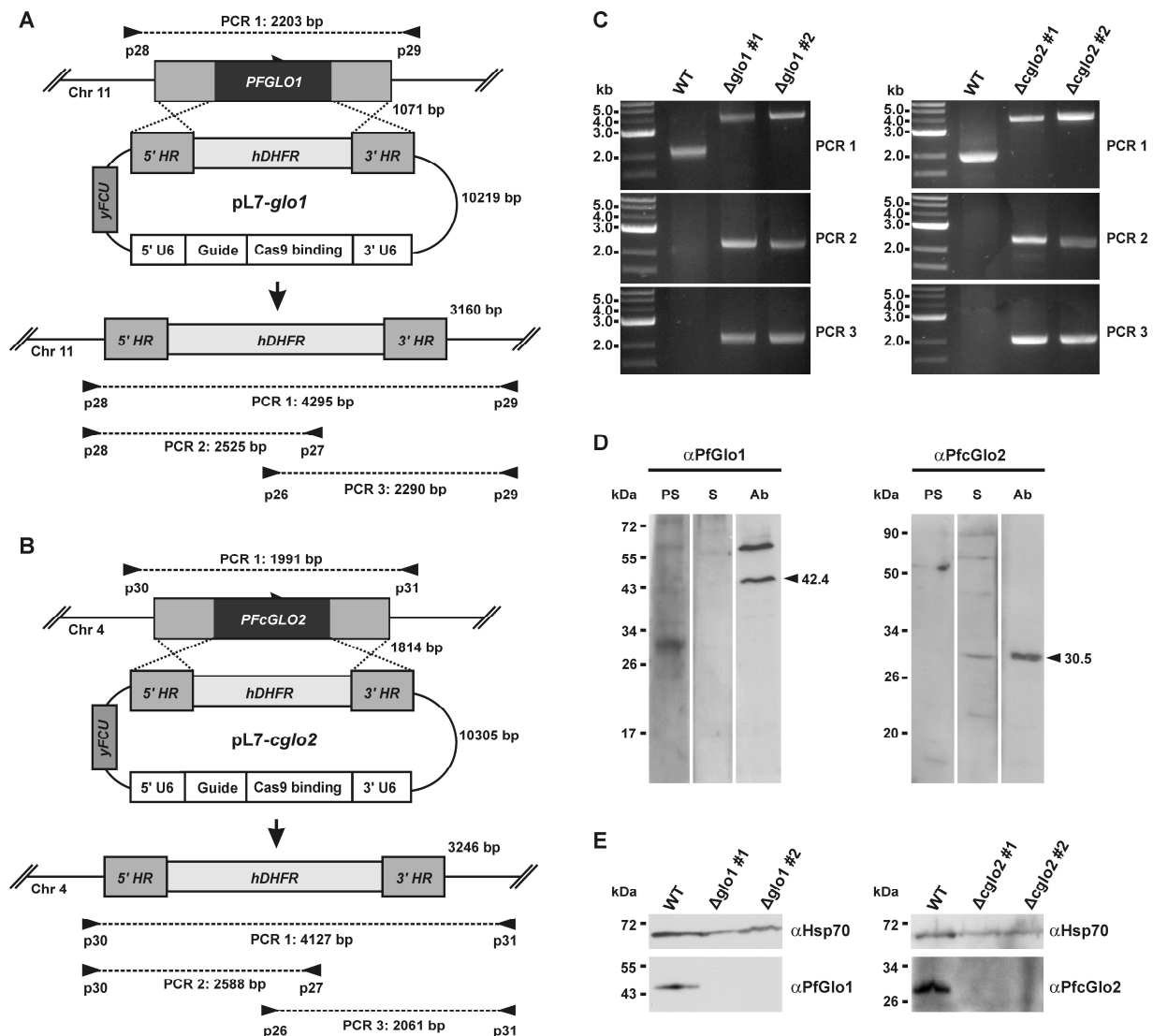


Figure 4.2. Generation and validation of *P. falciparum* Glo1 and cGlo2 knockout clonal lines. (A) and (B) Knockout scheme for *PfGlo1* and *PfcGlo2* respectively, adopting the CRISPR-Cas9 strategy (Ghorbal *et al.*, 2014). (C) PCR analysis of isolated genomic DNA from 3D7 Δ *glo1* and 3D7 Δ *cglo2* clonal lines generated after transfection, selection and limited dilution. The results are compared with the 3D7 wild-type strain as control. Analyses are shown for two clonal lines (#1 and #2) each of the 3D7 Δ *glo1* and 3D7 Δ *cglo2* strain. (D) Analysis of purified rabbit peptide antibodies against *PfGlo1* and *PfcGlo2* in *P. falciparum* 3D7 wild-type parasites. Lysate from 2×10^7 cells was loaded per lane on a 15% gel, separated by reducing SDS-PAGE and analyzed by western blotting. The expected sizes of *PfGlo1* and *PfcGlo2* are indicated by arrowheads. PS, S, Ab: Decoration with pre-immune serum, serum and affinity-purified antibody, respectively. (E) Western blot analyses of *PfGlo1* and *PfcGlo2* in extracts from two clonal lines of 3D7 Δ *glo1* and 3D7 Δ *cglo2* knockout strains from panel C using the purified antibodies from panel D. Analyses of *PfGlo1* and *PfcGlo2* in the same amount of lysate from the 3D7 wild-type strain served as control. As a loading control, membranes were decorated with an antibody against *P. berghei* Hsp70. The primer pairs used and the expected sizes of PCR products for the 3D7 wild-type strain as well as knockout clones are shown. Antibody purification and western blot analysis of the knockout clones was performed by Linda Liedgens. Taken and modified from (Wezena *et al.*, 2018).

and thus served as a positive drug selectable-marker. The guide sequence of each pL7 plasmid completed the requirements for a functional sgRNA. The sgRNA on each of the plasmids was therefore capable of binding Cas9 protein expressed by the pUF1-Cas9 plasmid and guiding it via the specific guide sequence to target and cause double strand breaks at specific gene loci. The double strand breaks could then be repaired by the 5' and 3' homologous regions (donor or template DNA) on the pL7 plasmids.

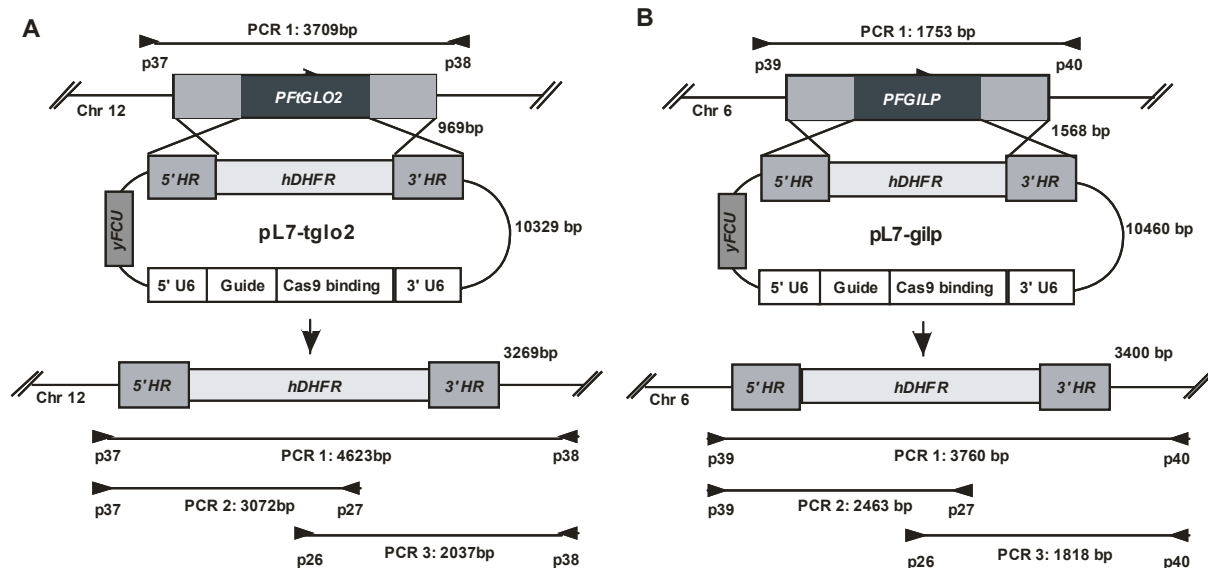


Figure 4.3. Strategy for the generation of *P. falciparum* 3D7 Δ tgo2 and 3D7 Δ gilp knockout clones. (A) and (B) Knockout scheme for *PFGLO2* and *PFGILP* respectively, adopting the CRISPR-Cas9 strategy (Ghorbal *et al.*, 2014). The primer pairs used and the expected sizes of PCR products for the 3D7 wild-type strain as well as knockout strains are shown.

P. falciparum 3D7 wild-type strains were first transfected with the pUF1-Cas9 plasmid which also carries the drug selectable marker yeast dihydroorotate dehydrogenase (*yDHODH*) gene. *yDHODH* confers resistance to atovaquone, an anti-protozoal mitochondrial electron transport inhibitor, by presenting a ubiquinone-independent DHODH for the essential pyrimidine bio-synthetic pathway (Ganesan *et al.*, 2011). Parasites were detected by Giemsa-stained blood smears 23 days post-transfection after selection with atovaquone. These transgenic parasites, 3D7^{Cas9}, were amplified and transfected with each of the pL7 plasmids. pL7 transfectants were detected within four weeks after positive selection and also survived 9 days of selection with the negative selectable marker 5-FC. 5-FC was used because the pL7 plasmid also carries the fusion suicide-gene yeast cytosine deaminase and uridyl phosphoribosyl transferase (*yfcu*), the product of which deaminates 5-FC to cytotoxic 5-fluorouracil leading to cell death (Braks *et al.*, 2006). 5-FC selection therefore eliminated parasites carrying unintegrated pL7 plasmid or parasites in which only a single crossover event occurred after transfection. Transfectants were controlled by PCR and western blot analyses for the disruption of the respective *PFGLO1*, *PFcGLO2*, *PFGLO2* and *PFGILP* target loci. Disruption of *PFGLO1* and *PFcGLO2*, the genes encoding the cytosolic glyoxalases was confirmed in a mixed population of transfectants.

4.3. Generation of single knockout clones by limiting dilution

Clonal parasite lines are essential for cellular, molecular and biochemical analyses of parasite strains because of the need for accurate, unambiguous and reproducible results (Hasenkamp *et al.*, 2012). Limiting dilution of culture to one or less parasites per culture well in a 96 well plate and cultivating the diluted cultures for 2-4 weeks is a common method of generating clonal parasite lines. Several versions of this method have been reported. The variations include the detection mode of parasites in 96 well plates. The cheapest, though quite tedious, variation is the detection of parasite growth in each well by light microscopy of Giemsa-stained blood smears. This thesis adopted the above method to select single knockout clones of transgenic *PFGLO1* and *PfCGLO2* knockout strains, now referred to as 3D7 Δ *glo1* and 3D7 Δ *cglo2*, respectively. Parasites were detected by microscopy on day 21 of cell culture. Of 24 wells that were cultured with approximately one parasite, growth was detected in 13 wells. Five (5) out of 24 culture wells of the 1/10 dilution of the approximately one-parasite culture were also positive for parasite growth by Giemsa-stained thin blood smears, while 1 well out of 24 culture wells of the 1/100 dilution of the approximately one-parasite culture was positive for parasite growth. No growth was detected in any of the 24 control wells.

4.4. PCR and western blot analyses of 3D7 Δ *glo1* and 3D7 Δ *cglo2* clonal lines

PCR analysis was repeated with gDNA of two clonal knockout lines each of the 3D7 Δ *glo1* and 3D7 Δ *cglo2* strains; *glo1*#1 & *glo1*#2 and *cglo2*#1 & *cglo2*#2 respectively. The results confirmed the disruption of *PFGLO1* and *PfCGLO2* gene loci and the integration of the *hDHFR* gene sequence in these loci (Figure 4.2 C). Single bands were visible on the analytic agarose gel of PCR products that were generated using primers that targeted the whole *PFGLO1* and *PfCGLO2* gene loci on the 3D7 Δ *glo1* and 3D7 Δ *cglo2* strains respectively (4.3 kb and 4.1 kb bands were respectively visible compared to 2.2 kb and 2.0 kb bands of the respective wild-type *PFGLO1* and *PfCGLO2* genes). This clearly showed the integration of the 2.1 kb expression cassette of *hDHFR*. PCR analysis using specific primers that targeted the integrated *hDHFR* and the 5' and 3' UTRs of the *PFGLO1* and *PfCGLO2* gene loci also confirmed the disruption of the native genes and the integration of the *hDHFR* gene sequence into the genome of the 3D7 Δ *glo1* and 3D7 Δ *cglo2* strains (2.5 kb and 2.3 kb bands were detected by PCR and agarose gel analyses of the 3D7 Δ *glo1* strain corresponding to the respective 5' and 3' UTR segments of the disrupted *PFGLO1* locus. 2.6 kb and 2.1 kb bands were also detected by PCR and agarose gel analyses of the 3D7 Δ *cglo2* strains, corresponding to the 5' and 3' UTR segments of the disrupted *PfCGLO2* locus). No bands were produced when *P. falciparum* 3D7 wild-type gDNA was analyzed for *hDHFR* integration. Western blot analysis confirmed the disruption of the two gene loci, and eliminated the possibility of gene multiplications and other genetic recombinations that may still have led to the expression of functional *PfGlo1* and *PfGlo2* enzymes in the respective knockout strains (Figure 4.2 E). In the western blot analysis, *PfGlo1* and *PfGlo2* proteins were detected at approximately 42 and 31 kDa respectively only in cell lysate of the *P. falciparum* 3D7 wild-type control strain. The PCR and western blot results together confirm

that the cytosolic glyoxalase enzymes, *PfGlo1* and *PfcGlo2*, are not essential for the blood-stage development of the *P. falciparum* 3D7 strain since single knockout clones were viable.

4.5. Attempts to disrupt the *PFtGLO2* and *PFGILP* loci were not successful

Four attempts to disrupt the *PFtGLO2* and *PFGILP* loci were unsuccessful. The four independent transfection attempts were performed using the same and slightly varied protocols as was used in the transfection of 3D7^{cas9} parasites with pL7-*PFGL01* and pL7-*PFcGLO2* plasmids. In the first attempt, transfections were maintained and selected with WR for 63 days but no parasites were detected in Giemsa-stained blood smears at various times during the culture. In the second attempt, parasites were detected in Giemsa-stained smears within 4 weeks post-transfection under WR selection. Transfectants also survived 9 days negative selection with 5-FC whilst maintaining WR pressure. Mixed population transfectants were ultimately analyzed by PCR for native gene disruption and the integration of the *hDHFR* expression cassette into the *PFtGLO2* or *PFGILP* locus. Analytical PCR using primers that targeted the whole gene locus of *PFtGLO2* and *PFGILP* generated DNA bands at 2.6 kb and 1.8 kb respectively on agarose gels. These band sizes corresponded to the lengths of the intact wild-type whole gene sequences, and showed that the native *PFtGLO2* and *PFGILP* genes were not disrupted. The expected band sizes of the disrupted *PFtGLO2* and *PFGILP* loci should be 4.7 kb and 3.9 kb on the 3D7 Δ *tglo2* and 3D7 Δ *gilp* strains respectively. Analytical PCR results using specific primers that targeted the probably integrated *hDHFR* expression cassette and the 5' and 3' UTRs of the native *PFtGLO2* and *PFGILP* loci produced no bands on agarose gels. The expected band sizes for the 5' and 3' segments of the *PFtGLO2* locus of the 3D7 Δ *tglo2* strain should be 3.1 kb and 2.0 kb respectively. The expected bands for the 5' and 3' segments of the *PFGILP* locus of the 3D7 Δ *gilp* strains should be 2.5 kb and 1.8 kb respectively. Different PCR programs were also tried to increase the chances of amplifying any integrated *hDHFR* expression cassette. These included increasing and decreasing the annealing and extension temperatures and times. However, all the results suggested that the reporter *hDHFR* gene was not integrated in the *PFtGLO2* and *PFGILP* native gene loci and so the target genes were not disrupted. In the third and fourth attempts, changes were made regarding the transfection protocol in order to increase the chance of disrupting the *PFtGLO2* and *PFGILP* genes. New transgenic 3D7^{cas9} parasites were generated for these attempts in order to eliminate the possibility that a mutated and inefficient Cas9 protein could result from the old population after many rounds of cell culture. A new dilution of WR was also used to increase the potency of the drug for positive selection. However, similar to the second transfection attempt, false-positive transfectants of the pL7 plasmids were detected by Giemsa-stained thin blood smears within four weeks of the third and fourth transfection attempts. In the fourth attempt, a repeat transfection of the pL7-*PFGL01* plasmid was also performed as a control of the protocol, along with the pL7-*PFtGLO2* and pL7-*PFGILP* plasmids transfections. Transfectants were detected in the culture of pL7-*PFGL01* control transfection about the same time as were detected in the pL7-*PFtGLO2* and pL7-*PFGILP* transfection cultures. PCR analysis of gDNA of the pL7-*PFGL01* control transfectants once again confirmed the disruption of the native gene and the integration of the *hDHFR* expression cassette into the *PFGL01* locus. This result showed that the transfection protocol

worked efficiently. The issues relating to the inability to disrupt the *Pf*GLO2 and *Pf*GILP gene loci therefore seem to be directly related to the architecture of the pL7-*Pf*GLO2 and pL7-*Pf*GILP knockout constructs, for example with the specificity of the guide sequence.

4.6. Growth curve and morphological analyses of knockout strains

Light microscopy examination of Giemsa-stained thin blood smears of the asexual stages of the 3D7 Δ *glo1* and 3D7 Δ *cgl2* strains helped analyze the phenotypic characteristics of these parasites (Figure 4.4 A, B & C). Analyses of different growth stages of over 20 parasites each of the two clonal knockout lines, Δ *glo1*#1 & Δ *glo1*#2 (of 3D7 Δ *glo1* strain) and Δ *cgl2*#1 & Δ *cgl2*#2 (of 3D7 Δ *cgl2* strain) detected no unusual morphological features of the knockout parasites in comparison with the 3D7 wild-type strain. Assessment of the viability and growth rate of three 3D7 Δ *glo1* clonal lines and two 3D7 Δ *cgl2* clonal lines showed a slight reduction in growth rate compared to the wild-type strain. From an averaged starting parasitemia of 0.1%, an asynchronous 3D7 wild-type culture reached a parasitemia of approximately 12% after 6 days of culture compared to 9% and 10% for 3D7 Δ *glo1* and 3D7 Δ *cgl2* clonal lines respectively under the same culture conditions. This reduction in growth rate was, however, found not to be significant according to statistical analyses. In summary, 3D7 Δ *glo1* and 3D7 Δ *cgl2* asexual blood-stage parasites have an inconspicuous morphology and show no obvious growth defect.

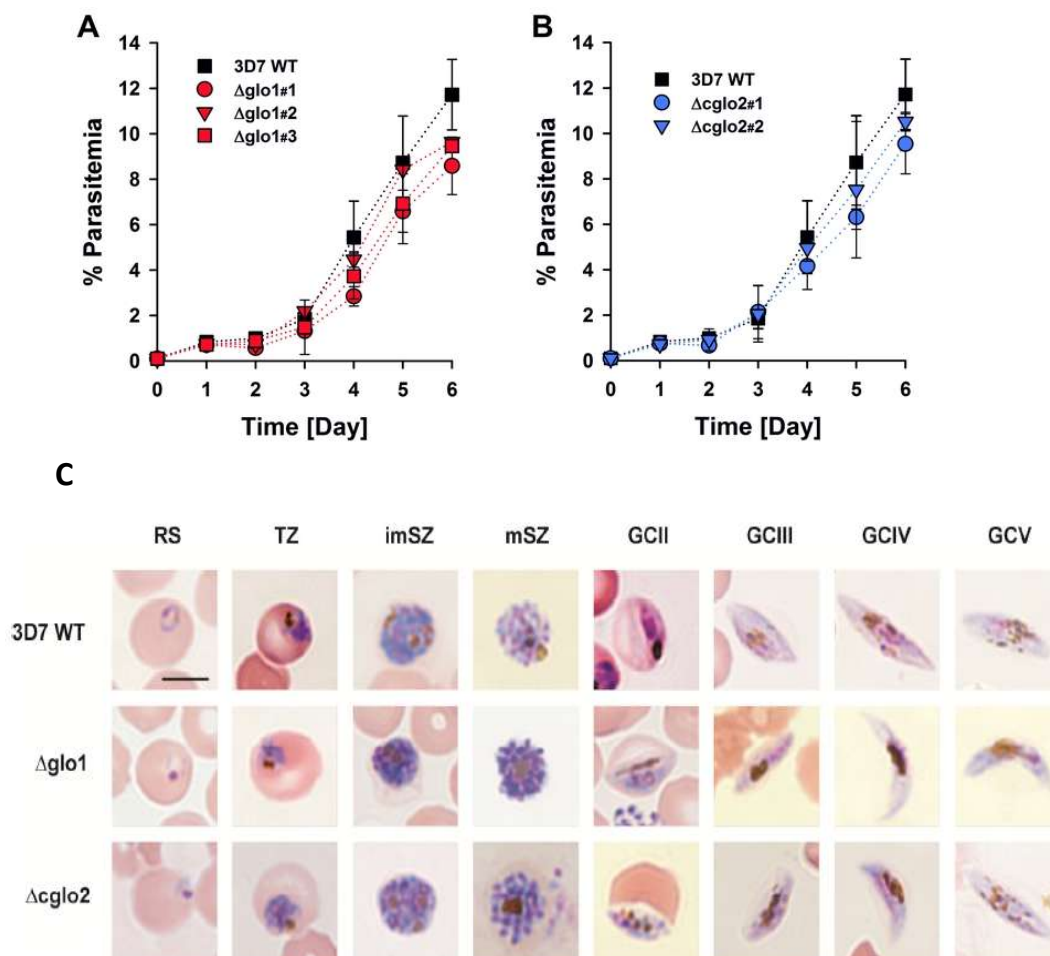


Figure 4.4. Growth curve analysis and general morphology of *P. falciparum* knockout strains 3D7 Δ *glo1* and 3D7 Δ *cglo2*. (A) Growth analysis of three clonal lines of 3D7 Δ *glo1* knockout strains in comparison to the 3D7 wild-type strain. (B) Growth analysis of two 3D7 Δ *cglo2* clonal lines in comparison with the 3D7 wild-type strain. The starting parasitemia of an asynchronous culture for all experiments was 0.1% and cultures were monitored for six days by counting Giemsa-stained blood smears. All data points represent the mean \pm S.D. from three independent experiments. Statistical analysis using the one way ANOVA method in SigmaPlot 12.5 did not reveal a significant growth difference between the knockout strains and the 3D7 wild-type strain ($p > 0.05$). (C) Morphology of the asexual blood and gametocyte stages of 3D7 Δ *glo1* and 3D7 Δ *cglo2* strains by Giemsa-stained blood smears. Microscopical examination of smears of ring stages (RS), trophozoites (TZ), immature schizonts (imSZ), mature (mSZ) schizonts as well as gametocytes (GC) stages II-V of the knockout strains revealed no observable differences in morphology compared to the same stages in the 3D7 wild-type blood-stage parasites. Bar, 5 μ m. Microscopy was performed by Alexandra Golzmann of the laboratory of Prof. Gabriele Pradel. Taken and modified from (Wezena *et al.*, 2018).

4.7. Glo1 and Glo2 activities of glyoxalase knockout strains

The contribution of *Pf*Glo1 and *Pfc*Glo2 to the overall Glo1 and Glo2 activities in purified *P. falciparum* parasite extracts was determined for the 3D7 wild-type strain in comparison with the clonal 3D7 Δ *glo1* and 3D7 Δ *cglo2* knockout lines (Figure 4.5). The average Glo1 activities of 3D7 wild-type, 3D7 Δ *glo1* and 3D7 Δ *cglo2* clones were 184, 19 and 281 μ U/mg protein respectively. Gene knockout clearly affected the activity levels of the enzymes in both knockout clones but in contrasting patterns. As expected, Glo1 activity in the 3D7 Δ *glo1* parasites significantly dropped by approximately 90% as compared to the activity in the 3D7 wild-type strain. The 10% residual Glo1 activity recorded in the 3D7 Δ *glo1* clones might either originate from a non-canonical parasite enzyme or from human Glo1 that is taken up into the parasite. In contrast, the Glo1 activity of the 3D7 Δ *cglo2* parasites unexpectedly increased by approximately 50% in comparison with that of the wild-type strain. This increase could be due to an up-regulation of the Glo1 gene in the 3D7 Δ *cglo2* parasites even though the averaged differences in Glo1 activity between wild-type strain and the 3D7 Δ *cglo2* clonal knockout lines varied and were not significant according to statistical analyses. With regards to Glo2 activities, the averaged values 295, 308 and 101 μ U/mg protein were recorded for 3D7 wild-type, 3D7 Δ *glo1* and 3D7 Δ *cglo2* clones respectively. The 3D7 Δ *cglo2* clones maintained about one third of the Glo2 activity recorded in the wild-type strain. This relatively high Glo2 activity recorded in the knockout lines might be explained by the *Pft*Glo2 activity in parasite extracts. As stated above, *Pft*Glo2 is an active enzyme in standard Glo2 assays. The residual Glo1 and Glo2 activities recorded in the respective knockout clones may explain the absence of a variant phenotype in these strains. While the residual Glo2 activity of around 30-40% is plausible in the 3D7 Δ *cglo2* clonal lines in the presence of a functional *Pft*Glo2 enzyme, a residual Glo1 activity of around 10% is quite surprising for 3D7 Δ *glo1* knockout parasites considering the absence of another functional canonical Glo1-isoform in *P. falciparum*.

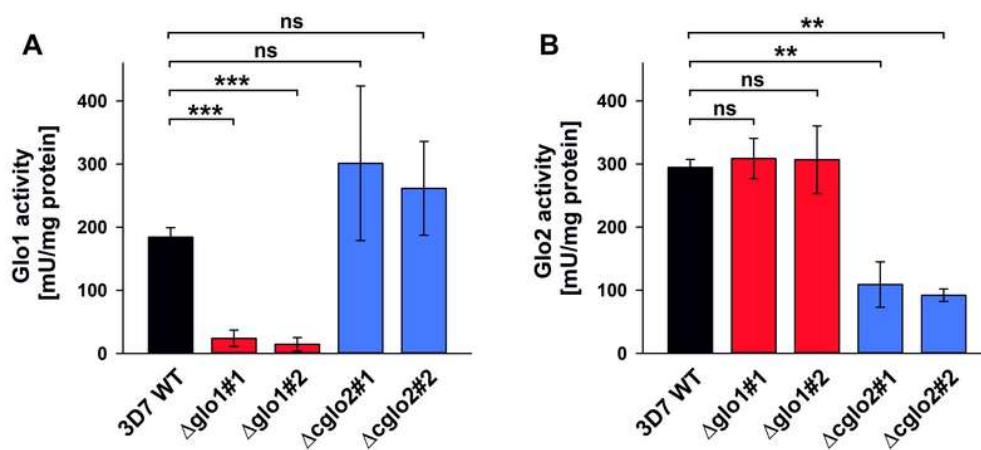


Figure 4.5. Glo1 and Glo2 activity measurements of *P. falciparum* 3D7Δglo1 and 3D7Δcglo2 knockout strains after erythrocyte removal by saponin lysis. (A) Normalized Glo1 activity measurements of knockout strains in comparison with the 3D7 wild-type strain at 240 nm. Parasite extracts from approximately 10^7 trophozoites were used. (B) Normalized Glo2 activity measurements of knockout strains in comparison with the 3D7 wild-type strain at 240 nm. Parasite extracts from approximately 1.7×10^7 trophozoites were used. All data points represent the mean \pm S.D. from two to four independent triplicate measurements. Statistical analyses were performed in SigmaPlot 12.5 using the one way ANOVA method (ns, not significant; ** $p < 0.01$; *** $p < 0.001$). Taken and modified from (Wezena *et al.*, 2018).

4.8. Susceptibility of glyoxalase knockout strains to 2-oxoaldehydes

IC₅₀ assays of the susceptibility of the clonal 3D7Δglo1 and 3D7Δcglo2 knockout lines to the external physiological substrates glyoxal, methylglyoxal and phenylglyoxal (Figure 4.7) are summarized in Figure 4.6. The IC₅₀ curves shown in Figure 4.7 are results from SYBR green 1 assays of bolus treatments of ring-stage knockout and 3D7 wild-type parasites clones with the 2-oxoaldehydes. The results, which were averaged from three to seven independent triplicate measurements, showed that the IC₅₀ values for glyoxal were approximately 75 μM, 40 μM and 76 μM for the 3D7 wild-type, 3D7Δglo1 and 3D7Δcglo2 parasite lines respectively. The average IC₅₀ values for methylglyoxal were 271 μM, 255 μM and 232 μM for 3D7 wild-type, 3D7Δglo1 and 3D7Δcglo2 parasite lines respectively. For phenylglyoxal, the average IC₅₀ values were in the millimolar range for all parasite lines. IC₅₀ values of 1.2 mM, 1.3 and 1.2 mM were recorded for this compound for the 3D7 wild-type, 3D7Δglo1 and 3D7Δcglo2 parasite lines respectively. The results revealed that the toxicity of the 2-oxoaldehydes depended on the size and/or polarity of the compounds with lowest IC₅₀ values for the lower molecular weight glyoxal and highest IC₅₀ values for higher molecular weight phenylglyoxal. The results also showed a significant decrease by up to 60% in IC₅₀ value for glyoxal for the 3D7Δglo1 knockout parasites in comparison to the wild-type strain, whereas no significant differences between wild-type and 3D7Δglo1 knockout parasites were observed after treatment with methylglyoxal and phenylglyoxal. No significant differences were observed between the susceptibility of the 3D7Δcglo2 knockout parasites and wild-type parasites towards the three external 2-oxoaldehydes. In summary, 3D7Δglo1 knockout parasites are more susceptible to external glyoxal, which is more toxic to the *P. falciparum* 3D7 strain than methylglyoxal and phenylglyoxal.

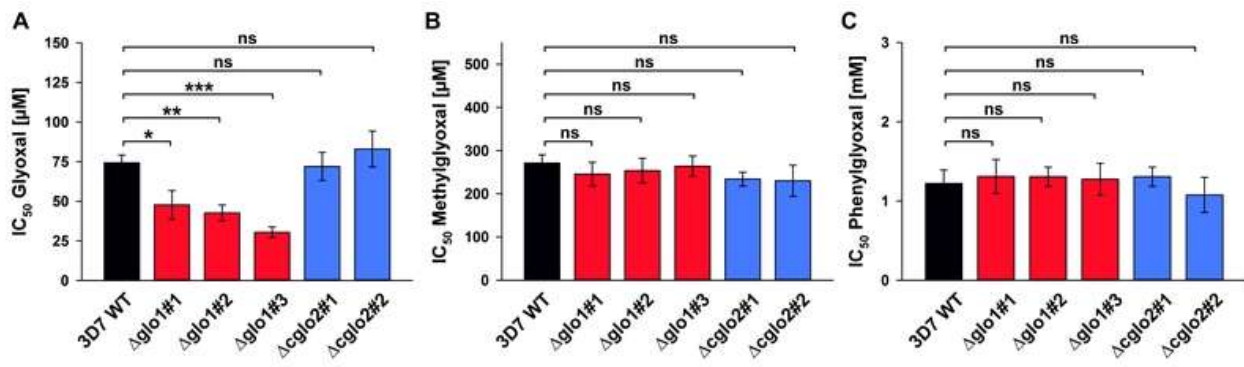


Figure 4.6. Summary of growth inhibitory effects of exogenous 2-oxoaldehydes on 3D7 Δ glo1 and 3D7 Δ cgl2 knockout strains. Ring-stage synchronous cultures with 1.5% starting parasitemia were treated with bolus amounts of (A) glyoxal, (B) methylglyoxal and (C) phenylglyoxal and maintained in 96-well plates. IC_{50} values were determined after 72 hr of incubation using a SYBR green 1 assay. All data points represent the mean \pm S.D. from triplicate measurements of three to seven independent experiments. Statistical analyses were performed in SigmaPlot 12.5 using the one way ANOVA method (ns, not significant; * $p < 0.05$; ** $p < 0.01$; *** $p < 0.001$). Taken and modified from (Wezena *et al.*, 2018).

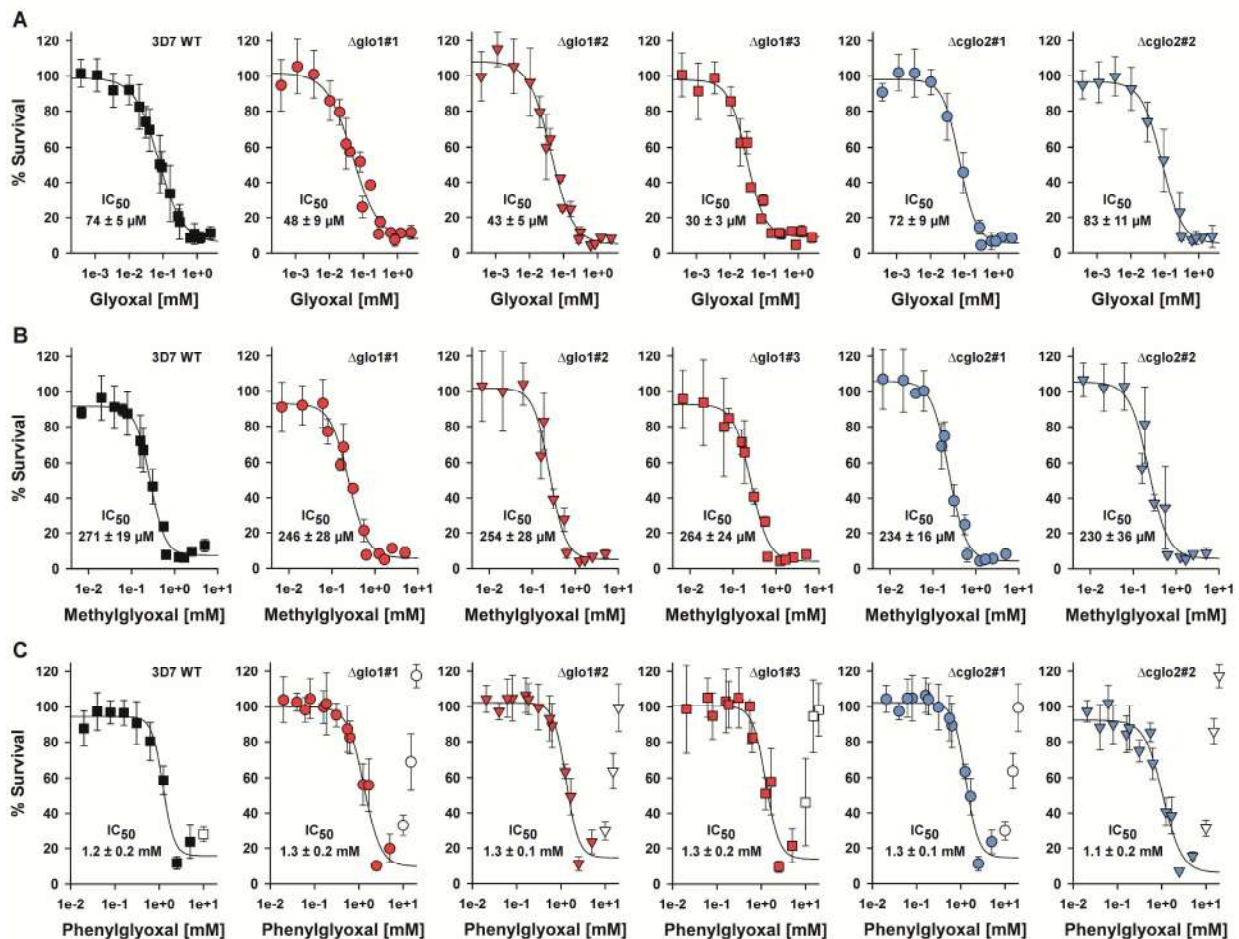


Figure 4.7. Growth inhibitory effects of exogenous 2-oxoaldehydes on synchronous ring-stage cell cultures of *P. falciparum* 3D7 Δ glo1 and 3D7 Δ cgl2 knockout strains. Cultures were maintained in 96-well plates with a starting hematocrit and parasitemia of 1.5% and 0.5% respectively. Cultures were treated with bolus amounts of (A) glyoxal, (B) methylglyoxal and (C) phenylglyoxal and the IC_{50} values were determined using a SYBR green I assay after 72 hr of incubation. All data points represent the mean \pm S.D. from triplicate measurements of three to seven independent experiments. Data points at phenylglyoxal concentrations ≥ 10 mM were omitted because of a strong autofluorescence. The IC_{50} values are summarized in Figure 4.6. Taken and modified from (Wezena *et al.*, 2018).

4.9. AGE accumulation in glyoxalase knockout strains

To assess the potential accumulation of AGE in the 3D7 Δ *glo1* and 3D7 Δ *cglo2* knockout strains, western blot analysis of purified trophozoite-stage parasite extracts was performed using the commercial polyclonal anti-AGE antibody, Ab23722 (Figure 4.7). This antibody has specificity for general AGE and is suitable for the detection of the products in parasite cell extracts. The staining pattern by the antibody revealed a few AGE bands and smears around 40, 70 and 180 kDa. When cell lysates from steady state parasites and cell lysates from parasites that were treated with 50 μ M glyoxal for 6 hr were analyzed, the AGE bands at 70 and 180 kDa were visibly more intense for the 3D7 Δ *glo1* and 3D7 Δ *cglo2* parasite extracts than for wild-type parasite extracts. Band patterns and comparative intensities in relation to the wild-type samples were, however, similar under both conditions. Analysis of band intensities from three independent experiments of treated and untreated parasite extracts was performed using the ImageJ software. The results showed an increase of about 80% in accumulated AGE in the 3D7 Δ *glo1* and 3D7 Δ *cglo2* parasite lines compared to the 3D7 wild-type parasites in extracts from both treated and untreated parasites. Results from the western blot analyses therefore support the accumulation of selected modified proteins in the glyoxalase knockout strains. However, parasite growth at the erythrocytic-stage appears to be normal and unaffected by the accumulation of the glycated products.

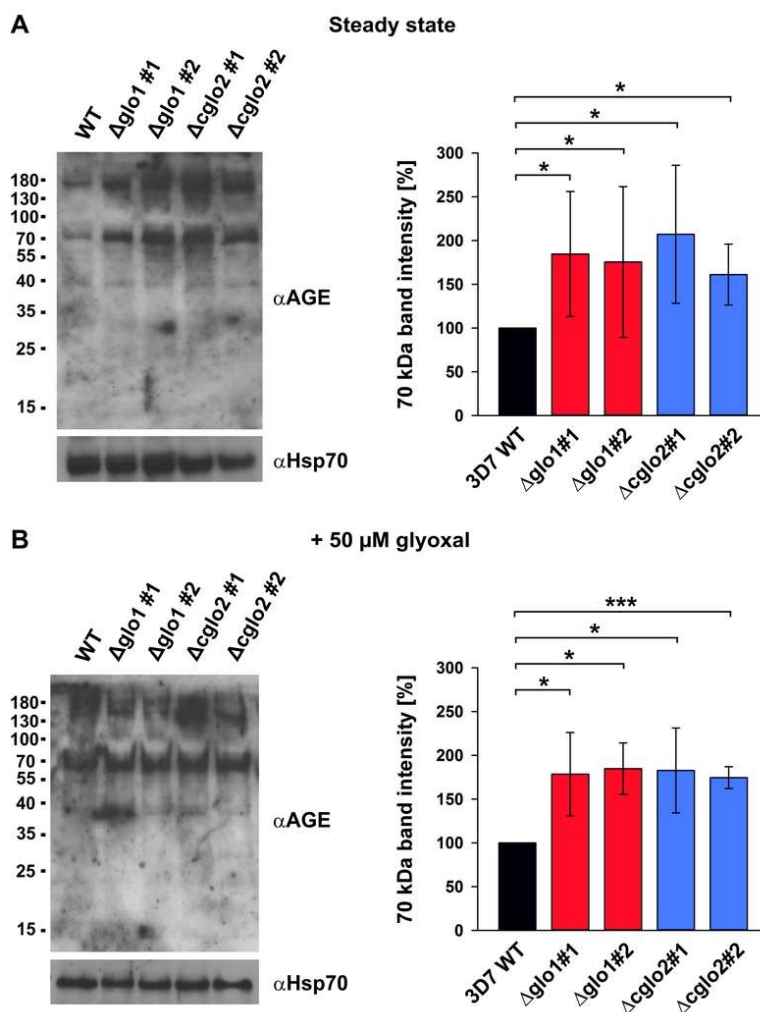


Figure 4.8. Western blot detection of AGE in parasite extracts from *P. falciparum* 3D7 Δ *glo1* and 3D7 Δ *cglo2* knockout strains after erythrocyte removal by saponin lysis. 3D7 wild-type parasite extracts served as a control. (A) Detection of AGE under steady-state conditions without treatment with external 2-oxoaldehyde. (B) Detection of AGE after a 6 hr bolus treatment with 50 μ M glyoxal (50 μ M glyoxal is used because this concentration corresponds approximately to the glyoxal IC₅₀ value determined in Figure 4.6). Extracts from 2×10^7 trophozoites were loaded per lane on a 15% gel, separated by reducing SDS-PAGE and decorated with a commercial polyclonal anti-AGE antibody. Detection of *P. berghei* Hsp70 on a parallel run blot using the same parasite extracts served as a loading control. Signal intensities were analyzed from three independent experiments using ImageJ and statistical analyses were performed in SigmaPlot 12.5 using the one way ANOVA method (* $p < 0.05$; *** $p < 0.001$). Taken and modified from (Wezena *et al.*, 2017).

4.10. Gametocytogenesis of glyoxalase knockout strains

Experiments aimed to investigate how the loss of *Pf*Glo1 or *Pf*cGlo2 activity as well as the accumulation of AGE would affect gametocyte commitment were performed by Alexandra Golzmann in the laboratory of Gabriele Pradel at the RWTH University of Aachen. The results revealed that the 3D7 Δ *glo1* and 3D7 Δ *cglo2* glyoxalase knockout strains were both able to undergo gametocyte commitment and to develop mature gametocytes as the 3D7 wild-type strain. The gametocyte stages formed in the three lines exhibited morphologies comparable to the wild-type strain during maturation (Figure 4.4 C). Surprisingly, however, the 3D7 Δ *cglo2* parasites had an increased gametocytemia compared to the parental line and the 3D7 Δ *glo1* parasites in more than three independent experiments (Figure 4.8). This result indicated that the lack of *Pf*cGlo2 results in increased gametocyte induction and gametocytogenesis. The 3D7 Δ *glo1* parasites were also shown to form a reduced number of gametocytes in all experiments compared with the two other strains.

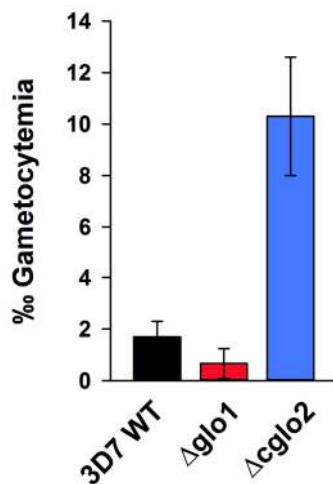


Figure 4.9. Analysis of gametocyte development of the *P. falciparum* 3D7 Δ *glo1* and 3D7 Δ *cglo2* knockout strains. Gametocyte commitment and induction were analyzed in the 3D7 Δ *glo1* and 3D7 Δ *cglo2* knockout strains in comparison with the 3D7 wild-type strain. Gametocytemia was determined by microscopy per 1000 red blood cells in Giemsa-stained blood smears 14 days post-induction. All data points are the mean \pm S.D. from triplicate measurements. Results shown are representative of three independent experiments. Taken from (Wezena *et al.*, 2017).

4.11. Antiproliferative effects of H₂O₂, ascorbate, NAc and DTT

The effect of standard pro- and antioxidants on the erythrocytic development of *P. falciparum* 3D7 wild-type strain was investigated using the SYBR green 1 assay. IC₅₀ values for H₂O₂, ascorbate, NAc and DTT were determined for synchronous ring-stage parasite cultures. Results averaged from three to six independent experiments showed IC₅₀ values for H₂O₂, ascorbate, NAc and DTT to be around 78 mM, 4.3 mM, 17 mM and 245 μ M respectively (Figure 4.9). The IC₅₀ value for H₂O₂ (Figure 4.9 D) is unexpectedly high considering the widely suggested susceptibility of *Plasmodium* species to reactive oxygen species (Dockrell *et al.*, 1986; Clark & Hunt, 1983), and the relevance of oxidative stress for parasite survival (Becker *et al.*, 2004; Jortzik & Becker, 2012). To completely kill parasites, even higher concentrations of H₂O₂ were required, that also caused intense catalase-dependent oxygen production and foaming of the culture (Wezena *et al.*, 2017).

During pre-trials to determine the order of magnitude of the IC₅₀ values, it was observed that the reducing agents ascorbate, NAc and DTT promoted gelling of the medium, formation of methemoglobin and hemolysis at high concentrations. The same effects were observed when

cultures were incubated for prolonged periods with the compounds. The same observation was made by Johannes Krafczyk while determining the IC_{50} values for the reducing agents for the *P. falciparum* Dd2 strain. While the gelation was also detected at DTT concentrations lower than 1 mM, methemoglobin formation and hemolysis appeared to require higher DTT concentrations. All the reducing agents were found to exhibit a significant gelation-dependent increase in background fluorescence in the SYBR green 1 assay. To correct the experimental results for this background effect, reference values from uninfected erythrocytes that were cultured in parallel with the same amount of the reducing agents were used. The final results showed that all three reducing agents have antiproliferative rather than growth-promoting effects (Figure 4.9 A, B & C). The parasites, however, appear to be more sensitive to DTT than to NAc and ascorbate.

The effects of ascorbate on the 3D7 strain were further analyzed by treating parasites in normal cultures with different concentrations of ascorbate (Figure 4.9 E). Cultures were grown for six days and the parasitemia was monitored daily by Giemsa-stained blood smears. The results showed that daily culture treatment with 2.5 mM and 5.0 mM ascorbate caused methemoglobin formation and hemolysis over time. These effects coincided with growth inhibition as the parasitemia after six days of culture was also reduced by around 46% and 90% in the plates treated with 2.5 mM and 5.0 mM ascorbate respectively. As observed in the IC_{50} assay results above, millimolar ascorbate concentrations as well as prolonged incubation periods were required for these effects to be detectable. Ascorbate thus exhibited slow growth inhibition kinetics for standard cultures of *P. falciparum* 3D7 strain with an IC_{50} value of > 1 mM.

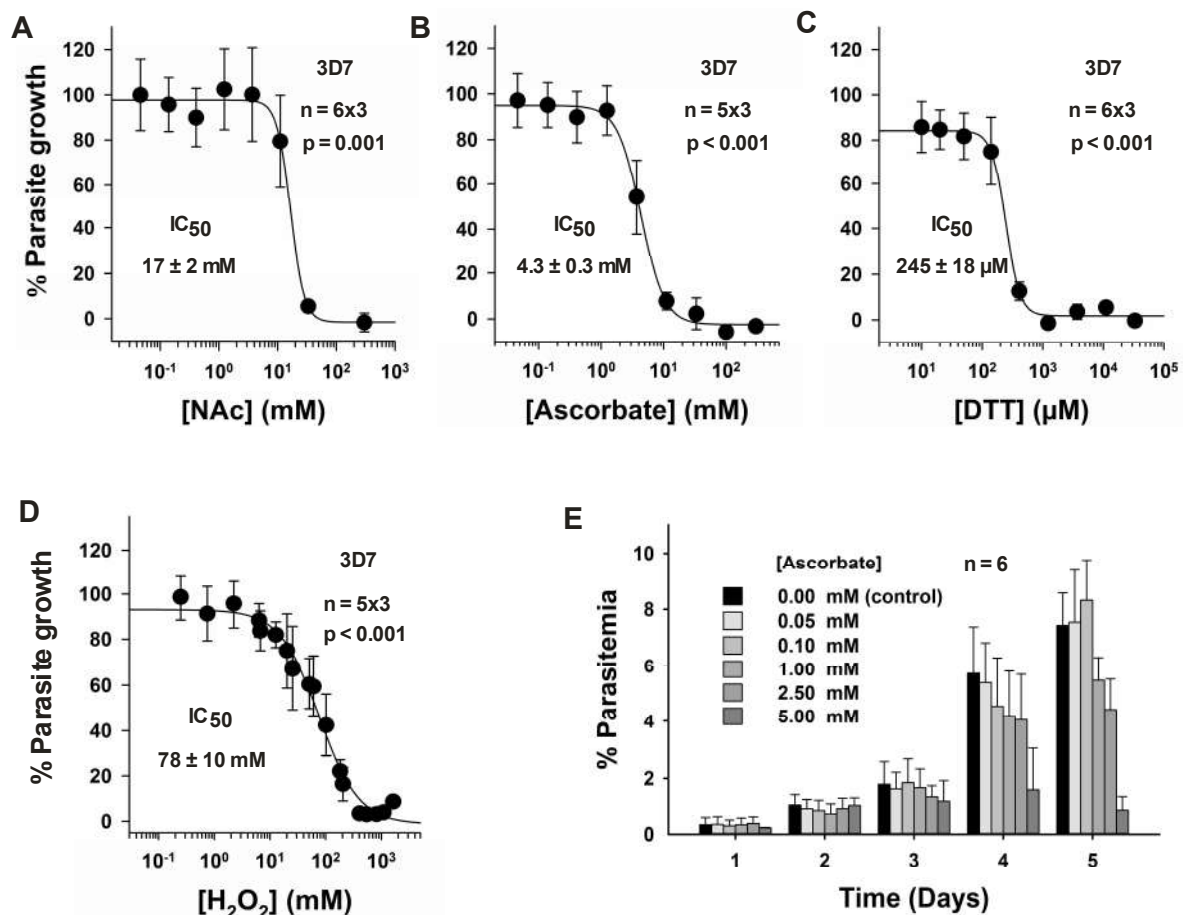


Figure 4.10. Growth inhibitory effects of hydrogen peroxide and the three reducing agents, NAc, ascorbate and DTT on *P. falciparum* 3D7 wild-type strain cultures. Panels (A-D) Ring-stage synchronized cultures were started in 96-well plates at a hematocrit of 1.5% and parasitemia of 0.5% for IC₅₀ determination. IC₅₀ values were determined using SYBR green I assay 72 hr after bolus treatment of cultures with NAc (A), ascorbate (B), DTT (C) and H₂O₂ (D). The number of replicates for each data point is indicated in each panel (e.g., n = 6 x 3 for six independent triplicate measurements). (E) Time-dependent growth inhibition of *P. falciparum* 3D7 wild-type strain by daily ascorbate treatment. Standard 14 mL 3D7 wild-type strain cultures synchronized at the ring-stage were started at a parasitemia of 0.1% and a hematocrit of 3%. Cultures were treated daily with the same concentration of ascorbate (0.05 mM, 0.10 mM, 1.00 mM, 2.50 mM and 5.00 mM) in fresh growth medium and the parasitemia was monitored over six days using Giemsa-stained blood smears. Data points represent the average of results from six independent 6-day experiments. Taken and modified from (Wezena *et al.*, 2017).

Table 4.1. Summary of the IC₅₀ values determined in this study compared with previously determined values from the Dd2 strain.

Strain	Oxidants		Reductants		
	H ₂ O ₂ (mM)	tBOOH (μ M)	Ascorbate (mM)	NAc (mM)	DTT (μ M)
3D7 ^a	77.8 \pm 9.6	81.1 \pm 6.4	4.3 \pm 0.3	16.6 \pm 2.1	245 \pm 18
Dd2 ^b	46.1 \pm 7.8	121 \pm 9	3.0 \pm 0.3	12.4 \pm 3.0	389 \pm 26

IC₅₀ value for tBOOH for the 3D7 strain was determined by Verena Staudacher. H₂O₂, tBOOH, ascorbate, NAc and DTT values for the Dd2 strain were determined by Johannes Krafczyk.

a Bolus treatment of asynchronous parasite cultures.

b Bolus treatment of synchronous ring-stage parasite cultures.

5. DISCUSSION

5.1. A revolutionary CRISPR-Cas9 system for *P. falciparum* genome editing

Malaria remains a major cause of global morbidity and mortality especially among children under five (5) years and pregnant women in the tropical regions of Africa (Bousema & Drakeley, 2011). Nearly half of the world's population is at risk of the disease that caused about 731 000 deaths in 2015 alone and around 350 to 500 million infections every year (Bousema & Drakeley, 2011; Rosenberg, 2008; WHO, 2017a). Of the five *Plasmodium* species that cause human malaria, *P. falciparum* is the most virulent and accounts for up to 85% of all global malaria cases (Dronamraju & Arese, 2006; Lee & Vythilingam, 2013). The combined effects of resistance to front-line malaria drugs, climate change and a rise in international travel have made control of the parasitic infection daunting and major gains made in the control of the disease are at risk of being eroded (Mirski *et al.*, 2011; Bai *et al.*, 2013). To sustain these gains and improve on the fight against malaria, new potent antimalarial drugs as well as effective vaccines are urgently required. An improved molecular understanding of the complex life cycle of the malaria parasite will not only help in the identification of new drug targets and the evaluation of vaccine candidates, but will also help characterize the molecular basis of current drug resistance. Information revealed by the sequencing of the *P. falciparum* genome is an added advantage that should immensely benefit molecular research into the malaria parasite in many fronts (Carvalho & Ménard, 2005). Genetic manipulation of the *P. falciparum* genome is, however, a daunting task hampered by peculiar difficulties, and mostly limited to the blood stages of the parasites life cycle (Cowman & Crabb, 2005). The reasons for this situation are numerous and are mainly based on the complex life cycle of the species and on the specific genome architecture of *P. falciparum* (Carvalho & Ménard, 2005). For instance, the parasite spends most of its life located intracellularly within the parasitophorous vacuole in the infected erythrocyte, with its nucleus separated from the environment by four membranes. This causes a marked reduction in transfection efficiency ($\sim 10^{-6}$ frequency in *P. falciparum*) of the *Plasmodium* parasite (Carvalho & Ménard, 2005; Crabb, 2002). Secondly, the genome of *P. falciparum* has a very high A-T content (81%) (Cowman & Crabb, 2005; Tuteja, 2007). This does not only make the preparation of transfection plasmids in *E. coli* difficult but also presents the very possible challenge of nonspecific DNA integration into the parasite genome during genetic manipulation (Cowman & Crabb, 2005; Tuteja, 2007). Thirdly, except for a few recent reports, only circular plasmid vectors have been used to successfully transfect *P. falciparum* parasites (Crabb, 2002). The use of linear DNA template shortens the time for the selection of integrants and circumvents the episomal maintenance of template DNA. It is the preferred template for homologous recombination in *P. berghei*, but, until recently, has not been workable in *P. falciparum*. This is presumably because linear DNA templates get degraded as they cross into the nucleus, making them unstable for ring-stage transfection (Cowman & Crabb, 2005). A longer period ($\sim 3-4$ months) is required to select for integrants after transfection with circular plasmids because these plasmids preferentially replicate episomally rather than integrate into the parasite genome (Carvalho & Ménard, 2005). Another issue is that double crossover is a rare random process in *P. falciparum* as circular plasmids would

preferentially undergo only a single crossover event especially without drug pressure and negative selection (Carvalho & Ménard, 2005). Finally, the limited number of robust selectable markers for successful gene editing in *P. falciparum* has restricted the performance of consecutive genetic manipulations on the same parasite (Koning-Ward *et al.*, 2015). The genome of blood-stage *Plasmodium* is haploid meaning that genetic manipulation involves targeting a single gene (Koning-Ward *et al.*, 2015). This has the advantage that, for most genes, a single recombination event is sufficient for generating a modified parasite clone (Carvalho & Ménard, 2005). It is, however, difficult to study essential genes under standard blood-stage culture conditions because disruption of such genes is lethal (Koning-Ward *et al.*, 2015).

Recently, an engineered CRISPR-Cas9 genome-editing system based on the type II CRISPR-Cas system of *S. pyogenes* was effectively used to achieve results for both gene disruption and single-nucleotide gene editing in *P. falciparum* (Lee & Fidock, 2014; Ghorbal *et al.*, 2014). Even though the earliest design of *P. falciparum* CRISPR-Cas9 system (Ghorbal *et al.*, 2014) involves a two-plasmid approach, the strategy was shown to be highly efficient. As long as the requirement for a unique guide sequence of the sgRNA was met, virtually every locus of the malaria parasite that carries a PAM sequence could be targeted for modification (Ghorbal *et al.*, 2014). Similar to other genome-editing tools, the CRISPR-Cas9 system can target and directly edit specific sites in the parasite genome. Having the choice of design of the guide sequence and the homologous regions for recombination helps avoid high A-T portions of target genes that will otherwise expose the strategy to non-specific recombination events. As the CRISPR-Cas9 system is not based on random induction of DNA double strand breaks (hallmark of conventional genome modification systems) selection of integrants can be achieved in a shorter period (within 3 weeks) (Ghorbal *et al.*, 2014). Compared with other genome-editing tools, the CRISPR-Cas9 system was demonstrated to be more workable with *P. falciparum* (Koning-Ward *et al.*, 2015; Ghorbal *et al.*, 2014). For these reasons, the CRISPR-Cas9 system, initially used by Ghorbal and colleagues was employed to disrupt the glyoxalase genes, *PFGLO1* and *PFcGLO2*, of *P. falciparum*. An attempt was also made to disrupt the genes, *PFGLO2* and *PFGLP* that encode the apicoplast targeted glyoxalase enzymes. Furthermore, the Glo1 inhibitors, compounds 1, 3 and 7, were employed to investigate the relevance of the hGlo1 enzyme for the *Plasmodium* parasite's blood-stage development.

5.2. Human Glo1 appears to be dispensable for asexual blood-stage development

Tight-binding Glo1-specific inhibitors (compounds 1, 3 and 7) inhibited host (erythrocyte) Glo1 activity and were therefore used as a chemical tool to address the relevance of the functional hGlo1 for parasite survival in the host-parasite unit. Contribution of the host glyoxalase system to parasite development can be envisioned in two possible ways: import of hGlo1 to help cope with elevated levels of 2-oxoaldehydes or the export of excess 2-oxoaldehydes into the host to be detoxified by the more abundant human glyoxalase system. The outcome of the study supports neither of the two possibilities but rather suggests that the activity of hGlo1 does not play a major role for the intraerythrocyte development of the parasite in cell culture. Inhibition experiments with the most potent of the inhibitors,

compound 1, however, still allowed for the assay of as much as one-third residual hGlo1 activity in the erythrocyte. This hGlo1 activity residue, though unlikely (please see below), may be sufficient to compensate for the loss of hGlo1 activity and thus aid the parasite to survive in the inhibited erythrocytes. One other significant observation from the inhibition study is that esterification of the tight-binding inhibitors can impact the growth inhibition of malaria parasites and the inhibition of the host cell Glo1 activity in different ways. Previously, direct growth inhibition of *P. falciparum* blood-stage cultures by the esterified analogues of compounds 1 and 2 (compounds 3 and 7) yielded a three-fold reduction in IC₅₀ values compared with the respective mother compounds (Wezena *et al.*, 2016). This result conforms to earlier findings that esterification of glutathione-derived inhibitors reduce the polarity of the compounds and improve their uptake (Wezena *et al.*, 2016). Surprisingly, however, under the same culture conditions, esterification did not result in a faster or more potent inhibition of hGlo1 in uninfected erythrocytes. Assuming that esterification improves uptake, compounds 3 and 7 appear to bind or inhibit hGlo1 less, leading to a reduction in inhibition potency of the compounds. The slightly higher inhibitory potency of compound 7 to hGlo1 compared to compound 3 can be explained by the stability of compound 7 to γ -glutamyltranspeptidase cleavage (More & Vince, 2009). In agreement with this possibility is the slightly lower IC₅₀ for compound 7 for direct growth inhibition of *P. falciparum* in comparison with compound 3 (Wezena *et al.*, 2016).

5.3. Cytosolic glyoxalases of *P. falciparum* are dispensable for blood-stage development

The cytosolic glyoxalases, *PfGlo1* and *PfcGlo2*, of *P. falciparum* are dispensable during asexual blood-stage development and, *PFGLO1* and *PFcGLO2* knockout parasites are viable with no significant growth defects in standard culture conditions. This result is in contrast to results from the only previous preliminary knockout analysis of *P. falciparum* glyoxalases using pHTK vectors, which suggested that the cytosolic glyoxalases might not be deletable (Deponte, 2014). Western blot analysis, however, supports the accumulation of selected modified proteins in the 3D7 Δ *glo1* and 3D7 Δ *cglo2* knockout strains both under steady-state conditions and under bolus treatment with external glyoxal. This is in agreement with results from studies of the glyoxalase system in yeast, bovine endothelial cells and in *Caenorhabditis elegans*. In the yeast study, *GLO1*-null mutants were reported to have an increased protein glycation even though the mutants were viable and did not exhibit any particular growth defects when compared to the wild-type cells (Gomes *et al.*, 2005; Bito *et al.*, 1997). The glyoxalase system was therefore strongly suggested to play a key role in controlling the levels of methylglyoxal in yeasts cells (Silva *et al.*, 2013; Inoue *et al.*, 2011). In bovine endothelial cells, *in vitro* overexpression of hGlo1 was also reported to prevent the accumulation of AGE (Shinohara *et al.*, 1998) while in *C. elegans* the overexpression of Glo1 decreased the methylglyoxal-derived modification of proteins resulting in an increase in the life span of the roundworm (Moros *et al.*, 2008). It is therefore plausible to suggest that, though *PFGLO1* knockout is not immediately lethal, it could lead to downstream defects in the life cycle of the parasite. The fact that 3D7 Δ *glo1* and 3D7 Δ *cglo2* knockout strains were observed to have a slightly reduced (though statistically insignificant) growth rate when compared with 3D7

wild-type strains gives a subtle support to the above suggestion. In addition, the lack of a severe phenotype for the knockout clones could be due to the fact that their metabolism is robust. This robustness allows for enzymes in different but related metabolic pathways to compensate for variations in an individual enzyme's activity without significant changes in flux (Silva *et al.*, 2013). In a final conformation with the above results, a recent study in the rodent parasite *P. berghei*, also revealed that *PBGLO1* (PBANKA_0933900) is dispensable and that knockout parasites have no growth defect (Bushell *et al.*, 2017). Notably, however, an approximately 10% Glo1 activity was surprisingly recorded in the purified *PFGLO1* knockout strains. This residual activity might either originate from a non-canonical parasite enzyme or from the hGlo1 enzyme that has been taken up. The possibility that the residual Glo1 activity may be sufficient to prevent the lethal effects of *PFGLO1* disruption, and therefore the presentation of a strong knockout phenotype is plausible. In the same scenario, the approximately 30% residual Glo2 activity recorded in purified *PfcGLO2* knockout strains may be sufficient to prevent the lethal effects of the *PfcGLO2* knockout event. A single IC₅₀ experiment with the Glo1 inhibitors, compound 3 and 7, for the 3D7Δ*glo1* and 3D7Δ*cglo2* knockout strains showed very similar IC₅₀ values compared to wild-type parasites (data not shown). These results are in contrast to the possibility that hGlo1 is taken up by the parasite and may compensate for the loss of *PFGLO1* in the 3D7Δ*glo1* knockout strains. If hGlo1 were taken up, the expectation would have been altered IC₅₀ values for the knockout strain because the inhibitors can also slowly inactivate the human enzyme (Wezena *et al.*, 2016). With regards to *PfGlo1*, the dispensability of the enzyme for parasite survival may also explain the high IC₅₀ values for tight-binding Glo1-inhibitors in previous cell culture experiments in contrast to low nanomolar inhibition constants against recombinant *PfGlo1* (Urscher *et al.*, 2012; Wezena *et al.*, 2016). A plausible explanation to these varying inhibitor outcomes is that, killing of parasites at micromolar instead of nanomolar inhibitor concentrations may be due to off-target effects. Concerning the dispensability of *PfcGLO2* for the blood-stage parasite development, it may be necessary to eliminate the residual enzyme activity recorded in the 3D7Δ*cglo2* knockout strains before a defective phenotype is observed. This feat can only be achieved by also deleting the *PftGLO2* and/or inactivating hGlo2 in the 3D7Δ*cglo2* knockout strains. In this case, a workable *PfcGlo2* inhibitor will then also have to target not only *PfcGlo2* but also *PftGlo2* and/or hGlo2 to be effective. The results also revealed a considerable increased Glo1 activity in the 3D7Δ*cglo2* parasites in comparison with that of the wild-type. Though the change is statistically insignificant, it may be explained by an up-regulation of the Glo1 gene in the 3D7Δ*cglo2* parasites.

A significant phenotypic difference between the wild-type and glyoxalase knockout parasites was observed for 3D7Δ*glo1* knockout parasites that were treated with external glyoxal. The 3D7Δ*glo1* knockout strains were more sensitive to external glyoxal treatment than the 3D7Δ*cglo2* knockout and wild-type strains. A clear relation between reduced Glo1 activity and susceptibility to glyoxal in the *PFGLO1* knockout strains suggests that *PfGlo1* plays an important physiological role in the parasite's response to glyoxal. No significant differences in susceptibility to external methylglyoxal or phenylglyoxal were, however, observed between both knockout strains and the wild-type parasites. The variant levels of susceptibility displayed by the parasites towards the different 2-oxoaldehydes might be explained by either different kinetics for the transport of glyoxal, methylglyoxal and phenylglyoxal across the three membranes that surround the parasite cytosol or by different glyoxalase efficiencies of

the host-parasite unit regarding the conversion of these 2-oxoaldehydes. It would thus appear that glyoxal enters the unit with more ease than the other oxoaldehydes or is better converted than methylglyoxal and phenylglyoxal. A third explanation could be that other enzymes of the host-parasite unit, such as 2-oxoaldehyde reductases or dehydrogenases, are able to metabolize methylglyoxal and phenylglyoxal but not glyoxal with sufficient efficiencies in the knockout strains.

5.4. Loss of *PfGLO2* in the asexual blood stages increased gametocytogenesis

Interestingly, the loss of *PfGLO2* in the asexual blood stages resulted in increased gametocyte formation. As mentioned above, commitment to gametocytogenesis is believed to take place at some point before erythrocytic schizogony, when individual schizonts produce merozoites that develop into gametocytes after invasion of red blood cells (Bruce *et al.*, 1990; Smith *et al.*, 2000.). Results from recent studies have implicated a number of *P. falciparum* proteins in the switch between asexual blood-stage replication and gametocyte formation. These proteins, including *P. falciparum* heterochromatin protein 1 and histone deacetylase 2, as well as down-stream transcription factors such as Ap2G, were shown to epigenetically regulate the process of gametocytogenesis in *P. falciparum* (Kafsack *et al.*, 2014; A. Sinha *et al.*, 2014; Coleman *et al.*, 2014; Brancucci *et al.*, 2014). A variety of internal and external stress factors such as high parasitemia, anemia, host immune response or drug treatment are also shown to influence the commitment of merozoites to gametocyte formation (Brancucci *et al.*, 2014; Smalley & Brown, 1981; Schneeweis *et al.*, 1991; Trager & Gill, 1992; Lingnau *et al.*, 1993; Puta & Manyando, 1997; Talman *et al.*, 2004). *S*-D-lactoylglutathione, the product of *PfGlo1* catalysis which will accumulate in the parasite cytosol in the absence of *PfGLO2* may be the newest addition to parasite compounds that contribute to gametocytogenesis. Lack of functional *PfGLO1*, however, did not trigger gametocyte commitment. It is therefore plausible to speculate that the accumulation of *S*-D-lactoylglutathione or another thioester substrate of *PfGlo2* (Vander Jagt *et al.*, 1990; Urscher & Deponte, 2009; Urscher *et al.*, 2011) might have caused the induction of gametocyte commitment. *S*-D-lactoylglutathione has earlier been associated with the control of microtubule length in human neutrophils (Thornally & Bellavite, 1987) and microtubule assembly (Clellan & Thornalley, 1993). Whether this control has a functional or structural link to gametocytogenesis is yet to be investigated. Also, altered *S*-D-lactoylglutathione concentrations were previously reported to activate *E. coli* potassium channels that share properties with cation-translocating channels in eukaryotes (Ferguson *et al.*, 1993; Ozyama *et al.*, 2010; Roosild *et al.*, 2010). Furthermore, altered *S*-D-lactoylglutathione concentrations might also affect the uptake of glutathione into organelles as previously reported for isolated rat liver mitochondria (Armeni *et al.*, 2014). Whether similar *S*-D-lactoylglutathione-dependent mechanisms play a role in gametocyte commitment in *P. falciparum* remains to be studied.

5.5. Disruption of *Pf*Glo2 and *Pf*GILP genes is challenging

Successful disruption of the genes encoding the cytosolic glyoxalases using the CRISPR-Cas9 strategy confirms the robustness of this new system for genome editing in *P. falciparum*. It also exemplifies the fact that negative results from knockout attempts using traditional strategies in *P. falciparum* are difficult to interpret because of methodological limitations even when positive and negative selections are applied (Duraisingh *et al.*, 2002). With this new strategy, some of the limitations of traditional knockout strategies as well as the peculiar bottle-necks presented by the *P. falciparum* genome (Duraisingh *et al.*, 2002; Cowman & Crabb, 2005) can be overcome by the targeted introduction of DNA double-strand breaks. Nevertheless, four attempts to disrupt *PFtGLO2* and *PFGILP* genes using the same CRISPR-Cas9 system failed. It was not possible to generate 3D7 Δ *tglo2* and 3D7 Δ *gilp* knockout parasites even though transfectants with resistance to both positive and negative selection were acquired. The most probable explanation for this outcome is off-target or unwanted integration of the positive selectable marker into the parasite genome. One limitation of the current CRISPR-Cas9 system is the use of a circular plasmid vector to deliver the homologous regions for double recombination. The risk associated with this limitation is the possibility of unwanted insertion into the genome via single crossover events (Duraisingh *et al.*, 2002). Additionally, a non-specific guide sequence or the effects of the extremely AT-rich homology regions for *PFtGLO2* and *PFGILP* loci are possible causes of unwanted integration. Methodological limitations are therefore the most probable cause of the negative outcome of these knockout attempts rather than essential roles of both genes. A recent study in the rodent parasite *P. berghei*, which revealed that the homologue *PBtGLO2* (PBANKA_0604400) is dispensable and that knockout parasites have no growth defect, supports this explanation (Bushell *et al.*, 2017). Going forward, the use of a linear template DNA (Crawford *et al.*, 2017; Ghorbal *et al.*, 2014), which is not only acquired without cloning steps, but also avoids the need for negative selection may enable the disruption of the *PFtGLO2* and *PFGILP* genes. The use of a linear DNA template will circumvent the episomal maintenance of plasmid DNA and therefore reduces the chances of off-target effects of genome-editing (Crawford *et al.*, 2017).

5.6. Standard redox agents inhibit the growth of *P. falciparum* in cell culture

For many years, the generation of oxidative stress has been widely suggested to play an important role in the survival or clearance of the malaria parasite during human infection (Becker *et al.*, 2004; Jortzik & Becker, 2012; Goyal *et al.*, 2012). One of several hypotheses on oxidative stress and malaria is that an impaired production of external reactive oxygen species by host immune mechanisms in response to infection might exacerbate malaria infections (Becker *et al.*, 2004; Sorci & Faivre, 2009; Clark & Hunt, 1983; Descamps-latscha *et al.*, 1987; Greve *et al.*, 1999). However, a problematic aspect of this hypothesis is that the host-parasite unit is packed with numerous redox enzymes such as hydroperoxidases that are very efficient in reducing and neutralizing H₂O₂ to water (Staudacher *et al.*, 2015; Jortzik & Becker, 2012; Koncarevic *et al.*, 2009; Low *et al.*, 2008). In addition, some redox agents such as the hydroxyl radical are too reactive to diffuse across several membranes or only do so in

limited amounts (Bienert *et al.*, 2006; Almasalmeh *et al.*, 2014). The very high IC₅₀ value for H₂O₂ (~78 mM) for the *P. falciparum* 3D7 wild-type strain recorded in this thesis indeed suggests that little external H₂O₂ reaches the parasite to generate more detrimental redox species such as the hydroxyl radical *in situ*. Similar findings were made when supraphysiological doses of the strong oxidants peroxynitrite and nitric oxide were used to treat the mouse malaria parasite *P. berghei*. The results in the latter study revealed that mice injected with treated inoculum exhibited similar parasitemia and showed no difference in disease development compared with the control. The reasons assigned to this finding were that haemoglobin or other intrinsic parasite defence systems protect the parasite from external oxidative stress (Sobolewski *et al.*, 2005). It is important to note, however, that the thesis IC₅₀ value for H₂O₂ was determined 72 h after a single bolus treatment. Challenging the cultures continuously with H₂O₂ might significantly alter the outcome as demonstrated previously for human embryonic kidney 293 cells (Sobotta *et al.*, 2013). Furthermore, prolonged growth assays might also result in detrimental developmental effects for subsequent cell cycles even at lower H₂O₂ concentrations. Changing the culture or growth conditions such as oscillating CO₂ and O₂ partial pressures or replacing albumax with human serum might also influence the IC₅₀ value. Earlier experiments performed by Verena Staudacher revealed that the IC₅₀ value for tBOOH for the 3D7 strain of *P. falciparum* was much lower at approximately 81.1 µM (Wezena *et al.*, 2017). A second study with the mouse parasite *Plasmodium vinckei* also revealed that intravenous injection of tBOOH resulted in iron-dependent hemolysis and rapid parasite death *in vivo* (Clark *et al.*, 1984). In the *P. vinckei* study, free radical species generated as a result of the dissociation of tBOOH were suggested to cause hemolysis, lipid peroxidation and parasite death (Clark *et al.*, 1984). Comparatively, the hydroperoxidase system of the host-parasite unit therefore seems to be much more robust against oxidative challenges with H₂O₂ than it is towards tBOOH. The inability of host catalase to reduce alkyl hydroperoxides might be one explanation for this situation. Another explanation for the higher susceptibility of *P. falciparum* to tBOOH compared with H₂O₂ might be that tBOOH is transported more rapidly and successfully across the erythrocyte, parasitophorous vacuole and parasite membranes and into the parasite cytosol.

Ascorbic acid is a compound required by almost all vertebrate species on a daily basis in relatively large amounts and it is known to play vital roles including acting as an antioxidant in these organisms (Meister, 1994; Drouin *et al.*, 2011). In the chloroplasts of photosynthetic organisms, ascorbic acid also plays, among others, a vital role of protecting against photoinhibition by helping detoxify reactive oxygen species such as singlet molecular oxygen (¹O₂) formed during the process of photosynthesis (Talla *et al.*, 2011; Sano *et al.*, 2001). Since malaria parasites infect vertebrates and harbor an apicoplast of algal origin (Janouškovec *et al.*, 2010; Dooren & Striepen, 2013), the effect of ascorbate on the growth of *P. falciparum* was also investigated in this thesis. Previous studies have shown that ascorbate exhibits stage- and host-dependent growth-promoting as well as antiproliferative effects on the development of *P. falciparum* at extremely high concentrations (Marva *et al.*, 1989; Soh *et al.*, 2012). In the above study, *in vitro* ring-form development was promoted as ascorbate routinely acts as an antioxidant (Marva *et al.*, 1989). During the trophozoite- and schizont-stages, however, ascorbate, probably acting as a potent prooxidant, was shown to suppress the parasite development (Marva *et al.*, 1989). Results from other studies have reported inverse correlations between serum ascorbate concentrations and malaria for infected and uninfected

adults and children (Hassan *et al.*, 2004; Venkatesh & Swamy, 2010; Onyesom *et al.*, 2010). In this thesis, a 4.3 mM IC₅₀ value for ascorbate was recorded for the *P. falciparum* 3D7 wild-type strain. This value is similar to the value of 3.0 mM for the Dd2 strain that was determined earlier in the laboratory by Johannes Krafczyk (Wezena *et al.*, 2017) and also in good agreement with a reported IC₅₀ value of around 5.0 ± 0.7 mM for the D6 strain using a hypoxanthine incorporation assay (Winter *et al.*, 1997). These values together indicate that physiological ascorbate concentrations, which are around 50 µM (Moeslinger *et al.*, 1995), do not play a role for the growth or control of *P. falciparum*. One case supporting this conclusion is the fact that RPMI medium for parasite culture does not contain ascorbate, although trace amounts of ascorbate may remain within the washed erythrocytes used for growing parasites. Secondly, gene searches in PlasmoDB (Aurrecochea *et al.*, 2009) did not reveal any candidates that encode ascorbate-metabolizing enzymes such as monodehydroascorbate reductase (Müller & Kappes, 2007). Third, results from this thesis showed that a continuous treatment of *P. falciparum* standard cultures with physiological ascorbate concentrations of 50 µM did not affect parasite growth and development (Figure 4.9 E). Therefore, if ascorbate were to really influence the development of the malaria parasite, the mode of action either relies on non-erythrocyte host cells or requires additional factors that are absent in the standard culture medium.

In vivo experiments in *Drosophila* previously demonstrated that 6.1 mM NAc exhibits pro-oxidative effects in some tissues by increasing the concentration of mitochondrial H₂O₂ and oxidized glutathione (GSSG) (Albrecht *et al.*, 2011). In a different study in *P. falciparum*, treatment of parasite cultures with 0.9 µM and 0.9 mM concentrations of NAc alone had no effects on parasite development (Arreesrisom *et al.*, 2007; Soh *et al.*, 2012). In this thesis, the IC₅₀ values for NAc were around 17 mM for the 3D7 strain which are similar to a previously recorded value of 12 mM for the Dd2 strain (Wezena *et al.*, 2017). These results explain the lack of effects of NAc in the previous *P. falciparum* studies as the concentrations tested were much lower than the IC₅₀ value recorded in the results of this thesis. Concerning DTT, a previous study reported that concentrations of between 12.5-200 µM enhanced the growth of the chloroquine-sensitive FC27 strain of *P. falciparum* with the optimum growth occurring at 12.5 µM (Senok *et al.*, 1997). Compared with the DTT IC₅₀ value of 245 µM for the 3D7 strain in this thesis and an earlier result of 389 µM for the Dd2 strain (Wezena *et al.*, 2017), it would appear that lower concentrations of DTT promote parasite growth while higher concentrations may have antiproliferating effects on the parasites. The results also show that *P. falciparum* 3D7 strain is more sensitive to DTT than to NAc and ascorbate. In comparison to previous laboratory results (Wezena *et al.*, 2017) for the chloroquine resistant Dd2 strain, the 3D7 strain also appears to be a little more sensitive to DTT. Generally, the antioxidants ascorbate, NAc and DTT all appear to exhibit non-physiological antiproliferative instead of growth-promoting effects to the parasite. One plausible reason for these results might be that these so-called antioxidants provide electrons for the Fenton reaction within the host-parasite system. Ascorbate, for instance, can reduce Fe (III) to Fe (II), which can then reduce H₂O₂ through the Fenton reaction to OH⁻ and a hydroxyl radical. Thus, these compounds acting as electron donors, might actually serve as pro-oxidants as suggested previously for ascorbate (Marva *et al.*, 1989; Marva *et al.*, 1992). Beside the detrimental Fenton reactions, ascorbate, NAc and DTT might also act as electron donors for the reduction of crucial disulfide bonds in important cellular proteins. Proteins such as albumin are vital in the host-parasite unit and are

actually imported into the parasite from the erythrocyte cytosol (Tahir *et al.*, 2003). To the parasite, albumin is important for growth and differentiation (Tahir *et al.*, 2003) and the reduced disulfide bonds in the protein might have an indirect antiproliferative effect. In addition, the reduction of important erythrocyte or merozoite surface proteins might directly alter the invasion efficiency and affect parasite proliferation. To better detect effects of surface protein reduction by antiproliferating agents, the use of asynchronous parasite cultures or the use of prolonged growth assays is more ideal. The SYBR green assay employed in this project does not discriminate between the DNA of growth-arrested schizonts, extracellular merozoites or successfully invaded merozoites. In conclusion, the results from this project revealed that the host-parasite unit is extremely robust towards redox challenges by H₂O₂, NAc and ascorbate, whereas a micromolar IC₅₀ value was determined for DTT. The mechanisms underlying these results were not investigated in this thesis and remain to be unravelled. In addition, note should be taken of the background fluorescence due to gelation of the medium and hemolysis when studying standard reducing agents using a SYBR green assay. This increased fluorescence has to be taken into account when determining IC₅₀ values.

5.7. Conclusion

For almost three decades, the glyoxalase system has gained interest as a possible target for antimalarial drug therapy. Results from this thesis have not only shown clearly that the two cytosolic glyoxalase enzymes of *P. falciparum* are not essential for blood-stage development of the parasite but also that these enzymes may not be suitable targets for the development of antimalarial drugs. Even though the lack of *PFGLO1* increases the susceptibility of the parasite to the 2-oxoaldehyde glyoxal, the 3D7Δ*glo1* and 3D7Δ*cglo2* knockout parasites are viable with no significant morphological or growth defects. Surprisingly, however, the results also show that the lack of *PFcGLO2*, which should result in the accumulation of S-D-lactyoglutathione in the parasite, leads to an increase in gametocytogenesis and might actually contribute to the transmission of the parasite. These results again raise questions concerning the actual function of the glyoxalase system in the cells. The thesis also generated results that suggest that hGlo2 of the host-erythrocyte does not contribute to the survival of *P. falciparum* parasites at the blood-stage of development. Finally, the results from this thesis indicate that external H₂O₂ is not a strong oxidizing agent for *P. falciparum* parasites in culture compared with tBOOH. The results also show that the prooxidant H₂O₂ and so-called antioxidants ascorbate, NAc and DTT, all inhibit growth of *P. falciparum* in cell culture. While the host-parasite unit is more tolerant to high levels of H₂O₂, ascorbate and NAc, it is more susceptible to DTT.

References

- Acharya, P., Garg, M., Kumar, P., Munjal, A., & Raja, K. D. (2017). Host–parasite interactions in human malaria: Clinical implications of basic research. *Frontiers in Microbiology*, **18**(8): 889.
- Aikawa, M. (1971). *Plasmodium*: The fine structure of malarial parasites. *Experimental Parasitology*, **30**(2): 284-320.
- Aikawa, M. (1977). Variations in structure and function during the life cycle of malarial parasites. *Bulletin of the World Health Organization*, **55** (2-3): 139-156.
- Akoachere, M., Iozef, R., Rahlfs, S., Deponte, M., Mannervik, B., Creighton, D. J., *et al.* (2005). Characterization of the glyoxalases of the malarial parasite *Plasmodium falciparum* and comparison with their human counterparts. *The Journal of Biological Chemistry*, **386**(1): 41–52.
- Albrecht, S. C., Barata, A. G., Großhans, J., Teleman, A. A., & Dick, T. P. (2011). *In vivo* mapping of hydrogen peroxide and oxidized glutathione reveals chemical and regional specificity of redox homeostasis. *Cell Metabolism*, **14**(6): 819–829.
- Allen, R. E., Lo, T. W. C., & Thornalley, P. J. (1993). Purification and characterisation of glyoxalase II from human red blood cells. *European Journal of Biochemistry*, **213**(3): 1261-1267.
- Almasalmeh, A., Krenc, D., Wu, B., & Beitz, E. (2014). Structural determinants of the hydrogen peroxide permeability of aquaporins. *Proceedings of the National Academy of Sciences of the United States of America*, **281** (3): 647–656.
- Amir, A., Cheong, F-W., De Silva, R. J., & Lau, Y-L. (2018). Diagnostic tools in childhood malaria. *Parasites and Vectors*, **11**: 53.
- Antinori, S., Galimberti, L., Milazzo, L., & Corbellino, M. (2012). Biology of human malaria *plasmodia* including *Plasmodium knowlesi*. *Mediterranean Journal of Hematology and Infectious Diseases*, **4**(1): e2012013.
- Arai, M., Nihonmatsu-Kikuchi, N., Itokawa, M., Rabbani, N., & Thornalley, P. J. (2014). Measurement of glyoxalase activities. *Biochemical Society Transactions*, **42** (2): 491-494.
- Ariza, A., Vickers, T. J., Greig, N., Armour, K. A., Dixon, M. J., Eggleston, I. M., *et al.* (2006). Specificity of the trypanothione-dependent *leishmania major* glyoxalase I: Structure and biochemical comparison with the human enzyme. *Molecular Microbiology*, **59**(4): 1239–1248.
- Armeni, T., Cianfruglia, L., Piva, F., Urbanelli, L., Caniglia, L. M., Pugnali, A., *et al.* (2014). S-D-lactoylglutathione can be an alternative supply of mitochondrial glutathione. *Free Radical Biology and Medicine*, **67**: 451-459.
- Aronsson, A.-C., Tibbelin, G., & Mannervik, B. (1979). Purification of glyoxalase I from human erythrocytes by the use of affinity chromatography and separation of the three isoenzymes. *Analytical Biochemistry*, **92**(2): 390-393.
- Arreesrisom, P., Dondorp, A. M., Looareesuwan, S., & Udomsangpetch, R. (2007). Suppressive effects of the anti-oxidant *N*-acetylcysteine on the anti-malarial activity of artesunate. *Parasitology International*, **56** (3): 221–226.

- Arrow, K. J., Panosian, C., & Gelband, H. (2004). Saving lives, buying time: Economics of malaria drugs in an age of resistance. Washington (DC): *The National Academies Press*.
- Aurrecochea, C., Brestelli, J., Brunk, B. P., Dommer, J., Fischer, S., Gajria, B., *et al.* (2009). Plasmodb: A functional genomic database for malaria parasites. *Nucleic Acids Research*, **37**: D539–D543.
- Bai, L., Morton, L. C., & Liu, Q. (2013). Climate change and mosquito-borne diseases in china: A review. *Globalization and Health*, **9**: 10.
- Bannister, L., & Mitchel, G. (2003). The ins, outs and roundabouts of malaria. *Trends in Parasitology*, **19** (5): 209-213.
- Bannister, L. H., Hopkins, J. M., Fowler, R. E., Krishna, S., & Mitchell, G. H. (2000). A brief illustrated guide to the ultrastructure of *Plasmodium falciparum* asexual blood stages. *Parasitology Today*, **16**(10): 427-433.
- Barrangou, R. (2015a). Diversity of CRISPR-Cas immune systems and molecular machines. *Genome Biology*, **16**: 247.
- Barrangou, R. (2015b). The roles of CRISPR-Cas systems in adaptive immunity and beyond. *Current Opinion in Immunology*, **32**: 36–41.
- Barrangou, R., & Marraffini, L. A. (2014). CRISPR-Cas systems: Prokaryotes upgrade to adaptive immunity. *Molecular Cell*, **54**(2): 234-244.
- Bartoloni, A., & Zammarchi, L. (2012). Clinical aspects of uncomplicated and severe malaria. *Mediterranean Journal of Hematology and Infectious Diseases*, **4**(1): e2012026.
- Becker, K., Tilley, L., Vennerstrom, J. L., Roberts, D., Rogersone, S., & Ginsburg, H. (2004). Oxidative stress in malaria parasite-infected erythrocytes: Host–parasite interactions. *International Journal for Parasitology*, **34** (2): 163–189.
- Bienert, G. P., Schjoerring, J. K., & Jahn, T. P. (2006). Membrane transport of hydrogen peroxide. *Biochimica et Biophysica Acta*, **1758** (8): 994–1003.
- Birnboim, H. C., & Doly, J. (1979). A rapid alkaline extraction procedure for screening recombinant plasmid DNA. *Nucleic Acids Research*, **7**(6): 1513-1523.
- Bito, A., Haider, M., Hadler, I., & Breitenbach, M. (1997). Identification and phenotypic analysis of two glyoxalase II encoding genes from *Saccharomyces cerevisiae*, *GLO2* and *GLO4*, and intracellular localization of the corresponding proteins. *The Journal of Biological Chemistry*, **272**: 21509-21519.
- Bloland, P. B. (2001). Drug resistance in malaria. *WHO/CDS/CSR/DRS/2001.4*
- Board, P. G. (1980). Genetic polymorphism of human erythrocyte glyoxalase ii. *The American Journal of Human Genetics*, **32**(5): 690 -694.
- Boucher, E. L., Hopp, S. C., Muthinja, M. J., Frischknecht, F., & Bosch, J. (2018). Discovery of *Plasmodium* (M)TRAP-aldolase interaction stabilizers interfering with sporozoite motility and invasion. *ACS Infectious Diseases*. In press.
- Bousema, T., & Drakeley, C. (2011). Epidemiology and infectivity of *Plasmodium falciparum* and *Plasmodium vivax* gametocytes in relation to malaria control and elimination. *Clinical Microbiology Reviews*, **24**(2): 377–410.
- Bouwman, H., Berg, H. v. d., & Kylin, H. (2011). DDT and malaria prevention : Addressing the paradox. *Environmental Health Perspectives*, **119** (6) : 744-747.

- Bradford, M. M. (1976). A rapid and sensitive method for the quantitation of microgram quantities of protein utilizing the principle of protein-dye binding. *Analytical Biochemistry*, **72**(1–2): 248-254.
- Braks, J. A. M., Franke-Fayard, B., Kroeze, H., Janse, C. J., & Waters, A. P. (2006). Development and application of a positive–negative selectable marker system for use in reverse genetics in *Plasmodium*. *Nucleic Acids Research*, **34**(5): e39.
- Brancucci, N. M., Bertschi, N. L., Zhu, L., Niederwieser, I., Chin, W. H., Wampfler, R., *et al.* (2014). Heterochromatin protein 1 secures survival and transmission of malaria parasites *Cell Host Microbe*, **16**(2): 165-176.
- Bruce, M. C., Alano, P., Duthie, S., & Carter, R. (1990). Commitment of the malaria parasite *Plasmodium falciparum* to sexual and asexual development. *Parasitology*, **100** (Pt 2): 191-200.
- Bushell, E., Gomes, A. R., Sanderson, T., Anar, B., Girling, G., Herd, C., *et al.* (2017). Functional profiling of a *Plasmodium* genome reveals an abundance of essential genes *Cell*, **170**(2): 260-272 e268.
- Butterworth, A. S., Robertson, A. J., Ho, M.-F., Gatton, M. L., McCarthy, J. S., & Trenholme, K. R. (2011). An improved method for undertaking limiting dilution assays for *in vitro* cloning of *Plasmodium falciparum* parasites. *Malaria Journal*, **10**: 95.
- Cameron, A. D., Olin, B., Ridderström, M., Mannervik, B., & Jones, T. A. (1997). Crystal structure of human glyoxalase I - evidence for gene duplication and 3D domain swapping. *The EMBO Journal*, **16** (12): 3386–3395.
- Cameron, A. D., Ridderström, M., Olin, B., Kavarana, M. J., Creighton, D. J., & Mannervik, B. (1999). Reaction mechanism of glyoxalase I explored by an x-ray crystallographic analysis of the human enzyme in complex with a transition state analogue. *Biochemistry*, **38**(41): 13480-13490.
- Cameron, A. D., Ridderström, M., Olin, B., & Mannervik, B. (1999). Crystal structure of human glyoxalase II and its complex with a glutathione thiolester substrate analogue. *Structure*, **7**(9): 1067–1078.
- Carvalho, T. G., & Ménard, R. (2005). Manipulating the *Plasmodium* genome. *Current Issues in Molecular Biology*, **7**(1): 39-56.
- Charunwatthana, P., Faiz, M. A., Ruangveerayut, R., Maude, R., Rahman, M. R., II, L. J. R., *et al.* (2009). N-acetylcysteine as adjunctive treatment in severe malaria: A randomized double blinded placebo controlled clinical trial. *Critical Care Medicine*, **37**(2): 516–522.
- Clark, I. A., Alleva, L. M., Mills, A. C., & Cowden, W. B. (2004). Pathogenesis of malaria and clinically similar conditions *Clinical Microbiology Reviews*, **17**(3): 509–539.
- Clark, I. A., & Hunt, N. H. (1983). Evidence for reactive oxygen intermediates causing hemolysis and parasite death in malaria. *Infection and Immunity*, **39**(1): 1-6.
- Clark, I. A., Hunt, N. H., Cowden, W. B., Maxwell, L. E., & Mackie, E. J. (1984). Radical-mediated damage to parasites and erythrocytes in *Plasmodium vinckei* infected mice after injection of *t-butyl* hydroperoxide. *Clinical and Experimental Immunology*, **56**(3): 524-530.
- Clellan, J. D. and Thornalley, P. J. (1993). The potentiation of GTP-dependent assembly of microtubules by *S*-D-lactoylglutathione. *Biochemical Society Transactions*, **21**:160S.

- Cohuet, A., Harris, C., Robert, V., & Fontenille, D. (2010). Evolutionary forces on anopheles: What makes a malaria vector? . *Trends in Parasitology*, **26**(3): 130-136.
- Coleman, B. I., Skillman, K. M., Jiang, R. H. Y., Childs, L. M., Altenhofen, L. M., Ganter, M., *et al.* (2014). A *Plasmodium falciparum* histone deacetylase regulates antigenic variation and gametocyte conversion. . *Cell Host Microbe*, **16**(2): 177-186.
- Collins, W. E., & Jeffery, G. M. (2007). *Plasmodium malariae* : Parasite and disease. *Clinical Microbiology Reviews*, **20**(4): 579–592.
- Cong, L., Ran, A. F., Cox, D., Lin, S., Barretto, R., Habib, N., Hsu, D. P., Wu, X., Jiang, W., Marraffini, L., & Zhang, F. (2013). Multiplex Genome Engineering Using CRISPR/Cas Systems. *Science*, **339**(819).
- Conway, D. J. (2015). Paths to a malaria vaccine illuminated by parasite genomics. *Trends in Genetics*, **31**(2): 97-107.
- Cooper, R. A. (1984). Metabolism of methylglyoxal in microorganisms. *Annual Review of Microbiology*, **38**: 49-68.
- Cordell, P. A., Futers, T. S., Grant, P. J., & Pease, R. J. (2004). The human hydroxyacylglutathione hydrolase (*HAGH*) gene encodes both cytosolic and mitochondrial forms of glyoxalase II. *The Journal of Biological Chemistry*, **279**(24): 28653–28661.
- Corin, S., & Weaver, S. A. (2005). A risk analysis model with an ecological perspective on DDT and malaria control in south africa. *Journal of Rural and Tropical Public Health*, **4**: 21-32.
- Cowman, A., & Crabb, B. (2005). Genetic manipulation of *Plasmodium falciparum* (Vol. ASM Press, Washington, DC). Washington, DC: ASM Press.
- Cowman, A. F., Berry, D., & Baum, J. (2012). The cellular and molecular basis for malaria parasite invasion of the human red blood cell. *Journal of Cell Biology*, **198** (6): 961–971.
- Cox-Singh, J., Davis, T. M. E., Lee, K.-S., Shamsul, S. S. G., Matusop, A., Ratnam, S., *et al.* (2008). *Plasmodium knowlesi* malaria in humans is widely distributed and potentially life-threatening. *Clinical Infectious Diseases*, **46**(2): 165–171.
- Cox, F. E. (2010). History of the discovery of the malaria parasites and their vectors. *Parasites and Vectors*, **3**(1): 5.
- Crabb, B. S. (2002). Transfection technology and the study of drug resistance in the malaria parasite *Plasmodium falciparum*. *Drug Resistance Updates*, **5** (3-4): 126–130.
- Crabb, B. S., Rug, M., Gilberger, T. W., Thompson, J. K., Triglia, T., Maier, A. G., *et al.* (2004). Transfection of the human malaria parasite *Plasmodium falciparum*. *Methods in Molecular Biology*, **270**: 263-276.
- Crawford, E. D., Quan, J., Horst, J. A., Ebert, D., Wu, W., & DeRisi, J. L. (2017). Plasmid-free crispr/cas9 genome editing in *Plasmodium falciparum* confirms mutations conferring resistance to the dihydroisoquinolone clinical candidate sj733. *PLoS ONE*, **12**(5): e0178163.
- Cruz, L. R., Spangenberg, T., Lacerda, M. V. G., & Wells, T. N. C. (2013). Malaria in south america: A drug discovery perspective *Malaria Journal*, **12**: 168.
- Cui, L., Mharakurwa, S., Ndiaye, D., Rathod, P. K., & Rosenthal, P. J. (2015). Antimalarial drug resistance: Literature review and activities and findings of the ICEMR network. *The American Journal of Tropical Medicine and Hygiene*, **93**(3): 57–68.

- Cyrklaff, M., Srismith, S., Nyboer, B., Burda, K., Hoffmann, A., Lasitschka, F., *et al.* (2016). Oxidative insult can induce malaria-protective trait of sickle and fetal erythrocytes. *Nature Communications*, **7**: 13401.
- Dakin, H. D., & Dudley, H. W. (1913). On glyoxalase. *The Journal of Biological Chemistry*, **14**: 423-431.
- Deitsch, K. W., Driskill, C. L., & Wellems, T. E. (2001). Transformation of malaria parasites by the spontaneous uptake and expression of DNA from human erythrocytes. *Nucleic Acids Research*, **29**(3): 850–853
- Deponte, M. (2013). Glutathione catalysis and the reaction mechanisms of glutathione-dependent enzymes. *Biochimica et Biophysica Acta*, **1830** (5): 3217–3266.
- Deponte, M. (2014). Glyoxalase diversity in parasitic protists. *Biochemical Society Transactions*, **42** (2): 473-478.
- Deponte, M., Sturm, N., Mittler, S., Harner, M., Mack, H., & Becker, K. (2007). Allosteric coupling of two different functional active sites in monomeric *Plasmodium falciparum* glyoxalase I. *The Journal of Biological Chemistry*, **282**(39): 28419–28430.
- Derbyshire, E. R., Mota, M. M., & Clardy, J. (2011). The next opportunity in anti-malaria drug discovery: The liver-stage. *PLoS Pathogens*, **7**(9): e1002178.
- Descamps-latscha, B., Lunel-fabiani, F., Karabinis, A., & Druilhe, P. (1987). Generation of reactive oxygen species in whole blood from patients with acute *falciparum* malaria. *Parasite Immunology*, **9**(2): 275-279.
- Diggs, C., Joseph, K., Flemmings, B., Snodgrass, R., & Hines, F. (1975). Protein synthesis *in vitro* by cryopreserved *Plasmodium falciparum*. *The American Journal of Tropical Medicine and Hygiene*, **24**(5): 760-763.
- Dixon, M. W. A., Dearnley, M. K., Hanssen, E., Gilberger, T., & Tilley, L. (2012). Shape-shifting gametocytes: How and why does *P. falciparum* go banana-shaped? *Trends in Parasitology*, **28** (11): 471–478.
- Djuika, C. F., Staudacher, V., Sanchez, C. P., Lanzer, M., & Deponte, M. (2017). Knockout of the peroxiredoxin 5 homologue pfaop does not affect the artemisinin susceptibility of *Plasmodium falciparum*. *Scientific Reports*, **7** 4410.
- Dluzewski, A. R., Ling, I. T., Hopkins, J. M., Grainger, M., Margos, G., Mitchell, G. H., Holder, A. A., & Bannister, H. L. (2008) Formation of the Food Vacuole in *Plasmodium falciparum*: A Potential Role for the 19 kDa Fragment of Merozoite Surface Protein 1 (MSP1₁₉). *PLoS ONE* **3**(8): e3085.
- Dockrell, H. M., Alavi, A., & Playfair, J. H. (1986). Changes in oxidative burst capacity during murine malaria and the effect of vaccination. *Clinical & Experimental Immunology*, **66**(1): 37–43.
- Doolan, D. L. (2002). *Malaria methods and protocols: Methods and protocols* (Vol. 72): Humana Press.
- Dooren, G. G. v., Marti, M., Tonkin, C. J., Stimmler, L. M., Cowman, A. F., & McFadden, G. I. (2005). Development of the endoplasmic reticulum, mitochondrion and apicoplast during the asexual life cycle of *Plasmodium falciparum*. *Molecular Microbiology*, **57**(2): 405–419.
- Dooren, G. G. v., Stimmler, L. M., & McFadden, G. I. (2006). Metabolic maps and functions of the *Plasmodium* mitochondrion. *FEMS Microbiology Reviews*, **30**(4): 596–630.

- Dooren, G. G. v., & Striepen, B. (2013). The algal past and parasite present of the apicoplast. *Annual Review of Microbiology*, **67**: 271–289.
- Dronamraju, K. R., & Arese, P. (2006). *Malaria: Genetic and evolutionary aspects*: Springer-Verlag New York.
- Drouin, G., Godin, J.-R., & Pagé, B. (2011). The genetics of vitamin C loss in vertebrates. *Current Genomics*, **12**(5): 371-378.
- Duraisingh, M. T., Triglia, T., & Cowman, A. F. (2002). Negative selection of *Plasmodium falciparum* reveals targeted gene deletion by double crossover recombination. *International Journal for Parasitology*, **32** (1): 81– 89.
- Elandalloussi, L. M., & Smith, P. J. (2002). Preparation of pure and intact *Plasmodium falciparum* plasma membrane vesicles and partial characterisation of the plasma membrane atpase. *Malaria Journal*, **1**(6).
- Ferguson, G. P., Munro, A. W., Douglas, R. M., McLaggan, D., & Booth, I. R. (1993). Activation of potassium channels during metabolite detoxification in *Escherichia coli* *Molecular Microbiology*, **9**(6): 1297-1303.
- Fleige, T., Fischer, K., Ferguson, D. J., Gross, U., & Bohne, W. (20017). Carbohydrate metabolism in the *Toxoplasma gondii* apicoplast: localization of three glycolytic isoenzymes, the single pyruvate dehydrogenase complex, and a plastid phosphate translocator. *Eukaryotic Cell*, **6**:984–96.
- Fidock, D. A., & Wellems, T. E. (1997). Transformation with human dihydrofolate reductase renders malaria parasites insensitive to wr99210 but does not affect the intrinsic activity of proguanil *Proceedings of the National Academy of Sciences of the United States of America*, **94**(20): 10931–10936.
- Francis, S. E., Sullivan, D. J., & Goldberg, D. E. (1997). Hemoglobin metabolism in the malaria parasite *Plasmodium falciparum*. *Annual Review of Microbiology*, **51**: 97–123.
- Frickel, E.-M., Jemth, P., Widersten, M., & Mannervik, B. (2001). Yeast glyoxalase i is a monomeric enzyme with two active sites. *The Journal of Biological Chemistry*, **276**(3): 1845–1849.
- Galinski, M. R., & Barnwell, J. W. (2009). Monkey malaria kills four humans. *Trends in Parasitology*, **25**(5): 200-204.
- Ganesan, S. M., Morrissey, J. M., Ke, H., Painter, H. J., Laroia, K., Phillips, M. A., *et al.* (2011). Yeast dihydroorotate dehydrogenase as a new selectable marker for *Plasmodium falciparum* transfection. *Molecular and Biochemical Parasitology*, **177**(1): 29–34.
- Ganguly, A. K., Ranjan, P., Kumar, A., & Bhavesh, N. S. (2015). Dynamic association of pfemp1 and kahrp in knobs mediates cytoadherence during *Plasmodium* invasion. *Scientific Reports*, **5**: 8617.
- Garcia, J. E., Puentes, A., & Patarroyo, M. E. (2006). Developmental biology of sporozoite-host interactions in *Plasmodium falciparum* malaria: Implications for vaccine design. *Clinical Microbiology Reviews*, **19**(4): 686–707.
- Garcia, L. S. (2010). Malaria. *Clinics in Laboratory Medicine*, **30** (1): 93–129.
- Gardner, M. J., Neil Hall, E. F., White, O., Berriman, M., Hyman, R. W., Carlton, J. M., *et al.* (2002). Genome sequence of the human malaria parasite *Plasmodium falciparum*. *Nature Reviews Microbiology*, **419**: 498–511.

- Gazzinelli, R. T., Kalantari, P., Fitzgerald, K. A., & Golenbock, D. T. (2014). Innate sensing of malaria parasites. *Nature Reviews Immunology*, **14**(11): 744-757.
- Gerald, N., B.Mahajan, & Kumar, S. (2011). Mitosis in the human malaria parasite *Plasmodium falciparum*. *Eukaryotic Cell*, **10**(4): 474-482.
- Ghorbal, M., Gorman, M., Macpherson, C. R., Martins, R. M., Scherf, A., & Lopez-Rubio, J.-J. (2014). Genome editing in the human malaria parasite *Plasmodium falciparum* using the CRISPR-Cas9 system. *Nature Biotechnology*, **32**(8): 819-821.
- Ginsburg, H. (2016). The biochemistry of *Plasmodium falciparum*, in advances in malaria research (Vol. Hoboken, NJ, USA). Hoboken, NJ, USA: *John Wiley & Sons, Inc.* .
- Gomes, A. R., Silva, S. M., Miranda, V. H., Ferreira, E. N. A., Cordeiro, A. A. C., & Freire, P. A.(2005). Protein glycation in *Saccharomyces cerevisiae* argpyrimidine formation and methylglyoxal catabolism. *FEBS Journal* **272**:4521-4531.
- Goonewardene, R., Daily, J., Kaslow, D., Sullivan, T. J., Duffy, P., Carter, R., *et al.* (1993). Transfection of the malaria parasite and expression of firefly luciferase. *Biochemistry*, **90** (11): 5234-5523.
- Goyal, M., Alam, A., & Bandyopadhyay, U. (2012). Redox regulation in malaria: Current concepts and pharmacotherapeutic implications. *Current Medicinal Chemistry*, **19**(10): 1475-1503.
- Greve, B., Lehman, L. G., Lell, B., Luckner, D., Schmidt-Ott, R., & Kremsner, P. G. (1999). High oxygen radical production is associated with fast parasite clearance in children with *Plasmodium falciparum* malaria. *The Journal of Infectious Diseases*, **179**(6): 1584-1586.
- Gueye, C. S., Newby, G., Gosling, R. D., Whittaker, M. A., Chandramohan, D., Slutsker, L., *et al.* (2016). Strategies and approaches to vector control in nine malaria-eliminating countries: A cross-case study analysis. *Malaria Journal*, **15**(2).
- Harwaldt, P., Rahlfs, S., & Becker, K. (2002). Glutathione S-transferase of the malarial parasite *Plasmodium falciparum*: Characterization of a potential drug target. *The Journal of Biological Chemistry*, **383**(5): 821-830.
- Hasenkamp, S., Russell, K. T., & Horrocks, P. (2012). Comparison of the absolute and relative efficiencies of electroporation-based transfection protocols for *Plasmodium falciparum*. *Malaria Journal*, **11**: 210.
- Hassan, G. I., Gregory, U., & Maryam, H. (2004). Serum ascorbic acid concentration in patients with acute *falciparum* malaria infection: Possible significance. *The Brazilian Journal of Infectious Diseases*, **8**(5): 378-381.
- Heiber, A., & Spielmann, T. (2014). Preparation of parasite protein extracts and western blot analysis. *Bio-protocol*, **4**(11): 8552.
- Hemingway, J., Shretta, R., Wells, T. N. C., Bell, D., Djimdé, A. A., Achee, N., *et al.* (2016). Tools and strategies for malaria control and elimination: What do we need to achieve a grand convergence in malaria? *PLoS Biology*, **14**(3): e1002380.
- Hempelmann, E. (2007). Hemozoin biocrystallization in *Plasmodium falciparum* and the antimalarial activity of crystallization inhibitors. *Parasitology Research*, **100**(4): 671-676.
- Hsiao, L. L., Howard, R. J., Aikawa, M., & Taraschi, T. F. (1991). Modification of host cell membrane lipid composition by the intra-erythrocytic human malaria parasite *Plasmodium falciparum*. *Biochem Journal*, **274**(1): 121-132.

- Hurd, H., Carter, V., & Nacer, A. (2005). Interactions between malaria and mosquitoes: The role of apoptosis in parasite establishment and vector response to infection. *Current Topics in Microbiology and Immunology*, **289**: 185-218.
- Inoue, Y., Maeta, K., & Nomura, W. (2011). Glyoxalase system in yeasts: Structure, function, and physiology. *Seminars in Cell and Developmental Biology*, **22** (3): 278–284.
- Iozef, R., Rahlfs, S., Chang, T., Schirmer, H., & Becker, K. (2003). Glyoxalase I of the malarial parasite *Plasmodium falciparum*: Evidence for subunit fusion. *FEBS Letters*, **554** (3): 284-288.
- Isah, M. B., & Ibrahim, M. A. (2014). The role of antioxidants treatment on the pathogenesis of malarial infections: A review. *Parasitology Research*, **113**(3): 801–809.
- Janouškovec, J., Horák, A., Oborník, M., Lukeš, J., & Keeling, P. J. (2010). A common red algal origin of the apicomplexan, dinoflagellate and heterokont plastids. *Proceedings of the National Academy of Sciences*, **107** (24): 10949–10954.
- Jomaa, H., Wiesner, J., Sanderbrand, S., Altincicek, B., Weidemeyer, C., Hintz, M., Türbachova, I., Eberl, M., Zeidler, J., Lichtenthaler, H. K., Soldati, D., & Beck, E. (1999). Inhibitors of the nonmevalonate pathway of isoprenoid bio-synthesis as antimalarial drugs. *Science*, **285**(5433):1573-6.
- Jortzik, E., & Becker, K. (2012). Thioredoxin and glutathione systems in *Plasmodium falciparum*. *International Journal of Medical Microbiology*, **302** (4-5): 187– 194.
- Josling, G. A., & Llinás, M. (2015). Sexual development in *Plasmodium* parasites: Knowing when it's time to commit. *Nature Review Microbiology*, **13**(9): 573-587.
- Kafsack, B. F., Rovira-Graells, N., Clark, T. G., Bancells, C., Crowley, V. M., Campino, S. G., *et al.* (2014). A transcriptional switch underlies commitment to sexual development in malaria parasites. *Nature*, **507**(7491): 248-252.
- Kamareddine, L. (2012). The biological control of the malaria vector. *Toxins*, **4**(9): 748–767.
- Kawatani, M., Okumura, H., Honda, K., Kanoh, N., Muroi, M., Dohmae, N., *et al.* (2008). The identification of an osteoclastogenesis inhibitor through the inhibition of glyoxalase I. *Proceedings of the National Academy of Sciences*, **105**(33): 11691-11696.
- Kerlin, D. H., & Gatton, M. L. (2013). Preferential invasion by *Plasmodium* merozoites and the self-regulation of parasite burden. *Parasitology Research*, **8**(2): e57434.
- Kim, S.-J., Kim, S.-H., Jo, S.-N., Gwack, J., Youn, S.-K., & Jang, J.-Y. (2013). The long and short incubation periods of *Plasmodium vivax* malaria in Korea: The characteristics and relating factors. *Infect Chemotherapy*, **45**(2): 184–193.
- Koncarevic, S., Rohrbach, P., Deponce, M., Krohne, G., Prieto, H. J., Yates III, J., *et al.* (2009). The malarial parasite *Plasmodium falciparum* imports the human protein peroxiredoxin 2 for peroxide detoxification. *Proceedings of the National Academy of Sciences*, **106**(32): 13323–13328.
- Koning-Ward, T. F. d., Gilson, P. R., & Crabb, B. S. (2015). Advances in molecular genetic systems in malaria. *Nature Reviews | Microbiology*, **13** (6): 373-387.
- Laemmli, U. K. (1970). Cleavage of structural proteins during the assembly of the head of bacteriophage T4. *Nature Biotechnology*, **227**(5259): 680–685.
- Lamarque, M., Tastet, C., Poncet, J., Demetree, E., Jouin, P., Vial, H., & Dubremetz, J.-F. (2008). Food vacuole proteome of the malarial parasite *Plasmodium falciparum*. *Proteomics-Clinical Applications*, **2**:1361–1374.

- Lambros, C., & Vanderberg, J. P. (1979). Synchronization of *Plasmodium falciparum* erythrocytic stages in culture. *Journal of Parasitology*, **65**(3): 418-420.
- Lee, A. H., Symington, L. S., & Fidock, D. A. (2014). DNA repair mechanisms and their biological roles in the malaria parasite *Plasmodium falciparum*. *Microbiology and Molecular Biology Reviews*, **78** (3): 469–486.
- Lee, K.-S., & Vythilingam, I. (2013). *Plasmodium knowlesi: Emergent human malaria in southeast asia*. Parasites and their vectors: Springer, Vienna.
- Lee, M. C., & Fidock, D. A. (2014). CRISPR-mediated genome editing of *Plasmodium falciparum* malaria parasites. *Genome Medicine*, **6**(8): 63.
- Lee, S. H., Nam, K. W., Jeong, J. Y., Yoo, S. J., Koo, Y.-S., Lee, S., *et al.* (2013). The effects of climate change and globalization on mosquito vectors: Evidence from Jeju island, South Korea on the potential for asian tiger mosquito (*aedes albopictus*) influxes and survival from Vietnam rather than Japan. *PLoS ONE*, **8**(7): e68512.
- Lim, L., & McFadden, G. I. (2010). The evolution, metabolism and functions of the apicoplast. *Philosophical Transactions of the Royal Society B*, **365**(1541): 749–763.
- Lingnau, A., Margos, G., Maier, W. A., & Seitz, H. M. (1993). The effects of hormones on the gametocytogenesis of *Plasmodium falciparum* *in vitro*. *Applied Parasitology*, **34**(3): 153-160.
- Liu, J., Istvan, E. S., Gluzman, I. Y., Gross, J., & Goldberg, D. E. (2006). *Plasmodium falciparum* ensures its amino acid supply with multiple acquisition pathways and redundant proteolytic enzyme systems. *Proceedings of the National Academy of Sciences*, **103**(23): 8840–8845.
- Lo, T. W. C., Westwood, M. E., McLellan, A. C., Selwood, T., & Thornalley, P. J. (1994). Binding and modification of proteins by methylglyoxal under physiological conditions. *The Journal of Biological Chemistry*, **269**(51): 32299-32305.
- Low, F. M., Hampton, M. B., & Winterbourn, C. C. (2008). Peroxiredoxin 2 and peroxide metabolism in the erythrocyte. *Antioxidants and Redox Signaling*, **10** (9): 1621-1630.
- Lu, J., Tong, Y., Pan, J., Yang, Y., Liu, Q., Tan, X., *et al.* (2016). A redesigned CRISPR-Cas9 system for marker-free genome editing in *Plasmodium falciparum*. *Parasites and Vectors*, **9**(198).
- Maeta, K., Izawa, S., Okazaki, S., Kuge, S. and Inoue, Y. (2004). Activity of the Yap1 transcription factor in *Saccharomyces cerevisiae* is modulated by methylglyoxal, a metabolite derived from glycolysis. *Molecular and Cellular Biology*, **24**, 8753–8764.
- Maier, A. G., Braks, J. A. M., Waters, A. P., & Cowman, A. F. (2006). Negative selection using yeast cytosine deaminase/uracil phosphoribosyl transferase in *Plasmodium falciparum* for targeted gene deletion by double crossover recombination. *Molecular & Biochemical Parasitology*, **150** (118–121).
- Maier, A. G., Cooke, B. M., Cowman, A. F., & Tilley, L. (2009). Malaria parasite proteins that remodel the host erythrocyte. *Nature Reviews Microbiology*, **7**(5): 341–354.
- Marasinghe, G. P. K., Sander, I. M., Bennett, B., Periyannan, G., Ke-WuYang, Makaroff, C. A., *et al.* (2005). Structural studies on a mitochondrial glyoxylase II. *The Journal of Biological Chemistry*, **280**(49): 40668–40675.
- Marva, E., cohen, A., saltman, P., chevion, M., & golenser, J. (1989). Deleterious synergistic effects of ascorbate and copper on the development of *Plasmodium falciparum*: An *in*

- vitro* study in normal and in G6PD-deficient erythrocytes. *Inmnorionol Journal for farasiroogy*, **19**(7): 779-785.
- Marva, E., Golenser, J., Cohen, A., Kitrossky, N., Har-el, R., & Chevion, M. (1992). The effects of ascorbate-induced free radicals on *Plasmodium falciparum*. *Tropical Medicine and Parasitology*, **43**(1): 17-23.
- McLellan, A. C., Thornally, P. J., Benn, J., & Sonksen, P. H. (1994). Glyoxalase system in clinical diabetes mellitus and correlation with diabetic complications. *Clinical Science*, **87**(1): 21-29.
- McQueen, P. G., & McKenzie, F. E. (2004). Age-structured red blood cell susceptibility and the dynamics of malaria infections. *Proceedings of the National Academy of Sciences*, **101** (24): 9161–9166.
- Meister, A. (1994). Glutathione-ascorbic acid antioxidant system in animals. *The Journal of Biological Chemistry*, **269**(13): 9397-9400.
- Mirski, T., Bartoszcze, M., & Bielawska-Drózd, A. (2011). Impact of climate change on infectious diseases. *Polish Journal of Environmental Studies*, **21**(3): 525-532.
- Miyake, Y., Karanis, P., & Uga, S. (2004). Cryopreservation of protozoan parasites. *Cryobiology*, **48**(1): 1-7.
- Moeslinger, T., Brunner, M., Voif, I., & Spieckermann, P. G. (1995). Spectrophotometric determination of ascorbic acid and dehydroascorbic acid. *Clinical Chemistry*, **41**(8): 1177-1181.
- Mohandas, N., & An, X. (2012). Malaria and human red blood cells. *Medical Microbiology and Immunology*, **201**(4): 593–598.
- Morcos, M., Du, X. L., Pfisterer, F., Hutter, H., Sayed, A. A. R., Thornalley, P., Ahmed, N., Baynes, J., Thorpe, S., Kukudov, G. et al. (2008). Glyoxalase-1 prevents mitochondrial protein modification and enhances lifespan in *Caenorhabditis elegans*. *Aging Cell*, **7**:260–269.
- More, S. S., & Vince, R. (2009). Inhibition of glyoxalase I : The first low-nanomolar tight-binding inhibitors. *Journal of Medicinal Chemistry*, **52**(15): 4650–4656.
- Morrisette, N. S., & Sibley, L. D. (2002). Cytoskeleton of apicomplexan parasites. *Microbiology and Molecular Biology Reviews*, **66**(1): 21–38.
- Müller, S., & Kappes, B. (2007). Vitamin and co-factor bio-synthesis pathways in *Plasmodium* and other apicomplexan parasites. *Trends in Parasitology*, **23**(3): 112–121.
- Neghina, R., Neghina, A. M., Marincu, I., & Iacobiciu, I. (2010). Malaria, a journey in time : In search of the lost myths and forgotten stories. *The American Journal of the Medical Sciences*, **340**(6): 492–498.
- Olsen, S. H., & Elvevoll, E. O. (2011). Ph-induced shift in hemoglobin spectra: A spectrophotometric comparison of atlantic cod (*gadus morhua*) and mammalian hemoglobin. *Journal of Agricultural and Food Chemistry*, **59**(4): 1415-1422.
- Olshina, A. M., Angrisano, F., Marapana, S. D., Riglar, T. D., Bane, K., Wong, W., Bruno Catime, B., Yin, M-X., Holmes, B. A., Frischknecht, F., David R Kovar, R. D., & Baum, J.(2015). *Plasmodium falciparum* coronin organizes arrays of parallel actin filaments potentially guiding directional motility in invasive malaria parasites. *The Malaria Journal*, **14**:280.

- Onyesom, I., Ekeanyanwu, R. C., & Achuka, N. (2010). Correlation between moderate *Plasmodium falciparum* malarial parasitaemia and antioxidant vitamins in serum of infected children in south eastern nigeria. *African Journal of Biochemistry Research*, **4**(12): 261-264.
- Ozyamak, K. E., Black, S. S., Walker, C. A., Maclean, M. J., Bartlett, W., Miller, S., *et al.* (2010). The critical role of S-D-lactoylglutathione formation during methylglyoxal detoxification in *escherichia coli*. *Molecular Microbiology*, **78**(6): 1577-1590.
- Painter H. J., Morrissey, J. M., Mather, M. W., Vaidya, A. B. (2007). Specific role of mitochondrial electron transport in blood-stage *Plasmodium falciparum*. *Nature*, **446**(7131):88-91.
- Perkins, S. L., & Austin, C. C. (2009). Four new species of *Plasmodium* from New Guinea lizards: Integrating morphology and molecules. *Journal of Parasitology*, **95** (2): 424–433.
- Petersen, I., Eastman, R., Lanzer, M. (2011). Drug-resistant malaria: molecular mechanisms and implications for public health. *FEBS Letters*, **585**(11):1551-62.
- Pimenta, P. F. P., Orfano, A. S., Bahia, A. C., Duarte, A. P. M., Ríos-Velásquez, C. M., Melo, F. F., *et al.* (2015). An overview of malaria transmission from the perspective of amazon anopheles vectors. *Mem Inst Oswaldo Cruz*, **110**(1): 23–47.
- Preisera, P., Kaviratna, M., Khana, S., Bannister, L., & Jarra, W. (2000). The apical organelles of malaria merozoites: Host cell selection, invasion, host immunity and immune evasion. *Microbes and Infection*, **2**(12): 1461–1477.
- Putz, C., & Manyando, C. (1997). Enhanced gametocyte production in Fansidar-treated *Plasmodium falciparum* malaria patients: Implications for malaria transmission control programmes. *Tropical Medicine & International Health*, **2**(3): 227-229.
- Racker, E. (1951). The mechanism of action of glyoxalase. *The Journal of Biological Chemistry*, **190**(2): 685-696.
- Ramasamy, R. (2014). Zoonotic malaria – global overview and research and policy needs. *Front Public Health*, **2** (123).
- Reinke, A. W., & Troemel, E. R. (2015). The development of genetic modification techniques in intracellular parasites and potential applications to *Microsporidia*. *PLoS Pathogens*, **11**(12): e1005283.
- Rich, S. M., & Ayala, F. J. (2006). Evolutionary origins of human malaria parasites, in: *Malaria: Genetic and evolutionary aspects. Emerging infectious diseases of the 21st century: Springer, Boston, MA.*
- Ridderström, M., Jemth, P., Cameron, A. D., & Mannervik, B. (2000). The active-site residue Tyr-175 in human glyoxalase II contributes to binding of glutathione derivatives. *Biochimica et Biophysica Acta*, **1481** (2): 344-348.
- Roosild, T. P., Castronovo, S., Healy, J., Miller, S., Pliotas, C., Rasmussen, T., *et al.* (2010). Mechanism of ligand-gated potassium efflux in bacterial pathogens. *Proceedings of the National Academy of Sciences of the United States of America*, **107**(46): 19784-19789.
- Rosario, V. (1981). Cloning of naturally occurring mixed infections of malaria parasites. *Science*, **212**(4498): 1037-1038.
- Rosenberg, R. (2008). Malaria: Some considerations regarding parasite productivity. *Trends in Parasitology*, **2008**(24): 11.

- Sano, S., Ueda, M., Kitajima, S., Takeda, T., Shigeoka, S., Kurano, N., *et al.* (2001). Characterization of ascorbate peroxidases from unicellular red alga *Galdieria partita*. *Plant and Cell Physiology*, **42**(4): 433–440.
- Schneweis, S., Maier, W. A., & Seitz, H. M. (1991). Haemolysis of infected erythrocytes - a trigger for formation of *Plasmodium falciparum* gametocytes? *Parasitology Research*, **77**(5): 458-460.
- Schofield, L., & Grau, G. E. (2005). Immunological processes in malaria pathogenesis. *Nature Reviews | Immunology*, **5**(9): 735.
- Schwank, S., Sutherland, C. J., & Drakeley, C. J. (2010). Promiscuous expression of α -tubulin II in maturing male and female *Plasmodium falciparum* gametocytes. *PLoS ONE*, **5**(12): e14470.
- Schwartz, E. (2012). Prophylaxis of Malaria. *Mediterranean Journal of Hematology and Infectious Diseases*, **4**. Open Journal System.
- Scire`, A., Tanfani, F., Saccucci, F., Bertoli, E., & Giovanni Principato, G. (2000). Specific interaction of cytosolic and mitochondrial glyoxalase II with acidic phospholipids in form of liposomes results in the inhibition of the cytosolic enzyme only. *Proteins: Structure, Function, and Genetics*, **41**:33–39.
- Senok, A. C., Nelson, E. A. S., Lil, K., & Oppenheimer, S. J. (1997). Thalassaemia trait, red blood cell age and oxidant stress: Effects on *Plasmodium falciparum* growth and sensitivity to artemisinin. *Transactions of the Royal Society of Tropical Medicine and Hygiene*, **91**(5): 585-589.
- Sherman, I. W. (1979). Biochemistry of *Plasmodium* (malarial parasites). *Microbiological Reviews*, **43**(4): 453-495.
- Shiff, C. (2002). Integrated approach to malaria control. *Clinical Microbiology Reviews*, **15**(2): 278–293.
- Shinohara, M., Thornalley, P. J., Giardino, I., Beisswenger, P., Thorpe, S. R., Onorato, J., & Brownlee, M. (1998). Overexpression of glyoxalase-I in bovine endothelial cells inhibits intracellular advanced glycation endproduct formation and prevents hyperglycemia-induced increases in macromolecular endocytosis. *Journal of Clinical Investigation*, **101**:1142–1147.
- Sies, H. (1986). Biochemistry of oxidative stress. *Angewandte Chemie International Edition*, **25**:1058e1071.
- Silva, M. S., Ferreira, A. E. N., Gomes, R., Tomás, A. M., Freire, A. P., & Cordeiro, C. (2012). The glyoxalase pathway in protozoan parasites. *International Journal of Medical Microbiology*, **302**(4-5): 225–229.
- Silva, M. S., Gomes, R. A., Ferreira, A. E. N., Freire, A. P., & Cordeiro, C. (2013). The glyoxalase pathway: The first hundred years . . . and beyond. *Biochemical Journal*, **453**(1): 1–15.
- Sinden, R. (2002). Molecular interactions between *Plasmodium* and its insect vectors. *Cellular Microbiology*, **4**(11): 713–724.
- Singer, M., & Frischknecht, F. (2017). Time for genome editing: next-generation attenuated malaria parasites. *Trends Parasitology*, **33**(3):202-213.
- Singer, M., Marshall, J., Heiss, K., Mair, R. G., Grimm, D., Mueller, A-K., & Frischknecht, F. (2015). Zinc finger nuclease-based double-strand breaks attenuate malaria parasites and reveal rare microhomology-mediated end joining. *Genome Biology*, **16**:249.

- Sinha, A., Hughes, K. R., Modrzynska, K. K., Otto, T. D., Pfander, C., Dickens, N. J., *et al.* (2014). A cascade of DNA binding proteins for sexual commitment and development in *Plasmodium*. *Nature*, **507**(7491): 253-257.
- Sinha, S., Medhi, B., & Sehgal, R. (2014). Challenges of drug-resistant malaria. *Parasite*, **21**: 61.
- Sinka, M. E., Bangs, M. J., Manguin, S., Rubio-Palis, Y., Chareonviriyaphap, T., Coetzee, M., *et al.* (2012). A global map of dominant malaria vectors. *Parasite Vectors*, **5**: 69.
- Smalley, M. E., & Brown, J. (1981). *Plasmodium falciparum* gametocytogenesis stimulated by lymphocytes and serum from infected gambian children. *Transactions of the Royal Society of Tropical Medicine and Hygiene*, **75**(2): 316-317.
- Smilkstein, M., Sriwilaijaroen, N., Kelly, J. X., Wilairat, P., & Riscoe, M. (2004). Simple and inexpensive fluorescence-based technique for high-throughput antimalarial drug screening. *Antimicrob Agents Chemotherapy*, **48**(5): 1803-1806.
- Smith, T. G., Lourenco, P., Carter, R., Walliker, D., & Ranford-Cartwright, L. C. (2000). Commitment to sexual differentiation in the human malaria parasite, *Plasmodium falciparum*. *Parasitology*, **121** (Pt 2): 127-133.
- Sobolewski, P., Gramaglia, I., Frangos, J. A., Intaglietta, M., & Heyde, H. v. d. (2005). *Plasmodium berghei* resists killing by reactive oxygen species. *Infection and Immunity*, **73**(10): 6704–6710
- Sobotta, M. C., Barata, A. G., Schmidt, U., Mueller, S., Millonig, G., & Dick, T. P. (2013). Exposing cells to H₂O₂: A quantitative comparison between continuous low-dose and one-time high-dose treatments. *Free Radical Biology and Medicine*, **60**: 325-335.
- Soh, P. N., Witkowski, B., Gales, A., Huyghe, E., Berry, A., Pipy, B., *et al.* (2012). Implication of glutathione in the *in vitro* antiplasmodial mechanism of action of ellagic acid. *PLoS ONE*, **7**(9): e45906.
- Sorci, G., & Faivre, B. (2009). Inflammation and oxidative stress invertebrate host–parasite systems. *Philosophical Transactions of the Royal Society B: Biological Sciences*, **364**(1513): 71–83.
- Southworth, P. M., Hyde, J. E., & Sims, P. F. (2011). A mass spectrometric strategy for absolute quantification of *Plasmodium falciparum* proteins of low abundance. *Malar Journal*, **10**(315)
- Spinello Antinori, L. G., Laura Milazzo and Mario Corbellino. (2012). Biology of human malaria plasmodia including *Plasmodium knowlesi*. *Mediterr J Hematol Infect Dis*, **4**(1).
- Staalsoe, T., Giha, H. A., Dodoo, D., Theander, T. G., & Hviid, L. (1999). Detection of antibodies to variant antigens on *Plasmodium falciparum*-infected erythrocytes by flow cytometry. *Cytometry*, **35**(4): 329-336.
- Staines, H. M., Ashmore, S., Felgate, H., Moore, J., Powell, T., & Ellory, J. C. (2006). Solute transport via the new permeability pathways in *Plasmodium falciparum*-infected human red blood cells is not consistent with a simple single-channel model. *Blood*, **108**(9): 3187–3194.
- Stanisic, D. I., Liu, X. Q., De, S. L., Batzloff, M. R., Forbes, T., Davis, C. B., *et al.* (2015). Development of cultured *Plasmodium falciparum* blood-stage malaria cell banks for early phase *in vivo* clinical trial assessment of anti-malaria drugs and vaccines. *Malaria Journal*, **14**(143).

- Staudacher, V., Djuika, C. F., Koduka, J., Schlossarek, S., Kopp, J., Büchler, M., *et al.* (2015). *Plasmodium falciparum* antioxidant protein reveals a novel mechanism for balancing turnover and inactivation of peroxiredoxins. *Free Radical Biology and Medicine*, **85**: 228–236.
- Sturm, A., Amino, R., Sand, C. v. d., Regen, T., Retzlaff, S., Rennenberg, A., *et al.* (2006). Manipulation of host hepatocytes by the malaria parasite for delivery into liver sinusoids. *Science*, **313**(5791): 1287-1290.
- Su, X. Z., Wu, Y., Sifri, C. D., & Wellems, T. E. (1996). Reduced extension temperatures required for PCR amplification of extremely A+T-rich DNA. *Nucleic Acids Research*, **24**(8): 1574–1575.
- Tahir, A. E. L., Malhotra, P., & Chauhan, V. S. (2003). Uptake of proteins and degradation of human serum albumin by *Plasmodium falciparum* – infected human erythrocytes. *Malaria Journal*, **2**(11).
- Talla, S., Riazunnisa, K., Padmavathi, L., Sunil, B., Rajsheel, P., & Raghavendra, A. S. (2011). Ascorbic acid is a key participant during the interactions between chloroplasts and mitochondria to optimize photosynthesis and protect against photoinhibition. *Journal of Biosciences*, **36**(1): 163–173.
- Talman, A. M., Paul, R. E. L., Sokhna, C. S., Domarle, O., Arieu, F. d., Trape, J.-F. o., *et al.* (2004). Influence of chemotherapy on the *Plasmodium* gametocyte sex ratio of mice and humans *The American Journal of Tropical Medicine and Hygiene*, **71**(6): 739-744.
- Tavares, R. G., Staggemeier, R., Borges, A. L. P., Rodrigues, M. T., Castelan, L. A., Vasconcelos, J., *et al.* (2011). Molecular techniques for the study and diagnosis of parasite infection. *Journal of Venomous Animals and Toxins including Tropical Diseases*, **17** (3): 239-248.
- Thornalley, P. J. (1988). Modification of the glyoxalase system in human red blood cells by glucose *in vitro*. *Biochemical Journal*, **254**(3): 751-755.
- Thornalley, P. J. (1993). The glyoxalase system in health and disease. *Molecular Aspects of Medicine*, **14**(4): 287-371.
- Thornalley, P. J. (1996). Pharmacology of methylglyoxal: Formation, modification of proteins and nucleic acids, and enzymatic detoxification—a role in pathogenesis and antiproliferative chemotherapy. *General Pharmacology*, **27**(4): 565-573.
- Thornalley, P. J. (1998). Glutathione-dependent detoxification of α -oxoaldehydes by the glyoxalase system: Involvement in disease mechanisms and antiproliferative activity of glyoxalase i inhibitors. *Chemico-Biological Interactions*, **111–112** 137–151.
- Thornalley, P. J. (2003). Glyoxalase i – structure, function and a critical role in the enzymatic defence against glycation. *Biochemical Society Transactions*, **31**(part 6): 1343-1348.
- Thornalley, P. J., & Bellavite, P. (1987). Modification of the glyoxalase system during the functional activation of human neutrophils. *Biochimica et Biophysica Acta*, **931**:120–129.
- Thornalley, P. J., Edwards, L. G., Kang, Y., Wyatt, C., Davies, N., Ladan, M. J., *et al.* (1996). Antitumour activity of *S-p*-bromobenzylglutathione cyclopentyl diester *in vitro* and *in vivo*. Inhibition of glyoxalase I and induction of apoptosis. *Biochemical Pharmacology*, **51**(10): 1365-1372.

- Thornalley, P. J., Strath, M., & Wilson, R. J. M. (1994). Antimalarial activity *in vitro* of the glyoxalase I inhibitor diester, *S-p*-bromobenzylglutathione diethyl ester. *Biochemical Pharmacology*, **47**(2): 418-420.
- Tjhin, E. T., Staines, H. M., Schalkwyk, D. A. v., Krishna, S., & Saliba, K. J. (2013). Studies with the *Plasmodium falciparum* hexokinase reveal that *PfHT* limits the rate of glucose entry into glycolysis. *FEBS Letters*, **587**(19): 3182–3187.
- Towbin, H., Staehelin, T., & Gordon, J. (1979). Electrophoretic transfer of proteins from polyacrylamide gels to nitrocellulose sheets: Procedure and some applications. *Proceedings of the National Academy of Sciences of the United States of America*, **76**(9): 4350-4354.
- Trager, W., & Gill, G. S. (1992). Enhanced gametocyte formation in young erythrocytes by *Plasmodium falciparum* *in vitro*. *Journal of Protozoology*, **39**(3): 429-432.
- Trager, W., & Jensen, J. B. (1976). Human malaria parasites in continuous culture. *Science*, **193**(4254): 673-675.
- Tuteja, R. (2007). Malaria - an overview. *FEBS Journal*, **274** (18): 4670–4679.
- Uotila, L. (1973). Purification and characterization of s-2-hydroxyacylglutathione hydrolase (glyoxalase II) from human liver. *Biochemistry*, **12**(20): 3944-3951.
- Urscher, M., Alisch, R., & Deponte, M. (2011). The glyoxalase system of malaria parasites—implications for cell biology and general glyoxalase research. *Seminars in Cell and Developmental Biology*, **22**(3): 262–270.
- Urscher, M., & Deponte, M. (2009). *Plasmodium falciparum* glyoxalase II: Theorell-chance product inhibition patterns, rate-limiting substrate binding via Arg257/Lys260, and unmasking of acid-base catalysis. *The Journal of Biological Chemistry*, **390**(11): 1171–1183.
- Urscher, M., More, S. S., Alisch, R., Vince, R., & Deponte, M. (2012). Tight-binding inhibitors efficiently inactivate both reaction centers of monomeric *Plasmodium falciparum* glyoxalase 1. *FEBS Journal*, **279**(14): 2568–2578.
- Urscher, M., Przyborski, J. M., Imoto, M., & Deponte, M. (2010). Distinct subcellular localization in the cytosol and apicoplast, unexpected dimerization and inhibition of *Plasmodium falciparum* glyoxalases. *Molecular Microbiology*, **76**(1): 92–103.
- Vander Jagt, D. L. V., Hunsaker, L. A., Campos, N. M., & Baack, B. R. (1990). D-lactate production in erythrocytes infected with *Plasmodium falciparum*. *Molecular and Biochemical Parasitology*, **42** (2): 277-284.
- Venkatesh, G., & Swamy, R. M. (2010). A study of electrocardiographic changes in smokers compared to normal human beings. *Biomedical Research*, **21** (4): 389-392.
- Vos, T., Allen, C., Arora, M., Barber, R. M., Bhutta, Z. q. A., Brown, A., *et al.* (2016). Global, regional, and national incidence, prevalence, and years lived with disability for 310 diseases and injuries, 1990–2015: A systematic analysis for the global burden of disease study 2015. *Lancet*, **388** (10053): 1545–1602.
- Waller, R. F., & McFadden, G. I. (2005). The apicoplast: A review of the derived plastid of apicomplexan parasites. *Current Issues in Molecular Biology*, **7**(1): 57-80.
- Walliker, D., Quakyi, I. A., Wellems, T. E., McCutchan, T. F., Szarfman, A., London, W. T., *et al.* (1987). Genetic analysis of the human malaria parasite *Plasmodium falciparum*. *Science*, **236**(4809): 1661–1666.

- Wang, H., Naghavi, M., Allen, C., Barber, R. M., Bhutta, Z. q. A., Carter, A., *et al.* (2016). Global, regional, and national life expectancy, all-cause mortality, and cause-specific mortality for 249 causes of death, 1980–2015: A systematic analysis for the global burden of disease study 2015. *Lancet*, **388**(10053): 1459–1544.
- Warhurst, D. C., & Williams, J. E. (1996). Laboratory diagnosis of malaria. *Journal of Clinical Pathology*, **49**: 533-538.
- Waterkeyna, J. G., Crabbb, B. S., & Cowman, A. F. (1999). Transfection of the human malaria parasite *Plasmodium falciparum*. *International Journal for Parasitology*, **29** 945-955.
- Webb, J. L. A. (2010). Humanity's burden: A global history of malaria *Social History of Medicine*, **23**(2): 441–443.
- Westra, E. R., Buckling, A., & Fineran, P. C. (2014). CRISPR–Cas systems: Beyond adaptive immunity. *Nature Reviews | Microbiology*, **12** (5): 317-326.
- Wezena, C. A., Alisch, R., Golzmann, A., Liedgens, L., Staudacher, V., Pradel, G., *et al.* (2018). The cytosolic glyoxalases of *Plasmodium falciparum* are dispensable during asexual blood-stage development. *Microbial Cell*, **5**(1): 32–41.
- Wezena, C. A., Krafczyk, J., Staudacher, V., & Deponte, M. (2017). Growth inhibitory effects of standard pro- and antioxidants on the human malaria parasite *Plasmodium falciparum*. *Experimental Parasitology*, **180** 64-70.
- Wezena, C. A., Urscher, M., Vince, R., More, S. S., & Deponte, M. (2016). Hemolytic and antimalarial effects of tight-binding glyoxalase 1 inhibitors on the host-parasite unit of erythrocytes infected with *Plasmodium falciparum*. *Redox Biology*, **8**: 348–353.
- White, N. J. (2008). *Plasmodium knowlesi*: The fifth human malaria parasite. *Clinical Infectious Diseases*, **46**(2): 172–173.
- WHO. (2009). World malaria report *World Health Organization*, Geneva, Switzerland.
- WHO. (2016a). Malaria fact sheet n°94. Who media centre *World Health Organization*, Geneva, Switzerland.
- WHO. (2016b). World malaria report *World Health Organization*, Geneva, Switzerland.
- WHO. (2017a). Malaria fact sheet n°94. Who media centre *World Health Organization*, Geneva, Switzerland.
- WHO. (2017b). World malaria report *World Health Organization*, Geneva, Switzerland.
- Wilson, R. J. M., & Williamson, D. H. (1997). Extrachromosomal DNA in the apicomplexa. *Microbiology and Molecular Biology Reviews*, **61**(1): 1–16.
- Winstanley, P. A. (2000). Chemotherapy for *falciparum* malaria: The armoury, the problems and the prospects. *Parasitology Today*, **16**(4): 146-153.
- Winter, R. W., Ignatushchenko, M., Ogundahunsi, O. A. T., Cornell, K. A., Oduola, A. M. J., Hinrichs, D. J., *et al.* (1997). Potentiation of an antimalarial oxidant drug. *Antimicrobial Agents and Chemotherapy*, **41**(7): 1449–1454.
- Wirth, C. C., Glushakova, S., Scheuermayer, M., Urska Repnik, S. G., Schaack, D., Kachman, M. M., *et al.* (2014). Perforin-like protein pplp2 permeabilizes the red blood cell membrane during egress of *Plasmodium falciparum* gametocytes. *Cellular Microbiology*, **16**(5): 709–733.
- World Health Organization. (2006). Indoor residual spraying: Use of indoor residual spraying for scaling up global malaria control and elimination. *World Health Organization*, Geneva, Switzerland.

- Yeh, E., & DeRisi, L. J. (2011). Chemical rescue of malaria parasites lacking an apicoplast defines organelle function in blood-stage *Plasmodium falciparum*. *PLoS Biology*, 9(8): e1001138.
- Zhang, F., Wen, Y., & Guo, X. (2014). CRISPR/Cas9 for genome editing: Progress, implications and challenges. *Human Molecular Genetics*, 23(1): R40–R46.